Neuronal regulation of haematopoietic stem cell ageing and age-related blood disorders through the microenvironment

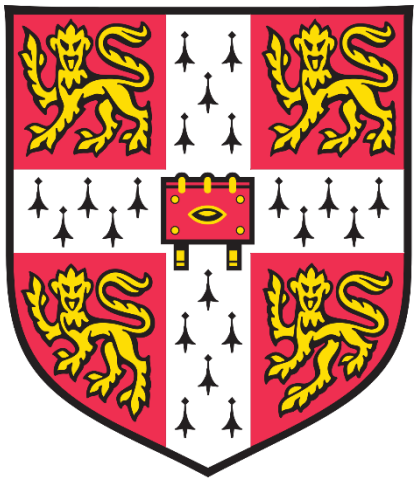

Ya-Hsuan Ho

Department of Haematology

University of Cambridge

This dissertation is submitted for the degree of Doctor of Philosophy

Wolfson College  September 2019

Declaration

This thesis is the result of my own work and includes nothing which is the outcome of work done in collaboration except as declared in the Preface and specified in the text. It is not substantially the same as any that I have submitted, or, is being concurrently submitted for a degree or diploma or other qualification at the University of Cambridge or any other University or similar institution except as declared in the Preface and specified in the text. I further state that no substantial part of my thesis has already been submitted, or, is being concurrently submitted for any such degree, diploma or other qualification at the University of Cambridge or any other University or similar institution except as declared in the Preface and specified in the text.

The total length of the main body of this dissertation is 23752 words, and therefore does not exceed the prescribed word limit (60000 words) for the relevant Degree Committee.

Ya-Hsuan Ho

September 2019

Abstract

Neuronal regulation of haematopoietic stem cell ageing and age-related blood disorders through the microenvironment

Ya-Hsuan Ho

Haematopoietic stem cells (HSCs) give rise to all blood and immune cells in our body. Residing in the bone marrow (BM), HSCs are surrounded by numerous cell types and the associated extracellular matrix, which form a unique microenvironment known as ‘’HSC niche’’. Sympathetic neurons are important BM niche regulators, controlling HSC traffic in and out of the BM through the activation of β-adrenergic receptors (β-ARs). However, whether BM sympathetic-adrenergic signalling regulates other functions of HSCs remains poorly understood.

Upon ageing, HSCs are functionally impaired, characterised by increased proliferation, decreased regenerative capacity, and myeloid/megakaryocytic-biased differentiation at the expense of lymphoid cell production. Ageing is associated with an increased risk to develop myeloid malignancies, but the contributions of HSC-intrinsic and -extrinsic ageing mechanisms remain debated. The current study aimed to understand how BM niches influence HSC fate in mouse models of ageing and age-related myeloid disorders, with a particular focus on microenvironmental regulation of myelopoiesis/megakaryopoiesis in response to neuronal inputs. During normal ageing, HSC niches decrease near bone but expand further from bone. Adrenergic signalling regulates lymphoid-myeloid balance during ageing. Whereas β2-AR promotes myeloid and megakaryocyte (Mk) differentiation through stromal-cell-derived interleukin-6 (IL-6), reduced β3-AR signalling accelerates ageing by remodelling HSC niches and diminishing lymphoid-biased HSCs. Similarly, non-HSC-autonomous premature haematopoietic ageing is observed in Hutchinson-Gilford progeria syndrome (HGPS). Chronic treatment of β3-AR agonist partially rejuvenates premature haematopoietic ageing in HGPS and restores exacerbated megakaryopoiesis in myeloproliferative neoplasms (MPNs).

In summary, these results suggest that HSC niche remodelling and a functional switch of sympathetic activity (β2-AR overriding β3-AR) contribute to myeloid expansion during normal ageing. Certain ageing features in HGPS and aged-related pathological conditions could be improved by targeting the microenvironment.

Acknowledgements

Firstly, I would like to thank my supervisor Simón Méndez-Ferrer for welcoming me into his laboratory to work on such an interesting project. His support throughout my PhD is invaluable.

Second, I would like to thank all the lab members (previous and present) of the Mendez-Ferrer's lab and collaborators throughout my PhD. In particular, I would like to thank Justyna Rak for starting the ageing project and performing some experiments. I would like to thank Andres Garcia-Garcia and Claudia Korn for providing insightful suggestions and contributions to the project. I would like to thank Claire Fielding and Chrysa Kapeni for experimental help and advices. I would like to thank Amie Waller and Holly Foster (from Cedric Ghevaert's lab) for assisting on human Mk differentiation experiments. I would like to thank David Macias (from Randall S. Johnson's lab) for measuring nitrate concentration. I would like to thank Cristina Gonzalez-Gomez and Alberto del Monte (Vicente Andres' lab) for helping the progeria experiments. I would like to thank Helen Jolin (Andrew McKenzie's lab) for helping with milliplex analyses.

Thirdly, I would like to thank Trinity college and Wolfson college (University of Cambridge) and R.O.C. government for providing funding to support my PhD.

Finally, I would like to thank my parents for their ongoing support. I would like to thank my brother for designing the beautiful cover image for my thesis. I would like to thank my wife for being there for me and always encouraging me when I was struggling throughout my PhD.

Paper arising from this PhD

Ho YH, Del Toro R, Rivera-Torres J, Rak J, Korn C, García-García, Macías D, González-Gómez C, Del Monte A, Wittner M, Waller AK, Foster HR, López-Otín C, Johnson RS, Nerlov C, Ghevaert C, Vainchenker W, Louache F, Andrés V2, Méndez-Ferrer S. **Remodeling of Bone Marrow Hematopoietic Stem Cell Niches Promotes Myeloid Cell Expansion during Premature or Physiological Aging**. **Cell Stem Cell**. 2019 Sep 5;25(3):407-418.e6.

Abbreviations

BM	bone marrow
HSC	haematopoietic stem cell
Mk	megakaryocyte
DKO	double knockout
LT-HSC	long-term haematopoietic stem cell
CXCL12	C-X-C motif chemokine 12
SCF	stem cell factor
TPO	thrombopoietin
EPO	erythropoietin
MSC	mesenchymal stromal cell
CAR	CXCL12-abundant reticular
LepR	leptin receptor
Vwf	Von Willebrand factor
PF4	platelet factor 4
TGFβ	transforming growth factor β
SNS	sympathetic nervous system
NE	norepinephrine
EPI	epinephrine
G-CSF	granulocyte-colony-stimulating factor
AR	adrenergic receptor
MPP	multipotent progenitor
CMP	common myeloid progenitor
MEP	megakaryocyte-erythrocyte progenitor
MkP	megakaryocyte progenitor
DMS	demarcation membrane system
TF	transcription factor
CFU-F	colony-forming unit fibroblast

OPN	osteopontin
CCL5	CC-chemokine ligand 5
ROS	reactive oxygen species
Terc	Telomerase RNA component
NO	nitric oxide
nNOS	neuronal nitric oxide synthase
EC	endothelial cell
TZV	Transitional zone vessel
EMNC	endomucin
MPNs	myeloproliferative neoplasms
CML	chronic myelogenous leukaemia
IL	interleukin
TNFα	tumour necrosis factor α
IFN	interferon
WT	wild-type
PV	polycythaemia vera
ET	essential thrombocythaemia
PMF	primary myelofibrosis
OCT	optimal cutting temperature
MDS	myelodysplastic syndrome
AML	acute myelogenous leukaemia
PFA	paraformaldehyde
EDTA	ethylenediaminetetraacetic acid
CLEC-2	C-type lectin-like receptor-2
ELISA	enzyme-linked immunosorbent assay
PPF	proplatelet formation
BMSC	bone marrow stromal cell

Contents

List of Figures

List of Tables

1. Introduction

1.1 Evolving concept of bone marrow (BM) haematopoietic stem cell (HSC) niches

Adult haematopoiesis takes place in the bone marrow (BM), where haematopoietic stem cells (HSCs) can self-renew, proliferate and differentiate to replenish the blood and immune systems. Given that most HSCs are quiescent under homeostasis, mature blood and immune cell production is believed to derive mainly from progenitor cells (rather than HSCs), which undergo stepwise differentiation to produce specific blood and immune cell lineages, including myeloid lineage cells, consist of granulocytes, monocytes, megakaryocytes (Mks) (precursors of platelets) and erythrocytes, and lymphoid lineage cells, comprising T-cells, B-cells and natural killer cells. Cumulative studies have demonstrated that HSCs are heterogenous and contain subsets with distinct myeloid, platelet or lymphoid-biased potentials (Ema et al., 2014). Additionally, they have shown that HSCs can bypass the intermediate steps to generate mature progenies under certain conditions, such as chronic inflammation and ageing (Nishikii et al., 2017).

Haematopoiesis is tightly controlled by cell-intrinsic mechanisms (lineage-specific transcription factors and epigenetic modifications) and the surrounding microenvironment, known as “HSC niche”. Osteoblasts (bone-forming cells) and osteolineage are the first niche cells found to be involved in HSC regulation. Early studies have indicated that osteoblasts differentiated from BM stromal cells secrete haematopoietic cytokines and could maintain HSCs in culture (Taichman and Emerson, 1994). In 2003, two studies described for the first time that transplanted HSCs lodge near the bone surface (endosteum) in the BM, where

their numbers are regulated by osteoblastic cells. Dr. Zhang et al. showed that transplanted long-term (LT) HSCs adhere to spindle-shaped N-cadherin^{+}CD45^{-} osteoblastic (SNO) cells, which control the size of HSC pool by BMP signalling (Zhang et al., 2003). Dr. Calvi et al. reported that osteoblasts activated with parathyroid hormone/parathyroid hormone-related protein receptor (PPRs) produce high levels of Notch ligand Jagged 1 and increase HSC number (Calvi et al., 2003). Later studies by Dr. Suda's group identified Tie2/angiopoietin-1 signalling and thrombopoietin (TPO)/MPL signalling as important regulators of HSC quiescence through the interaction with osteoblasts (Arai et al., 2004; Yoshihara et al., 2007). High calcium concentration in the endosteum also plays an indispensable role in supporting HSCs, since calcium-sensing receptor (CaR) knockout HSCs fail to migrate to endosteal BM surface after transplantation (Adams et al., 2006). In addition, endosteal BM is reportedly enriched in C-X-C motif chemokine 12 (CXCL12) (Sugiyama et al., 2006) and stem cell factor (SCF) (Kinashi and Springer, 1994), two key HSC cytokines, strengthening the hypothesis that the endosteal BM is an important reservoir for HSCs. However, the concept of osteoblastic/endosteal niche was thereafter challenged by Dr. Morrison's study, indicating that osteoblastic-specific deletion of CXCL12 or SCF only promotes the maintenance of early lymphoid progenitors but has little impact on HSCs (Ding and Morrison, 2013). Furthermore, N-cadherin in osteolineage cells seems to be dispensable for HSC maintenance under homeostasis (Greenbaum et al., 2012). These studies suggest that most HSCs are maintained in non-endosteal BM under steady state. Murine BM is highly vascularised, and the close developmental relationship between haematopoietic and endothelial lineages together suggest that HSCs are housed and regulated in perivascular regions. However, it is important to note that endosteal BM niches are densely vascularised. To date, at least two functionally distinct perivascular niches highly expressing CXCL12 and SCF have been identified: the peri-

arteriolar niches, which contain Nestin-GFP^{bright} and/or NG2^{+} mesenchymal stromal cells (MSCs), and the peri-sinusoidal niches, where sinusoid-associated CXCL12-abundant reticular cells (CAR), Nestin-GFP^{dim} and/or Leptin receptor^{+} (LepR^{+}) cells reside (Boulais and Frenette, 2015). Recent studies reveal that Mks also regulate HSC quiescence through transforming growth factor β (TGFβ), TPO and platelet factor 4 (PF4) secretion (Bruns et al., 2014; Nakamura-Ishizu et al., 2014; Zhao et al., 2014). Given the complexity of the BM architecture and the limitations of current genetically-modified mouse models, it remains controversial which specialised niches predominantly regulate HSC quiescence. It is likely that HSC quiescence is regulated by different signals in distinct BM regions and during steady state or stress haematopoiesis. However, HSC lineage commitment appears to be highly influenced by the location. Accumulating evidence suggests that lymphopoiesis preferentially occurs near the endosteum, while myelopoiesis/erythropoiesis/megakaryopoiesis takes place at non-endosteal regions. Supporting the concept, a recent study using von Willebrand factor (*Vwf*)-eGFP to label different HSC populations demonstrated that Vwf^{+} platelet/myeloid-biased HSCs are associated with Mks, whereas Vwf^{-} lymphoid/non-biased HSCs are close to arterioles (Pinho et al., 2018). Therefore, alterations in specialised niches might directly affect myeloid/lymphoid output, and imbalanced production of mature haematopoietic cells at specific niches might also remodel the microenvironment locally.

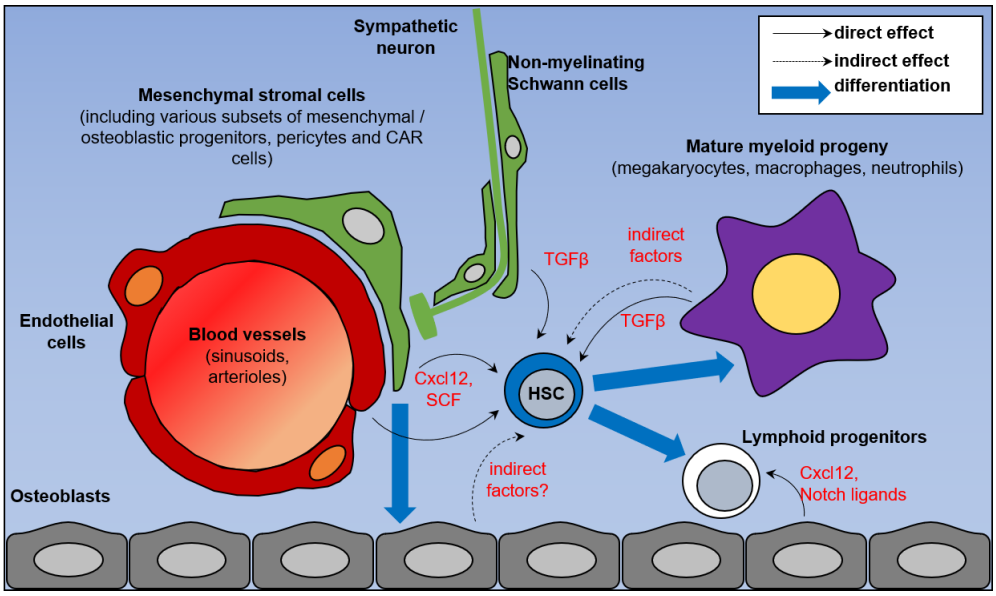

Figure 1. BM HSC niches.
HSCs are located at specialised ‘’niches’’ where their proliferation, differentiation and mobilisation are tightly controlled. BM niche components include mesenchymal stromal cells (MSCs), sympathetic neurons, non-myelinating Schwann cells, endothelial cells, osteoblasts and mature haematopoietic progenies. Based on BM anatomy, HSCs are differentially regulated at endosteal niches (close to bone surface) and/or non-endosteal niches (away from bone surface). Given BM is highly vascularised, most HSCs are adjacent to different types of vessels. At least two functionally distinct perivascular niches have been identified: arteriolar niches and sinusoidal niches. This image has been reproduced from (Sanchez-Aguilera and Mendez-Ferrer, 2017).

1.2 Neuronal regulation of haematopoiesis in the BM

The sympathetic nervous system (SNS) is one division of the autonomic nervous system (ANS) that participates in maintaining tissue homeostasis. Two types of neuron, the preganglionic neuron and the postganglionic neuron, are responsible for the transmission of SNS signals. Preganglionic fibres release acetylcholine, which activates nicotinic acetylcholine receptors on postganglionic neurons. In response to the stimulus, postganglionic fibres innervate targeted organs by locally releasing neurotransmitters, including dopamine, norepinephrine (NE) and epinephrine (EPI) (Feldberg, 1952). Sympathetic regulation of HSCs has been studied by Dr. Frenette's group, who reported that HSC egress and enforced mobilisation induced by granulocyte-colony-stimulating factor (G-CSF) is regulated by SNS signals in the BM (Katayama et al., 2006; Mendez-Ferrer et al., 2010). One regulation involves BM Nestin-GFP$^+$ MSCs, which are regulated by sympathetic nerve fibres via β3-adrenergic receptor (AR). This SNS-MSC regulatory axis regulates HSCs in part through chemokine CXCL12 (Mendez-Ferrer et al., 2010). In contrast, activation of β2-AR can directly promote haematopoietic stem and progenitor cell (HSPC) mobilisation (Spiegel et al., 2007), or indirectly induce clock gene expression by stromal cells (Mendez-Ferrer et al., 2010). Another study has shown that sympathetic tone in the BM primes anti-HSC-mobilizing functions of neutrophils (Kawano et al., 2017). Recent studies from our group have uncovered the role of sympathetic cholinergic nerve fibres in the regulation of HSC and leukocyte traffic (Garcia-Garcia et al., 2018). Although the regulation of HSC traffic by sympathetic nerve fibres has been well investigated, whether SNS regulates other functions of HSCs and/or their committed progenies remains largely unexplored.

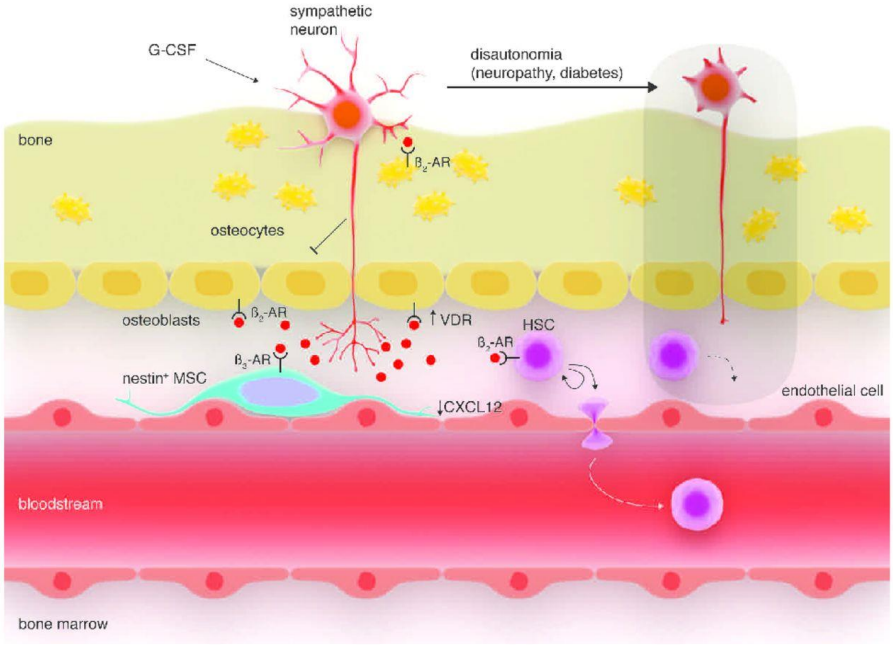

Figure 2. Sympathetic adrenergic regulation of HSC mobilisation by β-ARs. HSPCs trafficking is regulated by the sympathetic nervous system (SNS). Cooperation of β2-AR and β3-AR directly and/or indirectly (through Nestin-GFP^{+} MSCs) controls HSPC egress to circulation and homing to BM. This image has been reproduced from (del Toro and Méndez-Ferrer, 2013).

1.3 MKs and megakaryopoiesis and thrombopoiesis

Mks are platelet precursors in the BM, 70% of which are found adjacent to sinusoids. Mks are 10-15 times larger than red blood cells but they account for only 0.01 % of total BM nucleated cells. Whereas the major function of Mks is to produce platelets for blood clotting, recent studies also indicate that Mks are necessary for regulating HSC quiescence (Bruns et al., 2014; Nakamura-Ishizu et al., 2015; Zhao et al., 2014). Megakaryopoiesis is a process by which HSCs proliferate and differentiate to the large polyploid Mks. The traditional view involves a hierarchy of several consecutive commitment steps, during which HSCs sequentially transition from multipotent progenitor (MPP), common myeloid progenitor (CMP), megakaryocyte-erythrocyte progenitor (MEP), Mk progenitor (MkP), to multilobulated Mk (Malara et al., 2015). However, this stepwise Mk differentiation from HSCs has been questioned by recent studies proposing different routes to make blood cells and demonstrating that Mks can arise directly from HSCs (Huang and Cantor, 2009; Woolthuis and Park, 2016). As Mks mature, they undergo endomitosis by constantly doubling the numbers of chromosomes in the nucleus without cytoplasmic division (Jackson, 1990). In addition, their cytoplasm expands, followed by the formation of demarcation membrane system (DMS) and increased numbers of α-granules (Schulze et al., 2006). Terminally differentiated Mks migrate to the sinusoids for platelet release through a process called thrombopoiesis (Choi et al., 1996). Platelets are generated from the pseudopodial extensions of Mk, termed the proplatelets, which elongate along the endothelium and are fragmented by the bloodstream (Patel et al., 2005).

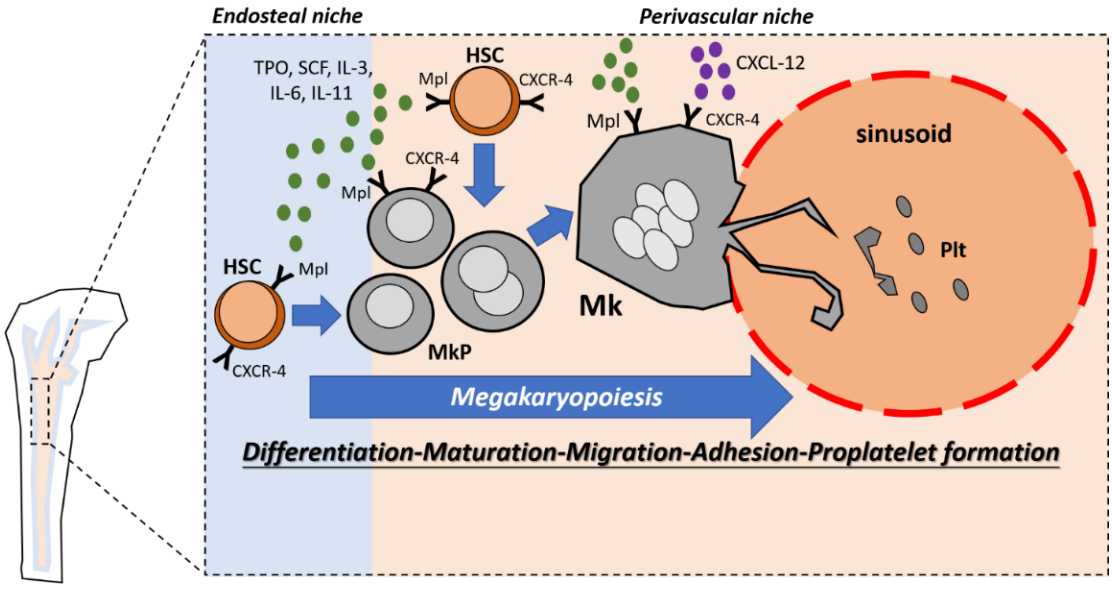

Figure 3. Megakaryopoiesis and thrombopoiesis.
Megakaryopiesis and thrombopoiesis include multistep biological processes: 1) HSCs undergo lineage-specific commitment to megakaryocyte progenitor (MkP). 2) MkPs differentiate to mature Mks. 3) Mature Mks migrate and adhere to the sinusoidal walls to generate platelets. The processes are tightly controlled by cell-intrinsic factors (mainly lineage-specific transcription factors) and microenvironmental signals (mainly cytokines and chemokines, such as TPO, SCF, IL3, IL6, IL11 and CXCL12).

Megakaryopoiesis and thrombopoiesis are controlled by microenvironmental cues and transcriptional factors (TFs). TPO, a glycoprotein cytokine primarily produced by the liver, is a master regulator of both processes (Vainchenker et al., 2013). The chemoattractant stromal cell-derived factor 1 (SDF-1)/CXCL12 directs Mk migration to the sinusoids for platelet production (Majka et al., 2000). GATA-1, FLI-1 and FOG play major roles in regulating HSC lineage commitment to Mk (Pimkin et al., 2014), whereas *NFE-2* governs platelet biosynthesis (Tijssen and Ghevaert, 2013). The spatial regulation of megakaryopoiesis in murine BM is controversial. The standard model suggests that Mk precursors migrate from endosteum to sinusoids for maturation (Eto and Kunishima, 2016). A revised model suggests that Mks and MkPs both reside at the sinusoid niche where megakaryopoiesis and thrombopoiesis directly take

place (Kunisaki et al., 2013; Stegner et al., 2017). In either case, these studies highlight the importance of the interaction between Mks and the microenvironment. Although many studies have indicated that different neurotransmitters can affect platelets, whether megakaryopoiesis/thrombopoiesis are regulated by SNS signals remains elusive. One study has suggested that Mk maturation and platelet production are regulated by adrenergic signals in the BM (Chen et al., 2016). However, whether neuronal signals regulate HSC lineage commitment to Mks was unclear.

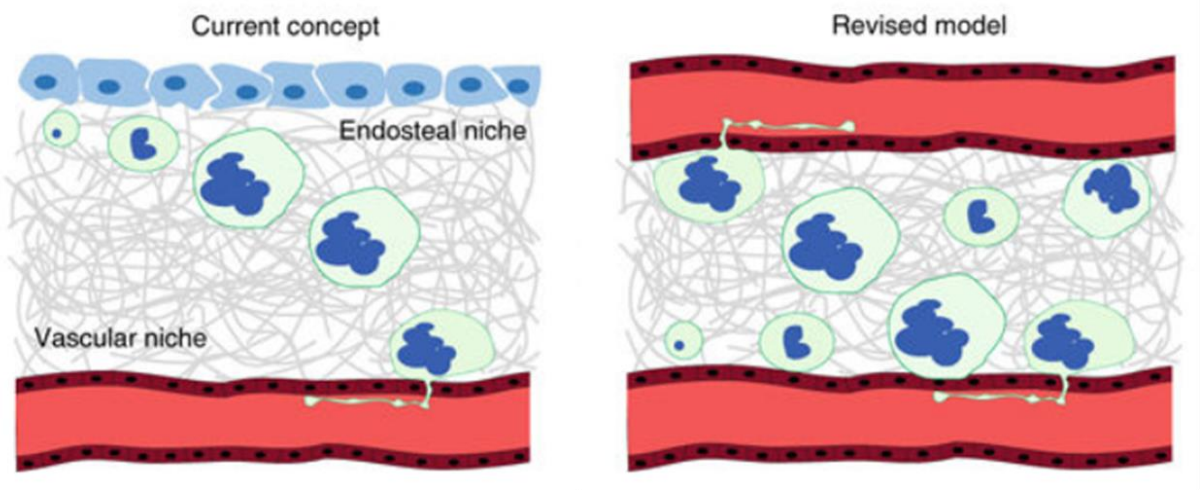

Figure 4. The current model and revised model of megakaryopoiesis and thrombopoiesis.
Traditional view suggests HSCs and MkPs migrate from endosteum to central marrow as they differentiate and mature to Mks. Current model suggests HSCs and MkPs are locating near sinusoids where megakaryopoiesis/thrombopoiesis is directly taking place. (Image taken from Stegner et al. Nature Communications 2017.)

1.4 HSC ageing and the aged BM microenvironment

Upon ageing, HSCs expand but their functions are impaired, characterised by reduced regenerative potential, decreased homing capacity and myeloid-biased differentiation at the expense of lymphopoiesis (Liang et al., 2005; Mohrin et al., 2015; Rossi et al., 2005; Sudo et al., 2000). The functional decline of aged HSCs correlates with their loss of cell polarity, which is in part mediated by elevated activity of the small RhoGTPase Cdc42 (Florian et al., 2012). Other HSC-intrinsic ageing drivers include DNA damage, reactive oxygen species (ROS)-induced oxidative stress, metabolic alterations, impaired autophagy and epigenetic dysregulations (de Haan and Lazare, 2018; Lee et al., 2019). Ageing also impacts HSCs by changing their BM distribution. Aged HSCs have been reported to locate further away from the bone surfaces after BM transplantation (Florian et al., 2012), correlating with increased marrow HSC numbers and enhanced HSC mobilisation into circulation (Xing et al., 2006). Recent studies using whole-mount immunofluorescence staining of murine long bones further revealed that aged HSCs are more distant to the endosteum, arterioles, Nestin-GFP^{high} cells and Mks, but their distance to sinusoids and Nestin-GFP^{low} cells is unchanged compared to young HSCs (Maryanovich et al., 2018; Sacma et al., 2019). These results suggest that BM microenvironment is altered with age, which might favour HSC lodging near non-endosteal/central niches (over endosteal niches). The following sections will discuss current studies on age-related BM niche remodelling, key microenvironmental players and the correlating mechanisms by which HSC localization and functions are regulated.

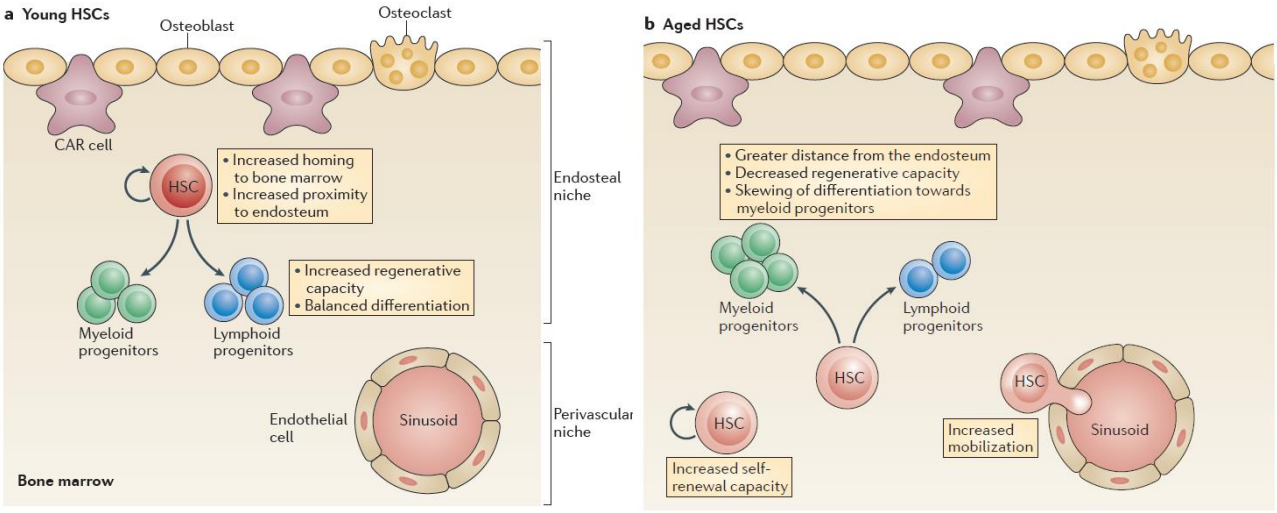

Figure 5. General features of HSC ageing.
Compared to young HSCs, aged HSCs exhibit reduced regenerative capacity, skewed differentiation towards myeloid/megakaryocytic progenitors, increased mobilisation and redistribution further away from endosteum. (Image taken from Geiger et al. Nature Reviews Immunology 2013.)

1.4.1 Dysfunction of BM MSCs during ageing

Alteration of MSC populations during ageing

Studies regarding the absolute number of MSCs during ageing are controversial, with some suggesting an overall increase (Garcia-Prat et al., 2013; Stolzing et al., 2008) while others suggest unchanged numbers (Siegel et al., 2013; Wagner et al., 2009). It is noteworthy that MSCs are heterogeneous, and conventional markers to immunophenotypically define functionally distinct MSCs are lacking. Using Nestin-GFP to label a subset of murine MSC population, scientists have revealed that Nestin-GFP$^+$ cells in endosteal BM are significantly decreased during ageing (Sacma et al., 2019), consistent with the reduction of arteriole-associated αSMA$^+$, PDGFRβ$^+$ and NG2$^+$ cells (Maryanovich et al., 2019). The age-related contraction of endosteal BM might initiate lymphoid deficiency at the level of HSCs, since lymphoid-biased HSCs seem to be enriched near bone, whereas more committed lymphoid lineage cells, such as common lymphoid progenitors and pro-B cells, localize near sinusoids (Balzano et al., 2019; Cordeiro Gomes et al., 2016; Ding and Morrison, 2013; Pinho et al., 2018). Functionally, old MSCs have lower colony-forming unit fibroblast (CFU-F) capacity *in vitro* and fail to produce HSC supporting molecules (Maryanovich et al., 2019). Revitalising MSCs with the ability to produce niche factors can prevent DNA damage in cultured HSCs (Nakahara et al., 2019).

MSC differentiation potential is imbalanced during ageing

MSCs exhibit reduced osteogenesis with age, which is associated with lower osteopontin (OPN) secretion to the extracellular matrix (Guidi et al., 2017). OPN negatively regulates HSC proliferation (Haylock and Nilsson, 2006; Nilsson et

al., 2005; Stier et al., 2005), and its decline might accelerate HSC divisions during ageing. Supporting this idea, treatment with thrombin-cleaved OPN partially reverses the age-associated phenotype of HSCs (Guidi et al., 2017). CC-chemokine ligand 5 (CCL5), a pro-inflammatory cytokine involved in bone remodelling (Wintges et al., 2013), is reportedly increased with age. Researchers also reported a direct contribution of CCL5 to myeloid-biased differentiation at the cost of T cells (Ergen et al., 2012), suggesting that CCL5 is important for ageing of the haematopoietic system and the microenvironment. In contrast, old MSCs show adipocyte skewing (Kim et al., 2012). Adipocytes are a BM niche component that regulate hematopoiesis after irradiation or leukemia (Boyd et al., 2017), although their roles negatively regulating HSC numbers (Naveiras et al., 2009) and haematopoiesis under homeostasis seem to be dispensable (Zhou et al., 2017). However, it has been reported that the functions of adipose tissues alter in response to ageing, such as ectopic lipid deposition, insulin resistance and increased inflammation (Mancuso and Bouchard, 2019). Accumulation of BM adipocytes upon ageing not only reduces haematopoietic reconstitution, but also disrupts bone fracture repair (Ambrosi et al., 2017). The later likely contributes to the increased risk of osteoporosis and bone fracture in the elderly population (Fazeli et al., 2013; Schwartz, 2015).

MSCs are senescent during ageing

BM ageing is also associated with senescence of MSCs, evidenced by increased p53/p21-mediated DNA damage, upregulation of p16(INK4a) and elevated levels of ROS (Kornicka et al., 2015; Zhang et al., 2011; Zheng et al., 2013). Dr. Ju et al. discovered an age-dependent shortening of telomeres in Telomerase RNA component knockout (*Terc*$^{-/-}$) MSCs, and lethally irradiated *Terc*$^{-/-}$ mice carrying wild-type BM cells display accelerated myelopoiesis (Ju et al., 2007). More

recently, proteomic analyses of human BM have unravelled nitric oxide (NO) synthesis and the urea cycle pathways as potential mediators for the crosstalk between old MSCs and HSCs (Hennrich et al., 2018). Murine MSCs highly express neuronal nitric oxide synthase (nNOS, encoded by gene *NOS1*), and *NOS1*$^{-/-}$ mice develop certain premature ageing features, such as increased peripheral platelets and granulocytes (Ho et al., 2019). Given the importance of NO in vascular biology and balanced inflammatory responses (Tripathi et al., 2007), it is likely that NO pathways participate in the aged vascular remodelling and myeloid expansion partly by modulating inflammation.

1.4.2 Remodelling of BM vasculature and its functions

Alteration of endothelial cells (ECs) during ageing

During ageing, a drastic remodelling of BM endothelial architecture occurs. Studies using whole-mount confocal imaging, two photon intravital microscopy and flow cytometry analysis, demonstrated an overall increase of vascular density in aged mice (Kusumbe et al., 2016; Maryanovich et al., 2019). Yet, distinct endothelial sub-populations behave differently with age. Arterioles are found to be decreased, while sinusoids appear to be unchanged upon ageing (Ho et al., 2019). Supporting these observations, arteriole segments covered by Nestin-GFP^{bright} cells are found to be shortened (Maryanovich et al., 2019). Transitional zone vessels (TZVs) containing type-H endomucin (EMNC)-high ECs (which are enriched in the murine trabecular BM, where they support developmental bone growth (Kusumbe et al., 2014)), are reduced in old mice (Ho et al., 2019; Kusumbe et al., 2016). In contrast, small capillaries (CD31^{high}EMCN^{-} cells with <6 μm diameter) are notoriously expanded in the central marrow (Ho et al., 2019).

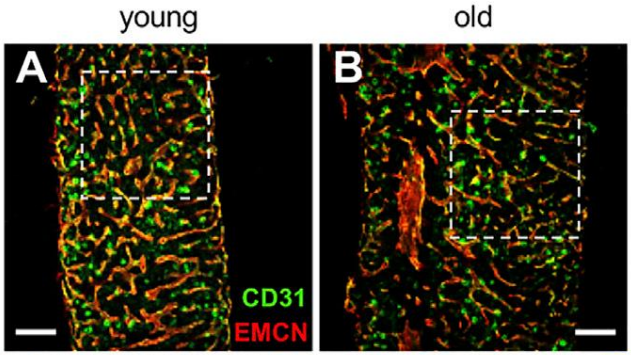

Figure 6. Remodelling of BM vasculature during ageing.
Whole-mount confocal imaging shows that TZVs (EMCN^{hi}CD31^{hi} endosteal vessels) are decreased, while small capillaries (CD31^{hi}EMCN^{-}, <6 μm diameter) are expanded in aged murine BM. (Image taken from Ho et al. Cell stem cell 2019. The staining was performed by Claudia Korn.)

The functions of ECs are compromised during ageing

The functions of ECs decline with age, characterized by increased vascular leakiness, reduced NO production, increased ROS levels and decreased angiogenic potential (Poulos et al., 2017). Poulos et al. previously reported that purified HSCs from young mice cocultured with ECs from old mice fail to show long-term and multilineage reconstitution, while old HSCs cocultured with young ECs maintain their self-renewal ability (Poulos et al., 2017). Infusion of young ECs into aged, conditioned mice revives the old haematopoietic system. Kusumbe et al. identified high Notch activity in type-H ECs and the associated perivascular cells (Kusumbe et al., 2016), suggesting that contraction of endosteal vessels upon ageing occurs concomitantly with impaired Notch signalling. Overexpression of Notch ligand, DLL4 in vascular ECs is shown to prevent myeloid-skewing of haematopoietic progenitors (Tikhonova et al., 2019), despite DLL4 being undetectable or unchanged in aged BM (Sacma et al., 2019). Nevertheless, Sacma et al. observed that the levels of Jag2, another Notch ligand, are reduced in Nestin-GFP^{high}/arteriolar cells with ageing. In contrast, Jag2 levels are higher in sinusoids/Nestin-GFP^{high} cells, and Jag2 blockade induces proliferation and clustering of aged HSCs near sinusoids (Sacma et al., 2019). Together, these results strongly suggest that altered Notch signalling critically contributes to HSC ageing in different ways depending on the niche: in the endosteal vessels, Notch signalling appears to regulate HSC lineage commitment, whereas it is required in the sinusoids to preserve old HSCs (since HSCs accumulate in sinusoidal niches as a function of age).

1.4.3 Inflammation

Ageing of the BM microenvironment is associated with increased pro-inflammatory cytokines in mice and humans (Kovtonyuk et al., 2016). Several lines of evidence have indicated that inflammatory signals drive myeloid/megakaryocytic differentiation. In age-related myeloid malignancies, such as myeloproliferative neoplasms (MPNs) and chronic myelogenous leukaemia (CML), serum interleukin 1 β (IL-1β) and interleukin 6 (IL-6) levels are elevated (Arranz et al., 2014; Reynaud et al., 2011). Dr. Pietras et al. reported that chronic IL-1 exposure induces HSC myeloid skewing at the expense of self-renewal (Pietras et al., 2016). IL-1α/β regulates thrombopoiesis *in vitro* (Beaulieu et al., 2014; Nishimura et al., 2015), possibly explaining high platelet counts in aged mice (Grover et al., 2016). Defective phagocytosis of macrophages during ageing induces acquisition of platelet-biased HSCs through IL-1β signalling (Frisch et al., 2019). IL-6 promotes thrombopoiesis either through a direct effect on BM Mk differentiation (Ho et al., 2019) or indirectly by upregulating hepatic TPO levels (Kaser et al., 2001). Dr. Yamashita et al. demonstrated that transient stimulation of tumour necrosis factor α (TNFα) prevents HSCs from necroptosis, and proposed that constitutive activation might lead to hyperproliferation of HSCs and exacerbated myelopoiesis in ageing and myeloproliferative disorders (Yamashita and Passegue, 2019). Mks express TGF-β to regulate HSC quiescence, while Mk-derived TGF-β also stimulates TPO synthesis by BM stromal cells to enhance megakaryopoiesis (Sakamaki et al., 1999). An elegant study by Dr. Haas et al. reported that acute inflammation induces proliferation of the stem cell-like Mk progenitor to quickly replenish platelet loss, and the process is in part mediated through the interferon (IFN) family (Haas et al., 2015).

Despite a well-known lymphocyte loss, only the proportion, but not absolute number of lymphoid-biased HSCs declines with age (Beerman et al., 2010). In fact, both platelet-biased and lymphoid-biased HSCs expand, alter gene expression programs and exhibit myeloid/platelet-skewing output (Grover et al., 2016). These findings suggest a cell fate change of HSCs upon ageing, and the net outcome is an increase of myeloid/platelet compartment at the expense of lymphoid compartment. Two possible non-mutually exclusive explanations are: 1) Different HSCs suffer the same genetic deformities upon ageing and/or 2) microenvironmental alterations specifically influence HSCs and direct their cell fate. Supporting the later, HSCs subpopulations have been found to respond differently to inflammatory challenge during ageing (Mann et al., 2018). Moreover, Dr. Montecino-Rodriguez et al. discovered that old lymphoid-biased HSCs recover their young lymphoid commitment potential when removed from the old microenvironment (Montecino-Rodriguez et al., 2019). Exogenous addition of IL-1 blocks lymphocyte differentiation from old lymphoid-biased HSCs, confirming the indispensable role of IL-1 in HSC cell fate decision. Consistently, Dr. Benjamin et al. demonstrated that IL-1 blockade is sufficient to restore age-dependent increase of megakaryocytic-biased HSCs *in vitro* (Frisch et al., 2019).

However, whether BM inflammation is the cause or consequence of HSC ageing remains debated. It is notable that mature myeloid/megakaryocytic cells are a major source of inflammatory cytokines (Pietras, 2017). Exacerbated myelopoiesis during ageing might also remodel the BM microenvironment, favouring HSC myeloid/megakaryocytic-skewing through inducing inflammation. A positive feedback loop of cytokine storm created by HSCs, their progeny cells and the niche compartments contribute to HSC ageing and might further predispose myeloid malignancies.

1.4.4 Neuronal regulation by sympathetic adrenergic signalling

It has been reported that BM sympathetic stimulation of β_2-AR or β_3-AR regulates HSC mobilisation (Mendez-Ferrer et al., 2010). A recent publication by Dr. Maryanovich et al. suggests that adrenergic nerve fibres marked with tyrosine hydroxylase (Th, rate-limiting enzyme in catecholamine synthesis) are reduced in old murine BM (Maryanovich et al., 2019). The study also indicates that surgical denervation of young BM induces premature ageing of the haematopoietic system, although certain experimental variables, such as the inflammation induced by the surgical denervation, might influence the observed phenotypes. Similar reduction of nerve fibres has been reported in a mouse model of the age-related MPNs (Arranz et al., 2014), suggesting that BM neuropathy might predispose to the development of myeloid malignancies with age. However, using whole-mount imaging and 3D reconstruction of different bones, other investigators from our group found that the BM area occupied by Th^+ adrenergic fibres are actually doubled during normal physiological ageing (Ho et al., 2019), consistent with the well-known increase in sympathetic activity in the elderly (Hart and Charkoudian, 2014; Ng et al., 1993; Veith et al., 1986; Ziegler et al., 1976). Additionally, the SNS has been known to control inflammation in a context-dependent manner (Pongratz and Straub, 2014). The concentration of catecholamines and the expressions of different ARs regulate the inflammatory state of the innate immune cells. Increased sympathetic activity during ageing might contribute to a cytokine storm by activating inflammatory cells, and subsequently affects lineage-bias of HSCs. Despite all the efforts made in recent days, however, neuronal regulation of HSCs during ageing remains poorly understood.

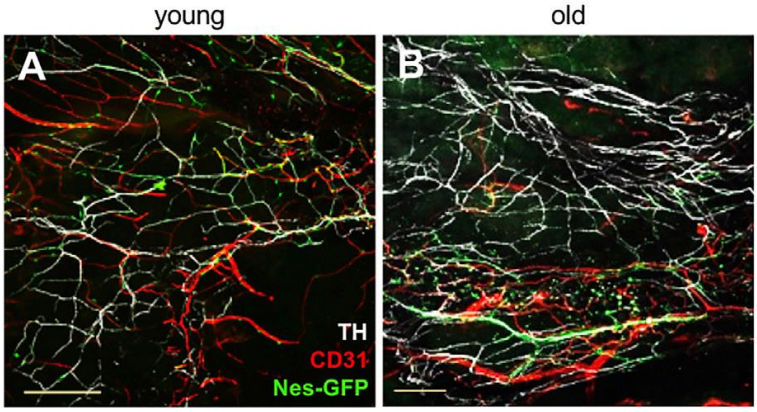

Figure 7. Increased sympathetic nerve fibres during ageing.
Whole-mount confocal imaging shows that Th^{+} sympathetic nerve fibres are increased in the skull of old mice compared to young mice. (Image taken from Ho et al. Cell stem cell 2019. The staining was performed by Justyna Rak and Andres Garcia-Garcia)

1.4.5 Other players in the BM microenvironment

Emerging data suggest that the progenies of HSCs can feed back to regulate their activity under homeostasis, raising the possibility that mature haematopoietic cells (or their interactions with others) also contribute to HSC ageing. For instance, clearance of senescent $CD62L^{low}CXCR4^{high}$ neutrophils by macrophages has been reported to modulate HSC niches (Casanova-Acebes et al., 2013). Dr. Frisch et al. discovered that aged macrophages are unable to engulf senescent neutrophils, leading to expansion of megakaryocytic-biased HSCs through IL-1β signalling (Frisch et al., 2019). Another key player is Mks, reportedly expressing PF4, CLEC-2, TPO and TGF-β to control HSC proliferation/quiescence (Bruns et al., 2014; Nakamura-Ishizu et al., 2014; Nakamura-Ishizu et al., 2015; Zhao et al., 2014). In murine BM, around 20% of HSCs are spatially associated with Mks (Bruns et al., 2014), and depletion of Mks expands platelet-biased HSCs (Pinho et al., 2018). BM Mks expand in ageing, and the distance of Mks to HSCs substantially increases (Maryanovich et al., 2019), suggesting a remodelling of Mk niches with age. However, the mechanism by which age-related alterations of Mks regulate HSC ageing is still elusive.

1.5 Premature haematopoietic ageing in Hutchinson-Gilford Progeria Syndrome (HGPS)

In HGPS, aberrant splicing of LMNA gene (encoding both lamin A and lamin C) leads to nuclear assembly of the truncated protein, prelamin A (progerin) (De Sandre-Giovannoli et al., 2003; Eriksson et al., 2003). Certain hallmarks of haematopoietic ageing in mice, such as increased platelet counts, have been observed in HGPS (Merideth et al., 2008). Interestingly, cells ageing naturally also express increased levels of progerin (Scaffidi and Misteli, 2006), raising the possibility that normal physiological conditions and progeria might share similar ageing mechanisms. Dr. Grigoryan et al. recently reported that HSCs deficient of LMNA display premature ageing-like phenotype (Grigoryan et al., 2018), suggesting a prominent role of lamin A/C in haematopoiesis at the level of HSCs. The strong impact of progeria on growth and sexual maturation might be paralleled with its influences on HSCs, since growth hormones and sex hormones regulate HSC proliferation and lineage commitment (Heo et al., 2015; Stewart et al., 2014). However, it is unclear which lamin isoforms (A or C) are expressed by HSCs and whether HSCs express progerin. In this regard, it remains unknown whether premature haematopoietic ageing in HGPS exists and whether it is a consequence of progerin accumulation in HSCs, other haematopoietic cells and/or the microenvironment. $Lmna^{G609G}$ knock-in mice ($Lmna^{G609G/G609G}$) display key features of the human disease, including accelerated ageing, shortened lifespan, and bone and cardiovascular defects (Hamczyk et al., 2018; Osorio et al., 2011; Villa-Bellosta et al., 2013). Our lab and collaborators have discovered that $Lmna^{G609G/G609G}$ mice exhibit myeloid/platelet-bias in the circulation, but the phenotype is not reproduced in wild-type (WT) recipients carrying $Lmna^{G609G/G609G}$ BM cells (Ho et al., 2019). These results suggest that

myeloid-skewing in progeroid mice might not be driven by HSC-autonomous defects.

1.6 Myeloproliferative neoplasms (MPNs)

MPNs are blood disorders with uncontrolled expansion of haematopoietic and myeloid progenitor cells (Nangalia et al., 2016). Three MPN subtypes, the polycythaemia vera (PV), essential thrombocythaemia (ET), and primary myelofibrosis (PMF) have been identified. PV is characterized by an elevation of red blood cells. ET is associated with high platelet counts in the peripheral blood concomitant with Mk hyperplasia in the BM. PMF is characterised by Mk hyperplasia and BM/spleen fibrosis, extramedullary haematopoiesis and leucocytosis (Vytrva et al., 2014). It has been reported that Mks in ET and PMF share common features, including atypical cluster formation, endosteal translocation and dysregulation of intrinsic pathways (Malherbe et al., 2016). However, the morphology of Mks is largely different in the two MPN subtypes. Mks in ET are reported to be giant, with staghorn-like nuclei, whereas Mks in PMF appear to be immature, characterized by cloud-shape nuclei and high nuclear/cytoplasmic ratio (Thiele et al., 2011). Emerging evidence has indicated that the increased numbers of Mks lead to myelofibrosis (Bain, 2010). Through the interaction with the BM niches, the pro-inflammatory cytokines TGF-β, PDGF, and bFGF are released from Mk α-granules and stimulate fibrotic tissue formation and osteoclerosis (Agarwal et al., 2016). These observations suggest that aberrant Mk phenotypes are a hallmark of MPNs and that abnormal megakaryopoiesis plays critical roles in MPN pathogenesis.

MPNs are driven by somatic mutations in the HSC compartment. A point mutation of G>T at the 617 position in exon 14 of the gene JAK2 (janus kinase 2) is a hallmark of MPNs. The majority of MPN patients are found with JAK2(V617F) mutation, with a frequency of 95 % in PV and 50-60 % in ET and PMF. Other mutations, such as CALR and MPL, are only specific to ET and PMF

patients (Kim et al., 2015) and similar to JAK2 mutations involve constitutive JAK-STAT activation. Despite acquired mutations being the main drivers of MPNs, the fact that PV and ET may develop into PMF suggests that disease progression also pivots on microenvironment. Accumulating evidence has indicated that malignant HSCs can alter the BM microenvironment, favouring disease progression (Korn and Mendez-Ferrer, 2017). This raises the possibility of targeting HSC niche in MPN therapy. In 2014, a paper published by our group demonstrated that neuropathy of HSC niche triggered by mutant HSCs contributes to MPN pathogenesis (Arranz et al., 2014). Sympathetic nerve fibres and Nestin-GFP$^+$ cell numbers are found to be significantly reduced in MPN patients and MPN murine model. Time-course analysis indicated that impaired SNS precedes apoptosis of Nestin-GFP$^+$ cells. Co-culture experiments *in vitro* further confirmed that IL-1β is responsible for neuroglial damage, which diminishes the number of Nestin-GFP$^+$ cells. Disease acceleration (particularly increased Mk expansion leading to myelofibrosis) was found upon nestin+ cell depletion or in β3-AR-deficient mice, suggesting that loss of β_3-AR or compromised Nestin-GFP$^+$ cells stimulates MPN progression. Strikingly, chronic treatment with neuroprotective agent or β_3-AR agonist blocks MPN progression in mice, as evidenced by reduced BM fibrosis and restored platelet/leukocyte counts in the peripheral blood. These results shed light on the idea that MPN progression is not only caused by HSCs alone, but also by alterations of the HSC niche. Improved reticulin fibrosis correlated with rescue of Nestin-GFP$^+$ niches has been recently reproduced in a multicentre Phase-II clinical study addressing the possible use of β_3-AR agonists in MPN patients (Drexler et al., 2019), but this treatment did not change mutant allele burden over 6 months. Overall, these data suggest that compensation of BM neuropathy might be a novel therapeutic strategy for MPNs. Nevertheless, how the unique neuro-MSC circuit affects

malignant megakaryopoiesis/thrombopoiesis in MPN requires further investigation.

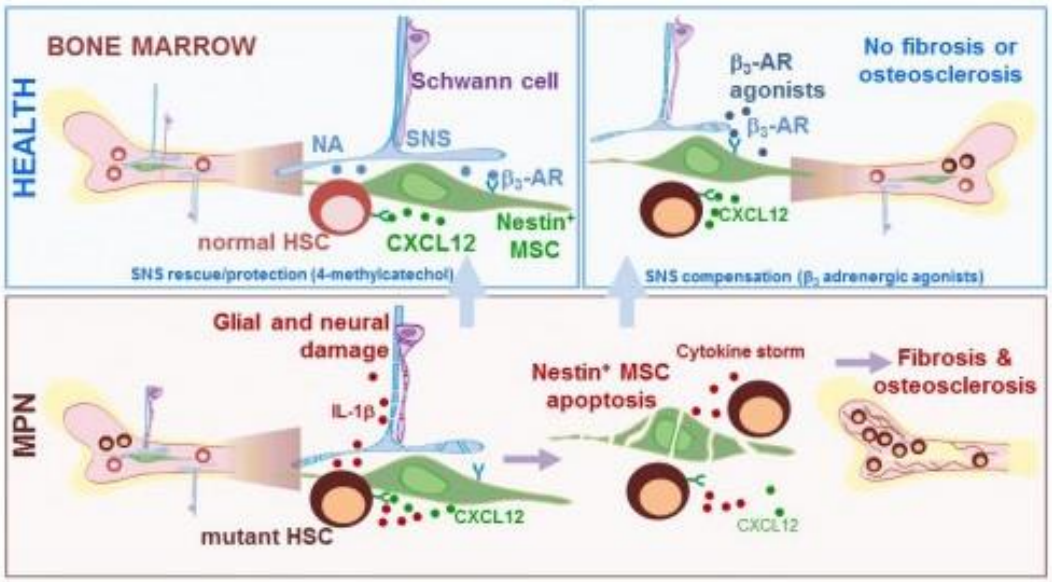

Figure 8. Neuropathy of BM microenvironment is essential for MPN progression.
Mutant HSC-derived IL-1β causes BM glial and neural damage, leading to Nestin-GFP$^+$ MSC apoptosis and accelerating disease progression. (Image taken from Arranz et al. Nature 2014.)

2. Rationale

Haematopoiesis is tightly controlled by HSC-intrinsic mechanisms and the microenvironmental cues under both homeostasis and stress conditions. The SNS controls HSC traffic through activating β-ARs and nicotinic receptors, but whether other HSCs functions are regulated in response to neuronal inputs is poorly understood. A recent publication reports that BM Th^+ sympathetic nerve fibres are decreased in old mice, and sympathetic denervation results in haematopoietic ageing in a β_3-AR-dependent manner. However, our group found increased BM sympathetic nerve fibres during ageing, which is consistent with the well-known increase of sympathetic activity in the elderly. The present study thus aims to investigate the roles of the BM microenvironment and its neural regulation in murine haematopoiesis during ageing and age-associated MPNs. The study will focus on addressing HSC myeloid/megakaryocytic-biased differentiation, and further extend the findings from normal physiological ageing to the treatment of age-related pathological conditions, such as HGPS and MPNs.

3.Materials and Methods

3.1 Mouse strains

Young (or adult) mice were analysed between 8-30 weeks of age, and old mice were 66-120 weeks old. Mice were housed in specific pathogen free facilities. All experiments using mice followed protocols approved by the Animal Welfare Ethical Committees, according to EU and United Kingdom Home Office regulations (PPL 70/8406). Nes-gfp (Mignone et al., 2004), Adrb2-/- (Chruscinski et al., 1999), FVB/N-Adrb3tm1Lowl/J (Susulic et al., 1995), Lmnatm1.1Otin (Osorio et al., 2011), Vwf-eGFP (Sanjuan-Pla et al., 2013), B6.129S4- Nos1tm1Plh/J (stock#2986) (Huang et al., 1993), B6.129S2-Il6tm1Kopf/J (stock#2650) (Kopf et al., 1994) (Jackson Laboratories), Mx1-cre;JAK2-V617 (Arranz et al., 2014), Tg(CAG-DsRed*MST)1Nagy/J (Stock No: 005441, Jackson Laboratories) and congenic CD45.1 and CD45.2 C57BL/6 mice (Charles River Laboratories) were used in this study.

Nomenclature	**Name (in the thesis)**
Nes-gfp	Nestin-GFP
Adrb2tm1Bkk/J	*Adrb2*$^{-/-}$
Adrb3tm1Lowl	*Adrb3*$^{-/-}$
Lmnatm1.1Otin	*Lmna*$^{G609G/G609G}$
Mx1-cre;JAK2-V617	Mx1-cre;JAK2(V617F)
Tg(CAG-DsRed*MST)1Nagy/J	DsRed
Vwf-eGFP	Vwf-eGFP
Nos1tm1Plh/J	*Nos*$^{-/-}$
Il6tm1Kopf/J	*IL6*$^{-/-}$
C57BL/6-Tg(UBC-GFP)30Scha/J	

Table 1. List of mouse strains.

3.2 Mouse studies

3.2.1 Reverse chimera experiments of WT, *Adrb2*$^{-/-}$ or *Adrb3*$^{-/-}$ mice

To generate chimeric mice carrying *Adrb2*$^{-/-}$ or *Adrb3*$^{-/-}$ BM cells, two-month-old C57BL/6 mice were lethally irradiated (12 Gy, two split doses) and i.v. transplanted with 2 X 10^6 nucleated BM cells from two-month-old WT, *Adrb2*$^{-/-}$ or *Adrb3*$^{-/-}$ mice. To test microenvironment-dependent effects of β-adrenergic signalling, WT, *Adrb2*$^{-/-}$ or *Adrb3*$^{-/-}$ (CD45.2) mice were lethally irradiated (12 Gy, two split doses) and i.v. transplanted with 2 X 10^6 nucleated BM cells from CD45.1 C57BL/6 mice. Haematopoietic cells in the BM were analysed 4 months after transplantation in both settings.

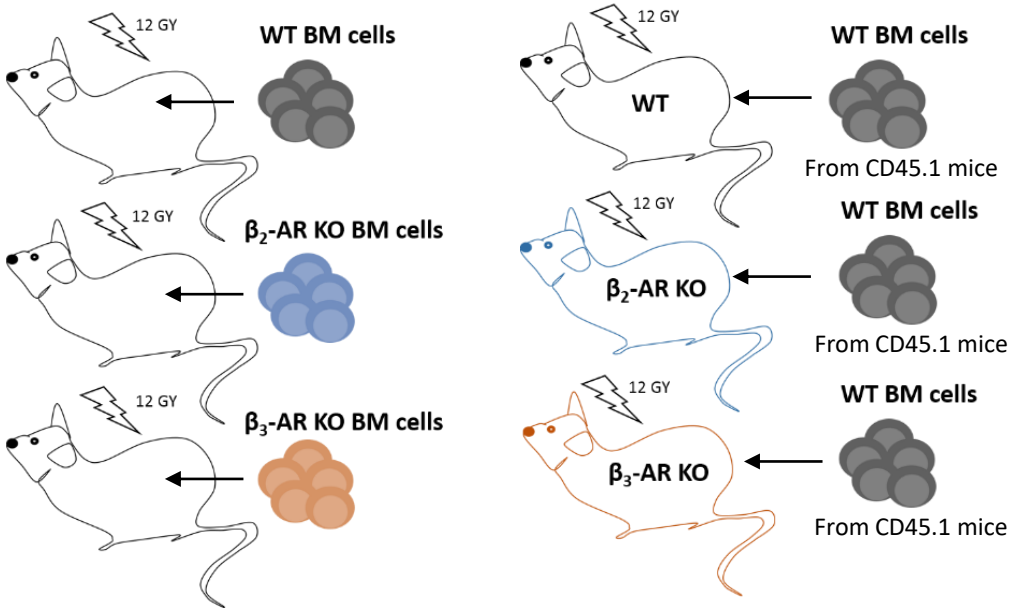

Figure 9. Scheme of reverse chimera experiments of WT, *Adrb2*$^{-/-}$ or *Adrb3*$^{-/-}$ mice.

3.2.2 Chronic treatment of progeroid mice with β3-AR agonist

For progeria studies, the selective β3-AR agonist BRL37344 (Sigma, St. Louis, MO) was administered at 2mg/kg through intraperitoneal (i.p.) injection once per day. Vehicle (saline solution) daily injections were performed in the same way. Treatment was initiated when *Lmna*$^{G609G/G609G}$ mice were 7 weeks old and lasted for 8 weeks. The experiment was collaboratively performed by Cristina Gonzalez-Gomez (research assistant in Vicente Andres's group, Centro Nacional de Investigaciones Cardiovasculares (CNIC), Spain).

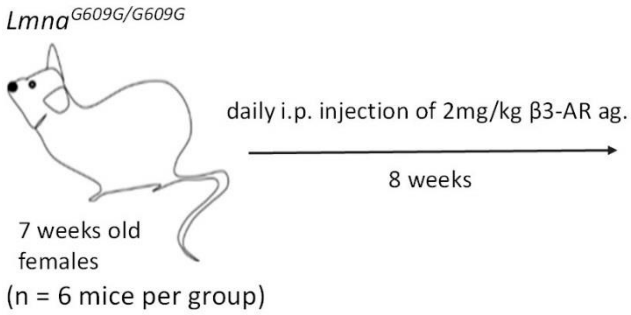

Figure 10. Scheme of progeroid mice treated with β3-AR agonist.

3.2.3 Chronic treatment of MPN mice with β3-AR agonist

For MPNs studies, Mx1cre;JAK2 (V617F) mice were given selective β3-AR agonist BRL37344 (Sigma, St. Louis, MO) at 2mg/kg through intraperitoneal (i.p.) injection twice per day. Vehicle (saline solution) daily injections were performed in the same way. Treatment lasted for 2 months. WT or *Adrb3*$^{-/-}$ mice were lethally irradiated (12 Gy, two split doses) and i.v. transplanted with 2 X 10^6 nucleated BM cells from Mx1cre;JAK2 (V617F) mice. The experiments were performed by Dr. Lorena Arranz (previous postdoctoral associate in the lab). Long bones were taken for immunofluorescence of Mks, performed by the author of this thesis. H&E staining was performed by the pathologists, and the sections were analysed by the author of this thesis.

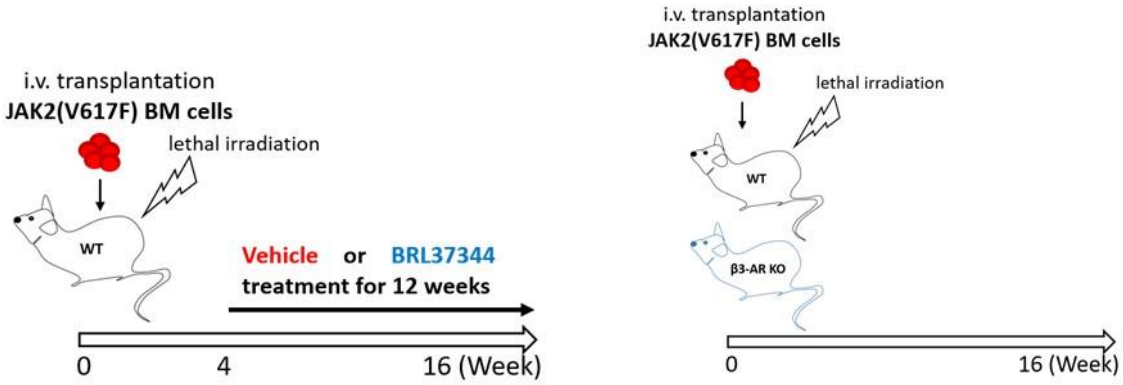

Figure 11. Scheme of MPN mice treated with β3-AR agonist, or β3-AR deficient mice transplanted with MPN BM cells.

3.3 Human studies

The SAKK 33/14 trial (NCT02311569) was planned and conducted in accordance with the Declaration of Helsinki, the Guidelines for Good Clinical Practice (GCP) issued by ICH and requirements of the respective national regulatory authorities. The local ethics committees of all participating centres gave approval to the trial and written informed consent was obtained from all patients prior to enrolment. Immunohistochemistry was performed by the pathologists, and the sections were analysed by the author of this thesis.

3.4 Murine BM cell extraction and flow cytometry analysis

Endosteal (e) and non-endosteal (n-e) BM fractions were isolated and analysed separately in this study, unless otherwise specified. Murine long bones were flushed gently to obtain single cell suspensions less tightly associated with the bone, which contain non-endosteal haematopoietic cells. The flushed-bones were then crushed in a mortar and filtered through a 40-mm strainer to obtain endosteal haematopoietic cells. Cells from both fractions were depleted of red blood cells by lysis in 0.15M NH4Cl for 10 min at 4℃. Cells were incubated with the appropriate dilution (2-5 mg/ml) of fluorescent antibody conjugates and 4',6-diamidino-2-phenylindole (DAPI) for dead cell exclusion, and analysed on LSRFortessa flow cytometer (BD Biosciences, Franklin Lakes, NJ) equipped with FACSDiva Software (BD Biosciences). The following antibodies were used: fluorescent CD45.1 (A20), CD45.2 (104), B220 (RA3-6B2), CD11b (M1/70), CD3ε (145-2C11), Ly-6G (1A8), sca-1 (E13-161.7), biotinylated lineage antibodies (CD11b, Gr-1, Ter119, B220, CD3ε) (BD Biosciences), c-kit (2B8) (eBioscience), CD150 (TC15-12F12.2), CD34 (RAM34) and CD41 (MWReg30) (BioLegend). Biotinylated antibodies were detected with fluorochrome conjugated streptavidin (BD Biosciences). Long-term HSCs (LT-HSCs) are immunophenotypically defined as $lin^-sca\text{-}1^+c\text{-}kit^+CD34^-CD150^+CD41^-$ cells. Myeloid-biased HSCs are immunophenotypically defined as $lin^-sca\text{-}1^+c\text{-}kit^+CD34^-CD150^+CD41^+$ cells. Lymphoid-biased HSCs are immunophenotypically defined as $lin^-sca\text{-}1^+c\text{-}kit^+CD34^-CD150^-CD41^-$ cells. $CD41^+$ LSK cells are immunophenotypically defined as $lin^-sca\text{-}1^+c\text{-}kit^+CD41^+$ cells. MkPs are immunophenotypically defined as $lin^-sca\text{-}1^-ckit^+$ $CD150^+CD41^+$ cells. Granulocytes are immunophenotypically defined as $CD45^+Ly\text{-}6G^+CD11b^+$ cells. B lymphocytes are immunophenotypically defined as $CD45^+B220^+$ cells.

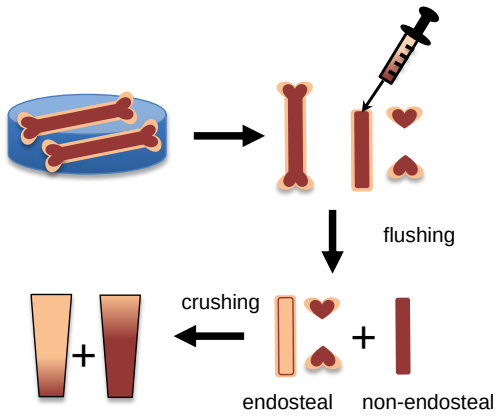

Figure 12. Scheme of endosteal and non-endosteal BM isolation from mouse long bones. (Image illustrated by Justyna Rak)

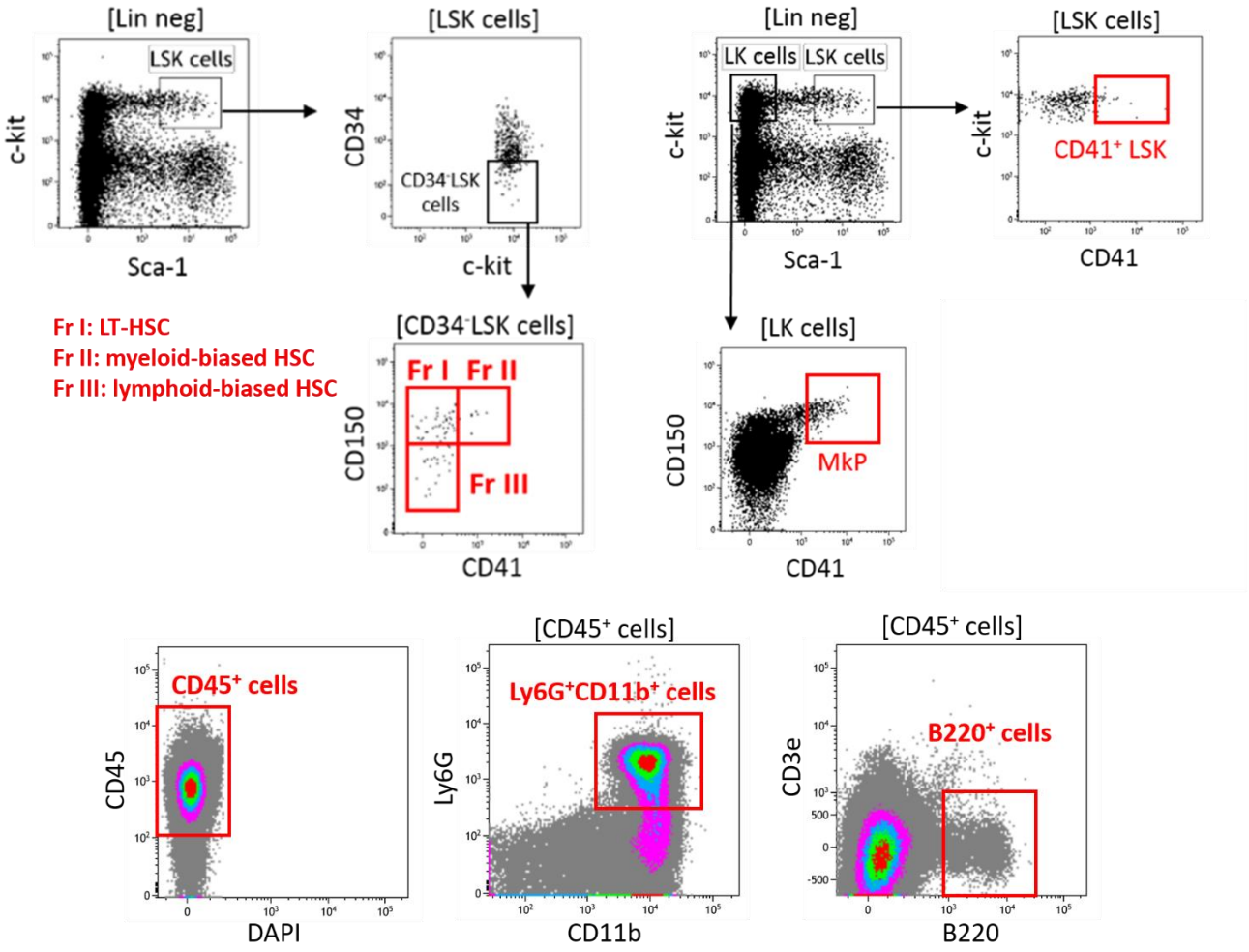

Figure 13. Flow cytometry graphs of haematopoietic populations.

Antibody (clone)	Supplier	Dilution
CD45.1 (A20)	BD Biosciences	1:200
B220 (RA3-6B2)	BD Biosciences	1:200
CD11b (M1/70)	BioLegend	1:200
CD3ε (145-2C11)	TONBO Biosciences	1:200
Ly-6G (RB6-(C5)	BioLegend	1:200
sca-1 (E13-161.7)	BioLegend	1:200
biotinylated lineage antibodies (CD11b, Gr-1, Ter119, B220, CD3ε)	BD Biosciences	1:100
c-kit (2B8)	eBioscience	1:200
CD150 (TC15-12F12.2)	BioLegend	1:200
CD34 (RAM34)	BD Biosciences	1:100
CD41 (MWReg30)	BioLegend	1:200
Brilliant Violet 510™ Streptavidin	BioLegend	1:400

Table 2. List of antibodies used for flow cytometry.

3.5 Cell culture

3.5.1 HPC-7 cells coculture with MS-5 stromal cells

HPC-7 cells were maintained in IMDM medium supplemented with 10% FCS and 100 ng/ml of mSCF (PeProTech 250-03). MS-5 cells were maintained in α-MEM medium supplemented with 10% FCS. To induce Mk differentiation, HPC-7 cells were cultured with or without MS-5 stromal cells in StemSpan H3000 medium, supplemented with 50 ng/ml of TPO (PeProTech 300-18) and 2U/mL of erythropoietin (EPO) (R&D 287-TC-500) up to 4 days. 10 mM of BRL37344 (β3-AR agonist; Sigma B169), 10 mM of clenbuterol (β2-AR agonist; Sigma C5423), 5 mM of H-89 (Protein kinase A inhibitor; Sigma B1427) and vehicle controls were added to the culture. To examine Mk differentiation, cells were incubated with anti-c-kit-FITC antibody (1:200, BD PharMingen 553354) and anti-CD41-PE antibody (1:200, BD PharMingen 558040). DAPI was added at 1:10,000 to discriminate dead cells. Samples were analysed by Gallios flow cytometer (Beckman Coconulter).

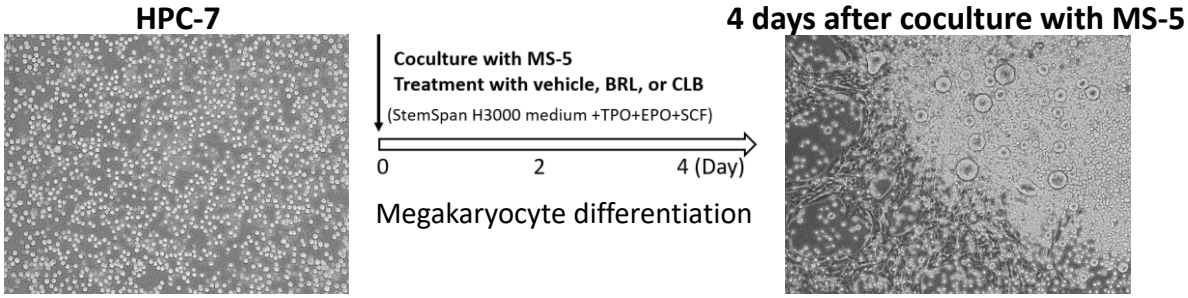

Figure 14. Scheme of HPC-7 cells coculture with MS-5 stromal cells.

3.5.2 Human cord blood-derived HSPCs coculture with MS-5 stromal cells

Human umbilical cord blood $CD34^+$ HSPCs were isolated using a CD34 Microbead kit (Miltenyi Biotec 130-046-702) following manufacturer's instructions, and were cultured with MS-5 stromal cells in Cellgro medium (CellGenix cat. no. 20802-0500), supplemented with 50 ng/ml of TPO (PeProTech 300-18) and 5 ng/ml of IL-1β (Cellgenix 1411-050) for 7-10 days, during which vehicle, 10 mM of BRL37344 (β3-AR agonist; Sigma B169) or 10 mM of clenbuterol (β2-AR agonist; Sigma C5423) were added to the culture. Cellgro medium was refreshed at day3 and day7 of the coculture. To examine Mk differentiation, cells were fixed and stained with anti-human CD61 antibody (Serotec MCA 728).

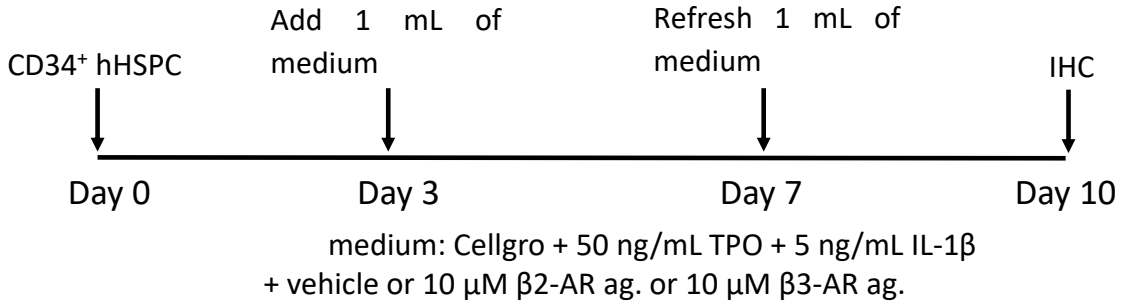

Figure 15. Scheme of human cord blood-derived $CD34^+$ HSPCs coculture with MS-5 stromal cells.

3.5.3 Lin$^-$ haematopoietic progenitors coculture with young and old primary murine stromal cells

Haematopoietic progenitors were immunomagnetically enriched from DsRed;Vwf-eGFP mouse BM by using lineage depletion cocktail (BD Biosciences). To isolate primary stromal cells, long bones from young or old mice were crushed with PBS in a mortar. Cell fractions were digested in 2 ml of collagenase type I (Stem Cell Technologies, cat. No. 07902) for 30 min at 37°C with agitation. The enzyme was quenched by adding 18 ml PBS/2%FCS. Cell suspensions were filtered, pelleted and red blood cell lysis was performed as stated above. Cells were then cultured in α-MEM medium supplemented with 20% FCS for at least 14 days until a confluent culture was formed. Lin$^-$ haematopoietic progenitors were cocultured with primary stromal cells in Cellgro medium (CellGenix cat. no. 20802-0500), supplemented with 50 ng/ml of TPO (PeProTech 300-18) and 5 ng/ml of IL-1β (Cellgenix 1411-050) for 4 days, during which vehicle or 10 mM of clenbuterol (β2-AR agonist; Sigma C5423) were added to the culture. Mk differentiation was examined by the frequency of DsRed$^+$Vwf-eGFP$^+$ cells in total DsRed$^+$ cells. Samples were analysed by LSRFortessa flow cytometer (BD Biosciences, Franklin Lakes, NJ).

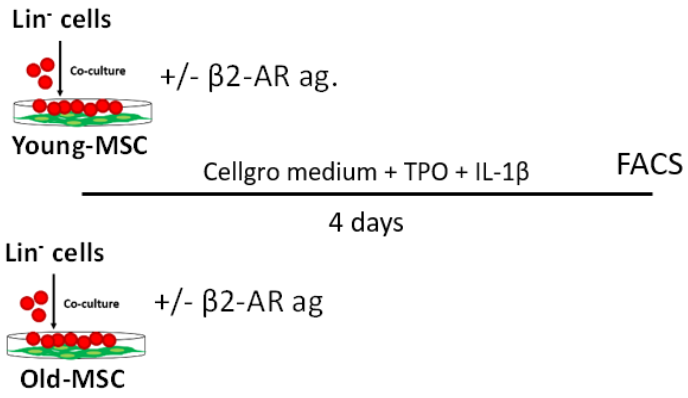

Figure 16. Scheme of Lin$^-$ haematopoietic progenitors coculture with young or old stromal cells.

3.5.4 Long-term mouse BM primary culture

For mouse BM long-term culture, femurs and tibias were flushed gently to obtain BM cells. Cells were seeded and cultured in MyeloCult M5300 medium (StemCell Technologies, cat. no. 05350) supplemented with 10^6 M hydrocortisone (Stem-Cell Technologies, cat. no. 07904) at 33℃ for 14 days. Half of the medium was refreshed at day 7. At day 14 of culture, half of the medium was refreshed again, supplemented with 50 ng/ml of TPO (PeProTech 300-18) for extra 4 days, during which vehicle, 10 mM of BRL37344 (β3-AR agonist; Sigma B169), 10 mM of clenbuterol (β2-AR agonist; Sigma C5423), or 100 mM of L-VINO (Insight Biotechnology 728944-69-2) were added to the culture. At day 18 of culture, cells were collected and subjected to flow cytometry analysis by LSRFortessa flow cytometer (BD Biosciences, Franklin Lakes, NJ).

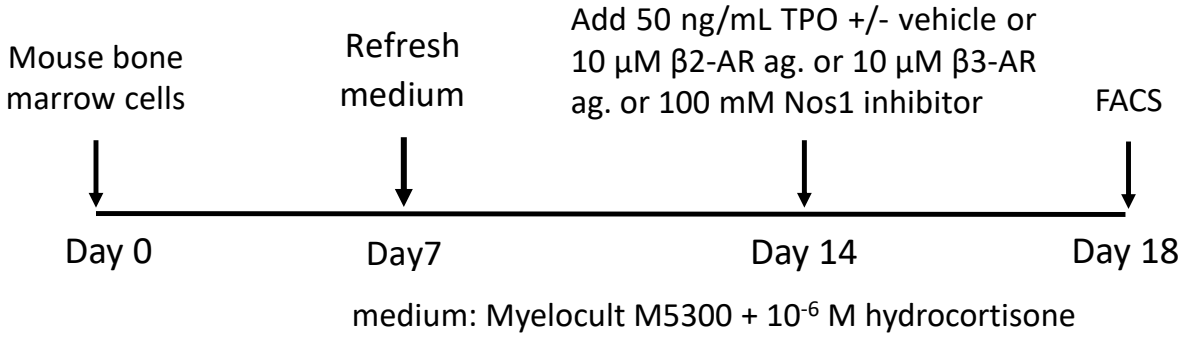

Figure 17. Scheme of long-term mouse BM primary culture.

Chemical/Cytokine	Supplier	Final concentration
mSCF	PeProTech	100 ng/ml
TPO	PeProTech	50 ng/ml
EPO	R&D	2U/mL
IL-1β	Cellgenix	5 ng/ml
hydrocortisone	Stem-Cell Technologies	10^6 M
BRL37344 (β3-AR agonist)	Sigma-Aldrich	10 mM
H-89 (PKA inhibitor)	Sigma-Aldrich	5 mM
Clenbuterol hydrochloride (β2-AR agonist)	Sigma-Aldrich	10 mM
L-VINO (Nos-1 inhibitor)	Insight Biotechnology	100 mM

Table 3. List of chemicals/cytokines used for *in vitro* culture.

3.6 Immunofluorescence staining

Murine long bones were isolated and quickly fixed in 2% paraformaldehyde (PFA) solution overnight at 4℃. Tissues were rinsed with PBS, and decalcified in 0.25 M ethylenediaminetetraacetic acid (EDTA) solution at 4℃ for 14 days. After decalcification, tissues were cryo-preserved with 15% sucrose solution for 12 h at 4℃, followed by 30% sucrose solution for 12 h at 4℃. After cryopreservation, tissues were embedded in optimal cutting temperature (OCT) compound, and subjected to cryosection. Immunofluorescence staining of cryostat sections was performed as previously described (Isern et al., 2014), with minor modifications. Briefly, whole-mount thick sections or thin sections were blocked with TNB buffer (0.1 M Tris–HCl, pH 7.5, 0.15 M NaCl, 0.5% blocking reagent, Perkin Elmer) for 1 h at RT. Primary antibody incubations were conducted for 2 h at RT or overnight at 4℃. Secondary antibody incubations were conducted for 1 h at RT. Repetitive washes were performed with PBS or PBS + 0.05% Triton X-100. Stained samples were counterstained for 10 mins with 5 mM DAPI and rinsed with PBS. Slides were mounted in Vectashield Hardset mounting medium (Vector Labs) and sealed with nail polish. Whole-mount tissues were stored in PBS. Details of specific staining used in this study are described below:

3.6.1 Whole-mount immunofluorescence staining of murine BM vasculature

For whole mount staining of vasculature, tibia or femur BM thick sections were obtained with a cryostat and remaining OCT was removed by PBS washes. Samples were blocked and permeabilized in 0.1% Triton X-100 (Sigma) TNB overnight at 4℃. On the next day, samples were incubated with goat anti-CD31 (R&D AF3628 1:100), and rat anti-EMCN (Insight Biotechnology sc-65495

1:100) diluted in 0.1% Triton X-100 TNB overnight at 4°C. Samples were rinsed with 0.05% Triton X-100 PBS for 8 hours and incubated overnight with secondary antibodies, including Dylight650 donkey anti-rat IgG (Thermo Fisher SA5-10029; 1:300) and Cy3-donkey anti-goat IgG (Jackson 705-165-147, 1:300) diluted in TNB. Samples were rinsed with 0.05% Triton X-100 PBS for 4 hours, washed with PBS and counterstained with DAPI (Sigma; 1:1000) to label cell nuclei. Images were acquired with Leica SP5 confocal microscope using 10x objectives and analysed with ImageJ. At least 3 independent and randomly selected BM areas were imaged and analysed per sample. For quantification of sinusoidal vessel area, $EMCN^+$ area >150 mm distant to the bone surface was measured and normalized to BM area. Arteriolar (> 6 mm diameter) and capillary (< 6 mm diameter) $CD31^{hi}EMCN^-$ vessel number was counted and normalized to BM area. To quantify TZVs, $CD31^{hi}EMCN^{hi}$ area < 150 mm close to the bone surface was quantified and normalized to the bone surface length.

3.6.2 Immunofluorescence staining of murine BM Mks and MkPs

For staining of Mks and MkPs, BM femur thin sections were blocked with TNB for 1h at RT. Samples were then incubated with primary antibodies for 2 h at RT or overnight at 4C, followed by secondary antibodies incubation for 1h at RT. Finally, samples were counterstained with DAPI to label cell nuclei. Repetitive washes were performed with PBS. At least 3 independent and randomly selected BM areas were imaged and analysed by ImageJ. The following primary antibodies were used: CD41 (1:200, PE conjugated rat monoclonal antibody, BD PharMingen 558040), CD42d (1:100, APC conjugated armenian hamster monoclonal antibody, eBioscience 17-0421-80) and c-kit (1:100, goat polyclonal antibody, R&D AF1356). The following secondary antibodies were used: Alexa

Fluor 647 Goat-anti-armenian hamster IgG (1:200, Abcam ab173004) and Alexa Fluor 647 donkey-anti-goat IgG (1:200, Life Technologies A21447).

3.6.3 Immunofluorescence staining of murine BM Mks and vasculature

For staining of Mk localization relative to sinusoids, BM femur thin sections were blocked with 0.1% Triton X-100 TNB for 1h at RT. Samples were then incubated with rat anti-EMCN (Insight Biotechnology sc-65495 1:100) antibody diluted in 0.1% Triton X-100 TNB overnight at 4℃. On the next day, samples were incubated with Alexa Fluor 647 goat-anti-rat IgG (1:200, Life Technologies, cat. no. A21247) secondary antibody for 1h at RT, followed by rat serum blocking (1:10 rat serum in 0.05% Triton X-100 TNB) for 10 min. Samples were incubated with third antibody, CD41 (1:200, PE conjugated rat monoclonal antibody, BD PharMingen 558040) for 2h at RT. Finally, samples were counterstained with DAPI to label cell nuclei. Repetitive washes were performed with PBS or 0.05% Triton X-100 PBS. At least 3 independent and randomly selected BM areas were imaged and analysed by ImageJ.

3.6.4 Immunofluorescence staining of murine BM Mks and HSCs

For HSCs and Mks staining, BM femur thin sections were blocked with TNB for 1h at RT and followed by Avidin/biotin blocking. Samples were then incubated with rat anti-CD150 (1:50, Biolegend Cat. No. 115902) and Armenian hamster anti-CD42d (1:100, eBioscience 17-0421-80) primary antibodies overnight at 4℃. On the next day, samples were incubated with Alexa Fluor 555 goat-anti-rat IgG (1:200, Life Technologies A21434) and Alexa Fluor 647 Goat-anti-armenian

hamster IgG (1:200, Abcam ab173004) secondary antibodies for 1h at RT, followed by rat serum blocking (1:10 rat serum in TNB) for 10 min. Samples were re-stained with biotinylated lineage antibodies (1:100, BD Biosciences) for 2h at RT. Finally, samples were incubated with Alexa Fluor 488 Streptavidin-conjugated antibody (1:200, Invitrogen S32354) for 1h at RT and counterstained with DAPI to label cell nuclei. At least 3 independent and randomly selected BM areas were imaged and analysed by ImageJ.

3.6.5 Immunofluorescence staining of human Mks in coculture

For staining of human cord blood-derived $CD34^+$ HSPC co-culture, cells were fixed with 1%PFA for 20mins at RT. After PBS washes, cells were blocked with 10% donkey serum (SigmaD9663) diluted in PBS for 1h at RT, followed by 2h incubation of mouse anti- human CD61 primary antibody (1:500,SerotecMCA728). After PBS washes, cells were incubated with Alexa Fluor 546 donkey-anti mouse IgG (1:200, Life Technologies, cat. no. A10036) secondary antibody for 1h at RT. Finally, samples were counterstained with DAPI to label cell nuclei. 10 independent and randomly selected fields in culture wells were imaged and analysed by ImageJ.

Antibodies	Supplier	Dilution
rat anti-CD150 antibody	Biolegend	1:50
Alexa Fluor 647 goat anti-rat IgG	Life Technologies	1:200
rat anti-EMCN antibody	Insight Biotechnology	1:100
goat anti-CD31 antibody	R&D	1:200
Alexa Fluor 546 Donkey anti-rabbit IgG	Invitrogen	1:200
Dylight650 donkey anti-rat IgG	Thermo Fisher	1:300
Cy3-donkey anti-goat IgG	Jackson	1:300
Rat anti-CD41 (PE conjugated) antibody	BD Pharmingen	1:200
Alexa Fluor 647 donkey-anti-goat IgG	Life Technologies	1:200
Alexa Fluor 647 Goat-anti-armenian hamster IgG	Abcam	1:200
mouse-anti-human CD61 primary antibody	Serotec	1:500
Alexa Fluor 546 donkey-anti-mouse IgG	Life Technologies	1:200
Alexa Fluor 488 Sreptavidin-conjugated antibody	Invitrogen	1:200
Alexa Fluor 555 goat-anti-rat IgG	Life Technologies	1:200
Human/Mouse CD117/c-kit Antibody (Polyclonal Goat IgG)	R&D	1:100
APC conjugated anti-mouse/rat CD42d antibody (armenian hamster IgG)	eBioscience	1:100

Table 4. List of antibodies for immunofluorescence staining.

3.7 RNA isolation and qPCR

RNA isolation was performed using Trizol Reagent (Sigma T9424). Reverse transcription was performed using the High-Capacity cDNA Reverse Transcription kit (Applied Biosystems 4368814), following the manufacturer's recommendations. qPCR was performed using the PowerUp SYBR Green Master Mix (Applied Biosystems A25742) and ABI PRISM7900HT Sequence Detection System. The expression level of each gene was determined by using the absolute quantification standard curve method. All values were normalized with Gapdh as endogenous housekeeping gene.

The following primers (mouse) were used:

NOS1-Fw: ACTGACACCCTGCACCTGAAGA
NOS1-Rv: GTGCGGACATCTTCTGACTTCC
NOS2-Fw: CAGCTGGGCTGTACAAACCTT
NOS2-Rv: CATTGGAAGTGAAGCGGTTCG
NOS3-Fw: CCTCGAGTAAAGAACTGGGAAGTG
NOS3-Rv: AACTTCCTTGGAAACACCAGGG
Gapdh-Fw: GCATGGCCTTCCGTGTTC
Gapdh-Rv: CTGCTTCACCACCTTCTTGAT

Table 5. List of qPCR primer sequences.

3.8 Enzyme-linked immunosorbent assay (ELISA)

MILLIPLEX MAP Mouse Cytokine/Chemokine Magnetic Bead Panel (MCYTOMAG-70K, Merck Millipore) was performed following the manufacture's protocol. BM extracellular fluids of mouse long bones were collected from the supernatants following BM extraction and subjected to the mouse cytokine panel.

3.9 Measurement of nitrate concentration

$NO_{(x)}$ content was measured in freshly-thawed samples (BM extracellular fluids) that had been kept at -80°C for less than 2 months using a nitric oxide analyser (NOA) 280i (Siever, GE Healthcare) according to the manufacturer's instructions. Data were collected, processed and analysed by using liquid software (Siever, GE Healthcare). Samples were prepared by the author of this thesis, and the measurement was performed by Dr. David Macias (research associate in Randall S. Johnson's group, University of Cambridge).

3.10 Statistical analyses

Statistical analyses and graphics were carried out with GraphPad Prism 7 software.

4. Results

4.1 Ageing inflames the BM microenvironment

Investigators (Dr. Justyna Rak, Claudia Korn and Andres Garcia-Garcia) from our lab have demonstrated that BM HSC-supporting niches remarkably alter with age: reduction of endosteal niches, characterised by impaired endosteal vessels, arterioles and their associated Nestin-GFP$^+$ cells; expansion of non-endosteal neurovascular niches, characterised by increased central small capillaries, their associated Nestin-GFP$^+$ cells and Th$^+$ sympathetic nerve fibres. It has been suggested that ageing and inflammation share similar haematopoietic alterations, such as myelopoiesis overriding lymphopoiesis. This myeloid dominance could be a trigger and/or consequence of increased inflammatory cytokines. Upregulation of circulating IL-6, TNFα, IL-1Rα, and C-reactive protein has been reported in the elderly. Increased inflammatory cytokines are known to happen in the circulation, but whether their concentrations follow spatial distribution in different BM niches during ageing has not been directly tested. To address this question, long bones from young and old mice were acquired, subjected to endosteal and non-endosteal BM separation (see section 3.4). Extracellular fluids from both BM fractions were extracted, and the concentration of inflammatory cytokine were measured by milliplex ELISA. In aged mice, the levels of IL-1α and IL-1β are significantly increased (Fig. 18A, C, H, H). IL-6 levels are elevated in endosteal BM (Fig. 18B and G), while IL-3 and IFNγ show similar trends (Fig. 18D, E, I and J). These results suggest that ageing not only up-regulates inflammatory cytokines in the circulation, but it also inflames the BM microenvironment, which might directly impact haematopoiesis.

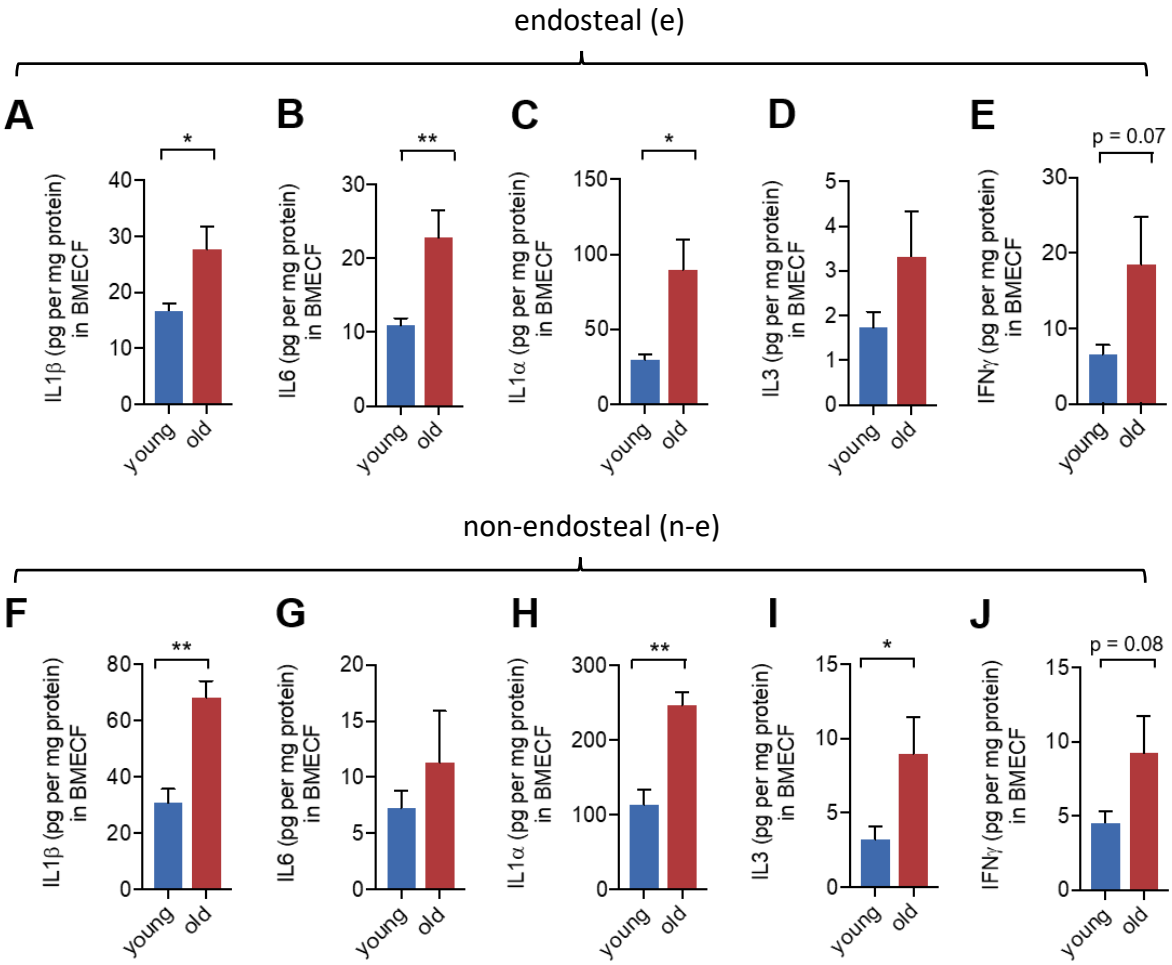

Figure 18. Ageing correlates with BM inflammation.
(A–J) Concentration of (A, F) IL-1b, (B, G) IL-6, (C, H) IL-1a, (D, I) IL-3, and (E, J) IFNγ in endosteal BM (A-E) or non-endosteal BM (F-J) extracellular fluid (BMECF) from young WT mice (n = 5) and old WT mice (n = 4). Data are means ± SEM. *p < 0.05; **p < 0.01. Unpaired two-tailed t test.

4.2 β-adrenergic signalling regulates megakaryopoiesis during ageing

Given that BM Th^+ fibres are expanded in aged mice, it is hypothesised that increased noradrenergic signalling might contribute to HSC ageing. To test the hypothesis, young and old mice lacking β2- and β3-ARs, two of the most important receptors transducing sympathetic nerve signals in the BM, were studied. Compared to young mice, old mice exhibit elevated platelet counts and increased frequency of peripheral granulocytes/monocytes paralleled with decreased percentage of lymphocytes in white blood cells, which confirms ageing of the haematopoietic system. Interestingly, platelet counts are normalised in old mice lacking both β2 and β3-ARs (double knockout, DKO) (Fig. 19L). Other peripheral blood parameters remained unchanged (Fig. 19M-P), suggesting that β-adrenergic signals might specifically regulate the megakaryocytic lineage. To examine BM Mks, immunofluorescence staining of $CD41^+CD42^+$ cells was performed. The numbers of $CD41^+CD42^+$ cells are significantly increased in old WT mice (compared to young WT mice), but are restored in old DKO mice (Fig. 19A-D and I). Old Mks undergo drastic morphological changes, with increased formation of proplatelet-like protrusions or cytoplasmic fragmentations. These features, correlated with increased apposition of Mks to the sinusoids, indicate promoted thrombopoiesis in aged BM (Fig. 19A-D). However, Mks in old DKO mice neither shows similar extent of proplatelet formation (PPF) (Fig. 19J), nor abnormal physical contact with sinusoids (Fig. 19E-H and K), suggesting that increased thrombopoiesis (a feature of old WT mice) is mitigated in old DKO mice. Undifferentiated myeloid/megakaryocyte progenitors originally sit near the endosteal surface, moving to central marrow as they differentiate and mature. To investigate Mk differentiation at the early progenitor level, BM cells from endosteal and non-endosteal fractions were isolated, respectively, and subjected

to flow cytometry analysis. In both fractions, the frequency of $CD41^+$ cells within the LSK population is increased by 5-fold in old WT mice. In contrast to old WT mice, however, the frequency of $CD41^+$ cells is much lower in old DKO mice, manifest in the endosteal BM (Fig. 19Q-S). Similarly, the numbers of $CD41^+ckit^+$ myeloid/megakaryocyte progenitors are doubled in the endosteal regions in old WT mice, but normalised in old DKO mice (Fig. 19T-X). Altogether, the results indicate that lack of β-adrenergic signalling in the BM affects megakaryopoiesis during ageing.

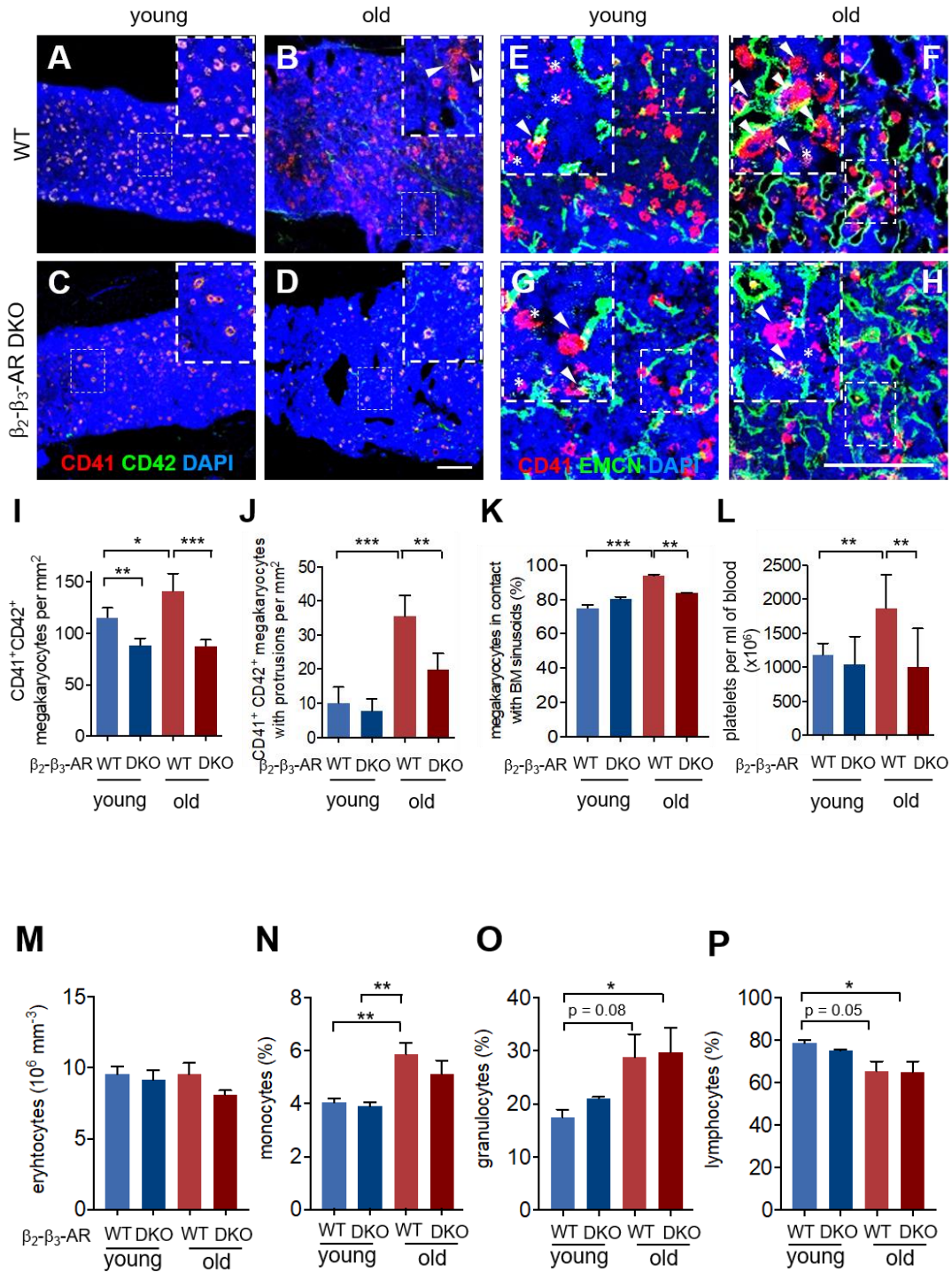
young
old
young
old
WT
β2-β3-AR DKO
A
B
E
F
C
D
G
H
CD41 CD42 DAPI
CD41 EMCN DAPI
I
J
K
L
CD41+CD42+ megakaryocytes per mm2
CD41+ CD42+ megakaryocytes with protrusions per mm2
megakaryocytes in contact with BM sinusoids (%)
platelets per ml of blood (x10^6)
β2-β3-AR WT DKO WT DKO
young old
M
N
O
P
eryhtocytes (10^6 mm^-3)
monocytes (%)
granulocytes (%)
lymphocytes (%)
p = 0.08
p = 0.05

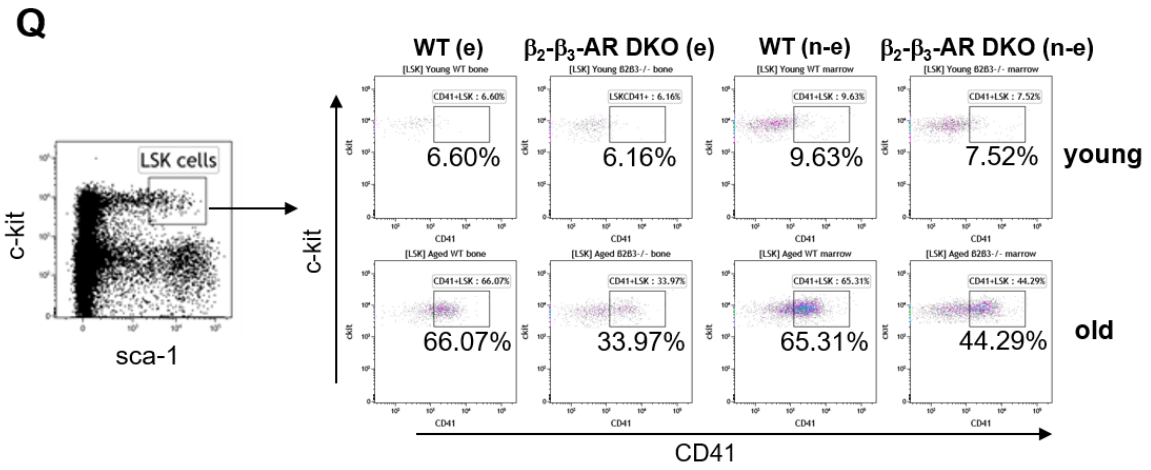
Q
WT (e)
β2-β3-AR DKO (e)
WT (n-e)
β2-β3-AR DKO (n-e)
LSK cells
c-kit
sca-1
CD41
young
old
6.60%
6.16%
9.63%
7.52%
66.07%
33.97%
65.31%
44.29%

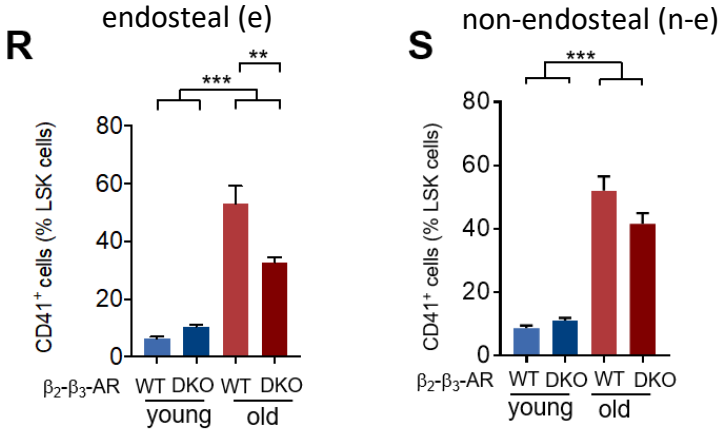
R
endosteal (e)
S
non-endosteal (n-e)
CD41+ cells (% LSK cells)
β2-β3-AR
WT DKO WT DKO
young
old

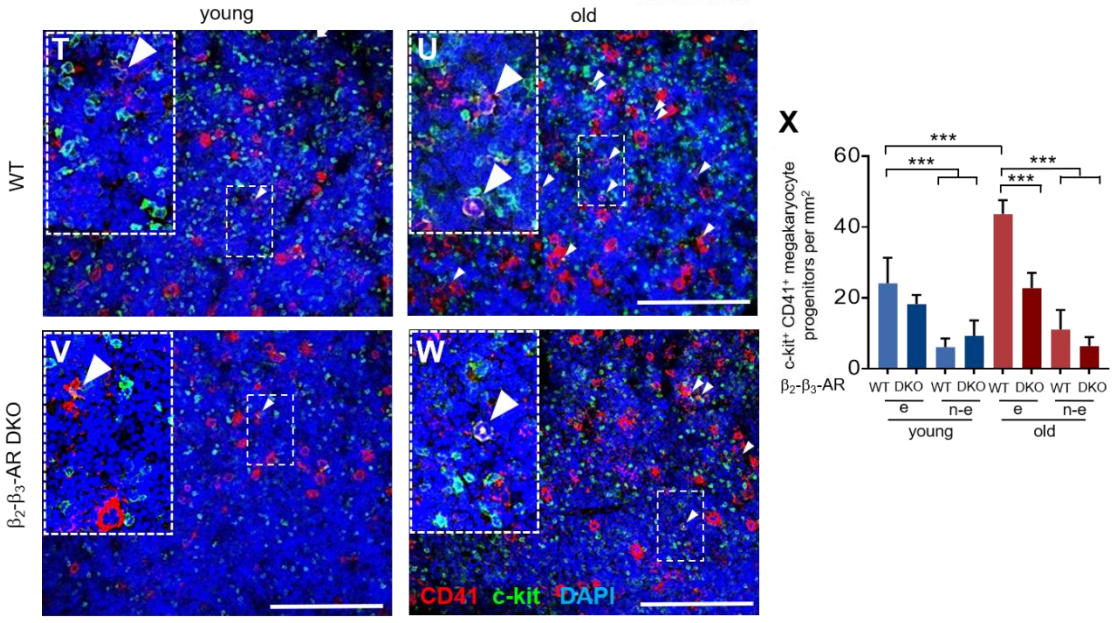
young
old
WT
β2-β3-AR DKO
T
U
V
W
CD41 c-kit DAPI
X
c-kit+ CD41+ megakaryocyte progenitors per mm2
β2-β3-AR
WT DKO WT DKO WT DKO WT DKO
e n-e e n-e
young
old

Figure 19. β-adrenergic signals regulate megakaryopoiesis during ageing. (A–D) Representative immunofluorescence staining for CD41 (red) and CD42 (green) in femoral BM sections of young (A) or old (B) WT mice and young (C) or old (D) *Adrb2*$^{-/-}$*Adrb3*$^{-/-}$ (double knockout [DKO]) mice. Arrowheads depict megakaryocytes with protrusions (CD41+ CD42+ cells with cell body extensions). Scale bar, 250 mm. (I and J) Number of CD41+CD42+ megakaryocytes (I) forming protrusions (J) per BM area (n = 4 young WT; n = 5 young DKO; n = 3 old mice). (E–H) Representative immunofluorescence staining for CD41 (red) and EMCN (green) in femoral BM sections of young (E) or old (F) WT mice and young (G) or old (H) DKO mice, depicting CD41+ megakaryocytes adjacent (arrowheads) or nonadjacent (asterisks) to EMCN+ vasculature. Scale bar, 100 mm. (K) Frequency of CD41+ cells in contact with EMCN+ vasculature (n = 4 young WT; n = 4 young DKO; n = 4 old WT; n = 3 old DKO). (L) Circulating platelets in young (n = 11) and old (n = 6) WT mice, compared with young (n = 9) and old (n = 5) DKO mice. (M) Circulating erythrocytes. (N-P) Frequencies of (N) monocytes, (O) granulocytes and (P) lymphocytes among white blood cells. (Q-S) Representative flow chart (Q) and quantification of the frequency of CD41+ myeloid or megakaryocyte progenitors within lin$^-$sca-1$^+$c-kit$^+$ (LSK) cells in endosteal BM (R) or non-endosteal BM (S) from young WT mice (n = 7), young DKO mice (n = 7), old WT mice (n = 5), and old DKO mice (n = 4). (T-W) Representative immunofluorescence staining for CD41 (red) and ckit (green) in femoral BM sections of WT or β2-β3-AR DKO mice of different age. Images were taken from the diaphysis regions; c-kit+CD41+ cells are depicted with white arrows. (X) c-kit+CD41+ cells per mm^2 (n = 4 young mice; n = 3 old mice) in endosteal (e) or non-endosteal (n-e) BM areas. Regions within 1/5 marrow width from the bone surface are defined as endosteal (both sides of the bone), while the remaining 3/5 marrow width in the central part are considered as non-endosteal. Young mice were analysed between 8–30 weeks of age, and old mice were 66–120 weeks old. Data are means ± SEM. *p < 0.05; **p < 0.01; ***p < 0.001 (one-way ANOVA followed by Bonferroni pairwise comparisons).

4.3 β2-AR and β3-AR have opposite, stage-divergent and stromal cell-dependent effects on Mk differentiation

β2-AR is widely expressed by many BM cells, including haematopoietic and non-haematopoietic cells. The expression of β3-AR is generally low/absent in hematopoietic cells and is rather restricted to the microenvironment. It has been reported that HSPC mobilisation is rhythmically controlled by the two receptors in different ways: β2-AR induces clock gene expression whereas β3-AR downregulates CXCL12 expressed by MSCs (Mendez-Ferrer et al., 2010). To understand how β2/3 adrenergic signalling regulates Mk differentiation, and whether the regulation is haematopoietic cell-autonomous or stromal cell-dependent, a coculture system was established by using HPC-7 cells (murine HSC-like cell line) and MS-5 stromal cells (murine mesenchymal cell line) (see 3.5.1). HPC-7 cells were cultured with or without MS-5 cell layers, in medium containing TPO together with selective β2-AR, β3-AR agonists or vehicle controls for 4 days (Fig. 20B). HPC-7 cells were categorized into three populations based on the expression of cell surface markers, c-kit and CD41: population I, c-kit^{high}CD41^{low} undifferentiated progenitor; population II, c-kit^{low}CD41^{low} intermediate progenitor; population III, CD41^{high} committed Mk progenitor (Fig. 20A). Upon TPO induction, HPC-7 cells follow two Mk differentiation routes: gradual transition from population I to II to III, or direct commitment from population I to III. In coculture with MS-5 stromal cells, β3-AR agonist significantly increases population I at day 2, but reduces population III at day 4. In contrast, β2-AR agonist expands population III at day 4 (Fig. 20D). Neither β2-AR nor β3-AR agonist affects HPC-7 differentiation in the absence of MS-5 stromal cells (Fig. 20C). These results suggest that β2-AR and β3-AR have opposite, stage-divergent and stromal dependent effects on Mk differentiation.

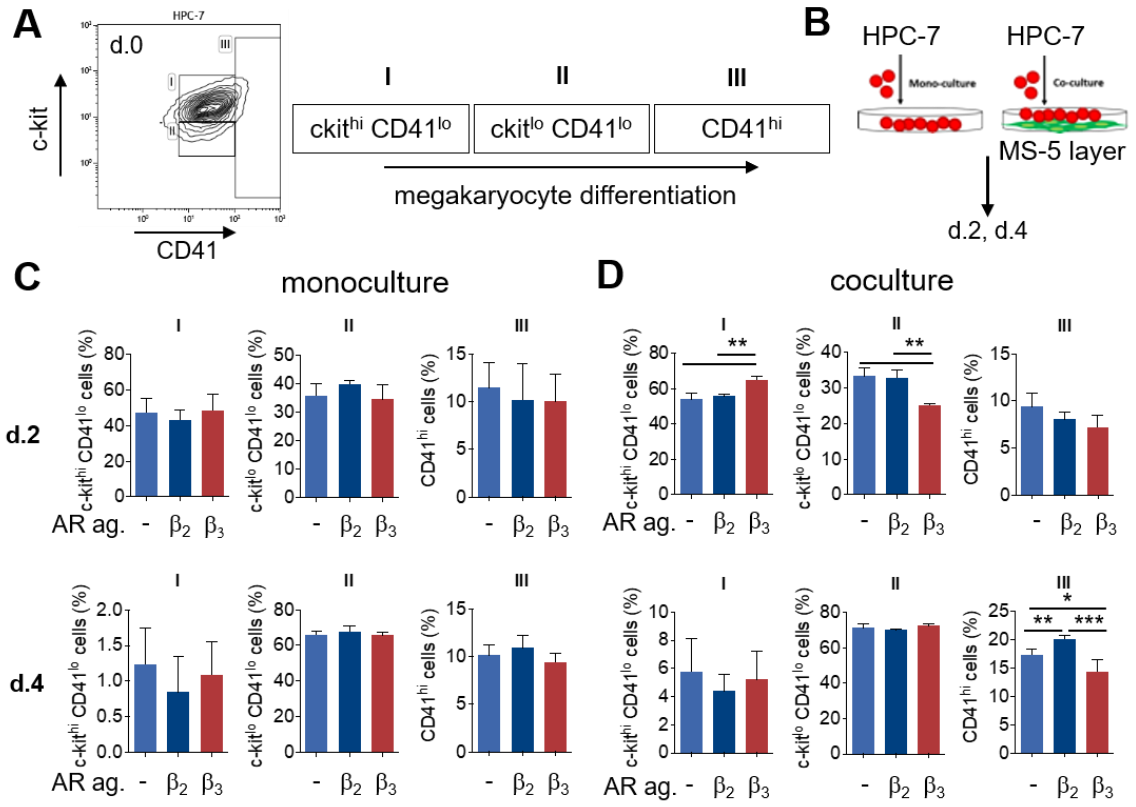

Figure 20. β2-AR and β3-AR have opposite, stage-divergent and stroma-dependent effects on Mk differentiation.

(A) Representative flow cytometry diagram of HPC-7 cells before treatment with cytokines (day 0). Scheme showing the cell populations indicating progressive megakaryocyte commitment: I, ckit^{hi}CD41^{lo} cells; II, ckit^{lo}CD41^{lo} cells; III, CD41^{hi} cells. Megakaryocyte differentiation trajectory flows from populations I to II to III, or I to III. (B) Scheme showing the experimental design. HPC-7 cells were cultured alone or co-cultured with MS-5 stromal cells in megakaryocyte differentiation medium. (C-D) Quantification of cell populations I, II and III after 2 or 4 days of treatment with vehicle, β2-AR agonist or β3-AR agonist in (C) monoculture or (D) coculture with MS-5 stromal layers (n = 4). Data are means ± SEM. * $p < 0.05$; ** $p < 0.01$; *** $p < 0.001$. (A, B, E-I) One-way ANOVA followed by Bonferroni pairwise comparisons.

4.4 Lack of β2-AR signalling in the microenvironment impairs Mk differentiation

Previous coculture experiments indicate that β2-AR indirectly promotes Mk differentiation through stromal cells. To validate the results, MS-5 stromal cells were cocultured with human cord-blood derived $CD34^+$ HSPCs in Mk differentiation medium, supplemented with or without β2-AR agonist for 10 days (see 3.5.2) (Fig. 21A). Immunofluorescence staining with human CD61 antibody demonstrates a significant increase of human megakaryocytic cells in β2-AR agonist treatment (Fig. 21B-D). To extend these observations to the context of ageing, a coculture system was established by using primary haematopoietic cells and stromal cells from mice of different ages (see 3.5.3). BM stromal cells were isolated from young or old mice. Lineage negative (Lin^-) haematopoietic progenitors were purified from young double-transgenic mice expressing DsRed under the control of the chicken β actin promoter and eGFP under the control of von Willebrand factor (Vwf) promoter (DsRed;Vwf-eGFP mice). TPO and the β2-AR agonist were given to the coculture for 4 days, in which differentiated megakaryocytic cells express both DsRed and eGFP, while undifferentiated haematopoietic progenitors only express DsRed (Fig. 21E). The frequency of $DsRed^+eGFP^+$ cells is tripled in coculture with old stromal cells compared to young stromal cells, suggesting ageing from the microenvironment promotes Mk differentiation. Consistent with the previous results, the presence of β2-AR agonist further increases Mk differentiation, in both young and old stromal cell settings (Fig. 21F). These results confirm a universal (independent of age), stromal cell-dependent and enhancing effect on Mk differentiation by β2-AR.

Given that the activation of β2-AR increases Mk differentiation *in vitro*, it is speculated that a mirror effect could be obtained from *in vivo* β2-AR depletion. To address the question, young and old mice deficient with β2-AR (but not β3-AR) were studied. Whereas there is no difference in peripheral platelet counts between WT and β2-AR deficient mice in adulthood, old β2-AR deficient mice do not increase platelet counts (Fig. 21G). To further investigate the effect of β2-AR on megakaryopoiesis in different BM niches, BM cells from endosteal and non-endosteal fractions were isolated, respectively, and subjected to flow cytometry analysis. The frequency of $CD41^+$ LSK cells (same analysis as described in 4.2) is significantly decreased in young β2-AR deficient mice, and the reduction persists until ageing (Fig. 21H and I), which is in line with the observations in DKO mice (Fig.19Q-S). Similarly, MkPs are decreased in both young and old β2-AR deficient mice, compared to their age-matched WT controls (Fig. 21J and K). To test whether the effect on megakaryocytic cells ($CD41^+$ LSK cells and MkPs) is mediated through the microenvironment, reverse chimera experiments were performed, in which lethally irradiated WT or β2-AR deficient mice were transplanted with WT or β2-AR deficient BM cells (see 3.2.1). 4 months after transplantation, β2-AR deficient mice carrying WT BM cells recapitulate the endosteal-specific reduction of megakaryocytic cells in primary mice (Fig. 21H'', I'', J'' and K''), while WT recipients with β2-AR deficient BM cells do not reproduce the phenotype (Fig. 21H', I', J' and K'). It is notable that in non-endosteal BM, both chimeras and primary mice also show a tendency (but not statistically different) toward reduced megakaryocytic cells. These results suggest that β2-AR has a niche-dependent effect on megakaryopoiesis near endosteum, while present certain HSC-autonomous effect in the central marrow.

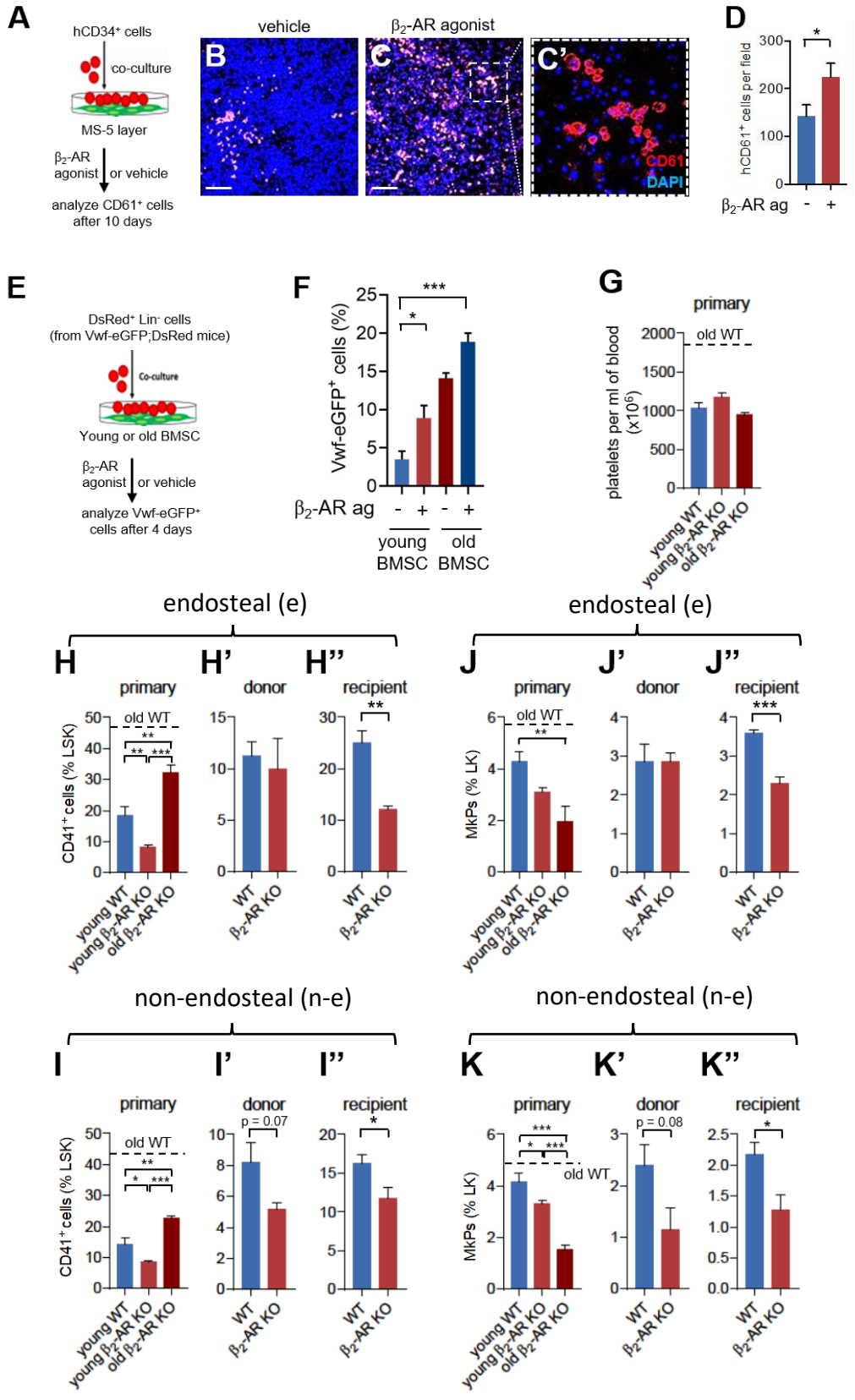
A
hCD34+ cells
co-culture
MS-5 layer
β2-AR agonist or vehicle
analyze CD61+ cells after 10 days
vehicle
β2-AR agonist
B
C
C'
CD61
DAPI
D
hCD61+ cells per field
β2-AR ag - +
E
DsRed+ Lin- cells (from Vwf-eGFP;DsRed mice)
Co-culture
Young or old BMSC
β2-AR agonist or vehicle
analyze Vwf-eGFP+ cells after 4 days
F
Vwf-eGFP+ cells (%)
β2-AR ag - + - +
young BMSC
old BMSC
G
primary
old WT
platelets per ml of blood (x10^6)
young WT
young β2-AR KO
old β2-AR KO
endosteal (e)
H
H'
H''
primary
donor
recipient
old WT
CD41+ cells (% LSK)
WT
β2-AR KO
J
J'
J''
MkPs (% LK)
non-endosteal (n-e)
I
I'
I''
p = 0.07
K
K'
K''
p = 0.08

Figure 21. β2-AR signalling in endosteal BM is essential for Mk differentiation during ageing.

(A) Scheme of human umbilical-cord-blood derived CD34+ HSPCs cocultured with MS-5 stromal cells. (B–D) Representative immunofluorescence (B and C) and number (D) of CD61+ (red) human megakaryocytes in cocultures treated with (B) vehicle or (C) β2-AR agonist (clenbuterol, 10 mM) for 10 days (n = 3). Scale bar, 250 mm. (C') Inset of (C). (E) Scheme of Lin- cells derived from Vwf-eGFP; DsRed mice cocultured with bone marrow stromal cells (BMSCs) from young or old mice. (F) Frequency of Vwf-eGFP+ cells in DsRed+ cells in cocultures treated with vehicle or β2-AR agonist (clenbuterol, 10 mM) for 4 days (n = 3). (G) Circulating platelets in young WT (n = 11), young *Adrb2*$^{-/-}$ (n = 3), or old *Adrb2*$^{-/-}$ (n = 3) mice. (H-K'') Frequency of (H-I'') CD41+ myeloid or megakaryocyte progenitors within lin-sca-1+c-kit+ (LSK) cells or (J-K'') CD150+CD41+ megakaryocyte progenitors (MkPs) within lin-c-kit+ (LK) cells in endosteal BM (H, H', H'', J, J', J'') or non-endosteal BM (I, I', I'', K, K', K'') of the following mice: (H, I, J, K) young WT (H, I, n = 6; J, K, n = 3), young *Adrb2*$^{-/-}$ (H, I, n = 6; J, K, n = 8) or old *Adrb2*$^{-/-}$ (n = 4) mice; (H', I', J', K') lethally irradiated WT recipients of WT (n = 5) or *Adrb2*$^{-/-}$ (n = 4) BM cells; (H'', I'', J'', K'') lethally irradiated WT (n = 5) or *Adrb2*$^{-/-}$ (n = 4) recipients of WT BM cells. Data are means ± SEM. *p < 0.05; **p < 0.01; ***p < 0.001. (D, H', H'', I', I'', J', J'', K', K'') Unpaired two-tailed t test. (F, G, H, I, J, K) one-way ANOVA and Bonferroni pairwise comparisons.

4.5 β2-AR promotes Mk differentiation through MSC-derived IL-6

To get mechanistic insight of β2-AR-dependent megakaryopoiesis, multiple ELISA screening of pro-inflammatory cytokines involved in ageing and Mk differentiation was performed. Extracellular fluids extracted from young murine endosteal or non-endosteal BM fractions were subjected to analysis. IL-6 and IFNγ levels are generally higher in endosteal BM than non-endosteal BM, and both cytokines are downregulated specifically in endosteal BM of β2-AR deficient mice (Fig. 22A and B). IL-6 levels are also significantly increased in the ageing BM (Fig. 18B and G), suggesting that IL6 might be downstream of β2-AR in endosteal niches. MS-5 stromal cells were treated with the selective β2-AR agonist, which demonstrates that *IL6* mRNA transcripts are doubled in response to β2-AR activation. Yet the increase is abrogated when protein kinase A (PKA), a secondary effector to transduce β2-AR signalling, is pharmacologically inhibited (Fig. 22C). To strengthen the connection between β2-AR and IL-6 *in vivo*, an IL-6 deficient mouse model (see 3.1) was studied. It has been reported that these mice are protected from the decrease of circulating lymphocytes with age. Moreover, old IL-6 deficient mice develop less severe anaemia, whereas their platelet counts are slightly lower than their WT counterparts (McCranor et al., 2013). Immunofluorescence staining of BM $CD41^{+}CD42^{+}$ cells demonstrates that both β2-AR and IL-6 deficient mice (in adulthood) display significantly fewer Mks compared to WT controls (Fig. 22D-G). To test whether β2-AR locally regulates Mk differentiation through IL-6 in the BM, a long-term primary culture system was established to mimic murine BM microenvironment *ex vivo*. Total BM cells from WT or IL-6 deficient mice were grown in myeloid-culture medium for 2-3 weeks until stromal cell layers were formed and haematopoietic cells were grown. After the primary culture was

developed, TPO was given for extra 4 days to induce Mk differentiation, during which the β2-AR agonist or vehicle control were added to the culture (Fig. 22H). The number of $CD41^{+}$LSK cells is significantly increased in response to β2-AR in WT BM culture. However, activation of β2-AR fails to increase $CD41^{+}$LSK cells in IL-6 deficient BM culture (Fig. 22I). Taken together, these results suggest that β2-AR in endosteal niches promotes Mk differentiation through stromal cell-derived IL-6.

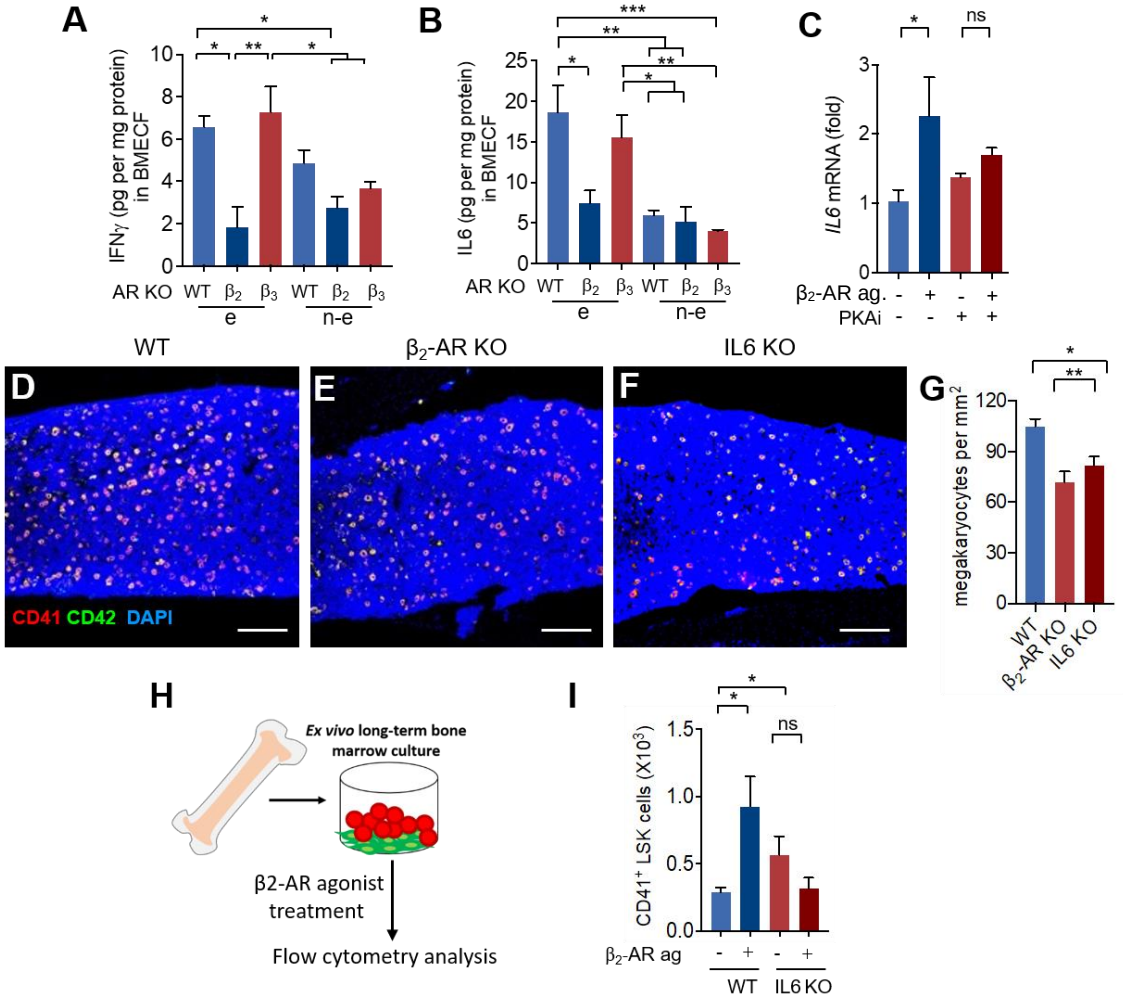

Figure 22. β2-AR promotes Mk differentiation through stromal cell-derived IL-6.

(A-B) Concentration of (A) IFNγ and (B) IL-6 in endosteal (e) or non-endosteal (n-e) BM supernatant from adult WT (n = 6), *Adrb2*$^{-/-}$ (n = 4), or *Adrb3*$^{-/-}$ (n = 7) mice. (C) *Il6* mRNA expression (fold change) in MS-5 stromal cells treated with β2-AR agonist (clenbuterol, 10 mM), PKA inhibitor (H-89, 5 mM), or vehicle for 2 days (n = 3). (D–G) Representative immunofluorescence (D–F) and quantification (G) of CD41+ (red) CD42+ (green) megakaryocytes (yellow) in adult WT (n = 5), *Adrb2*$^{-/-}$ (n = 3), or *Il6*$^{-/-}$ (IL6 KO) (n = 5) mice. Scale bar, 250 mm. (H) Scheme of long-term BM culture from WT or *Il6*$^{-/-}$ mice. (I) Myeloid or megakaryocyte progenitors (CD41+ LSK cells) in primary BM culture from WT or *Il6*$^{-/-}$ mice treated with β2-AR agonist (clenbuterol, 10 mM) or vehicle for 4 days (n = 4). Data are means ± SEM. *p < 0.05; **p < 0.01; ***p < 0.001. One-way ANOVA followed by Bonferroni pairwise comparisons.

4.6 Lack of β3-AR signalling in the microenvironment impacts HSC lineage bias

The cell line experiments indicate that β3-AR has an opposite effect on the size of $CD41^+$ cells. Activation of β3-AR decreases megakaryocytic cells possibly through preventing Mk differentiation from HSCs. However, in the primary culture systems (lin^- cells cultured with young/old stromal cells, or $hCD34^+$ HSPCs cultured with MS-5 cells), terminal Mk differentiation appears to be unaffected by β3-AR agonist (data not shown). A recent paper reported that adult β3-AR deficient mice exhibit myeloid-bias in the circulation, paralleled with reduced lymphoid multipotent progenitors (LMPP) in the BM. It is therefore hypothesized that β3-AR does not directly regulate Mk differentiation, but controls the switch of myelopoiesis/lymphopoiesis at the early stem and progenitor cell level. To test the hypothesis, young and old mice deficient with β3-AR (but not β2-AR) were studied. BM cells from endosteal and non-endosteal fractions were isolated, and the frequency of different HSC populations (LT-HSCs, myeloid-biased HSC and lymphoid-biased HSCs) was analysed by flow cytometry (Fig. 23A). Upon ageing, LT-HSCs and myeloid-biased HSCs are expanded while lymphoid-biased HSCs are reduced in WT BM (both endosteal and non-endosteal fractions), an evidence of myeloid skewing. Interestingly, lymphoid-biased HSCs are lowered by one-third, specifically in endosteal BM of adult β3-AR deficient mice, to a similar extent of old WT mice. Old β3-AR deficient mice do not aggravate the loss of lymphoid-biased HSCs (Fig. 23B, C, D, E, F and G). To test whether the effect is mediated through the microenvironment, lethally irradiated WT or β3-AR deficient mice were transplanted with WT or β3-AR deficient BM cells (see 3.2.1). The reverse chimera experiments confirm that the regulation of β3-AR is niche-dependent, since lymphoid-biased HSCs are not attenuated in WT recipients carrying β3-AR

deficient BM cells (Fig. 23B', B'', C', C'', D', D'', E', E'', F', F'', G' and G''). Based on the phenotype in lineage-biased HSCs, the corresponding haematopoietic progenies (mature myeloid or lymphoid cells) in the BM was further investigated. Despite the differences being nonsignificant, adult β3-AR deficient mice exhibit a tendency toward increased frequency of granulocytes (Ly-6G$^+$CD11b$^+$ cells) but decreased B lymphocytes, manifest in non-endosteal BM. Compared to old WT mice, old β3-AR deficient mice show similar reduction of B lymphocytes (Fig. 23H-K). However, β3-AR deficient mice (compared to their age-matched WT controls) do not show clear differences in circulating myeloid or lymphoid cells (Fig. 23L and M). Interestingly, impaired lymphoid-biased HSCs near endosteum correlates with increased concentration of IL-1α and IL-1β (Fig. 23N and O), which have been reported to enhance myeloid/megakaryocytic differentiation or suppress lymphopoiesis. These results suggest that lack of β3-AR in endosteal niches majorly impairs lymphoid-biased HSCs, which might accelerate skewed myeloid differentiation upon ageing.

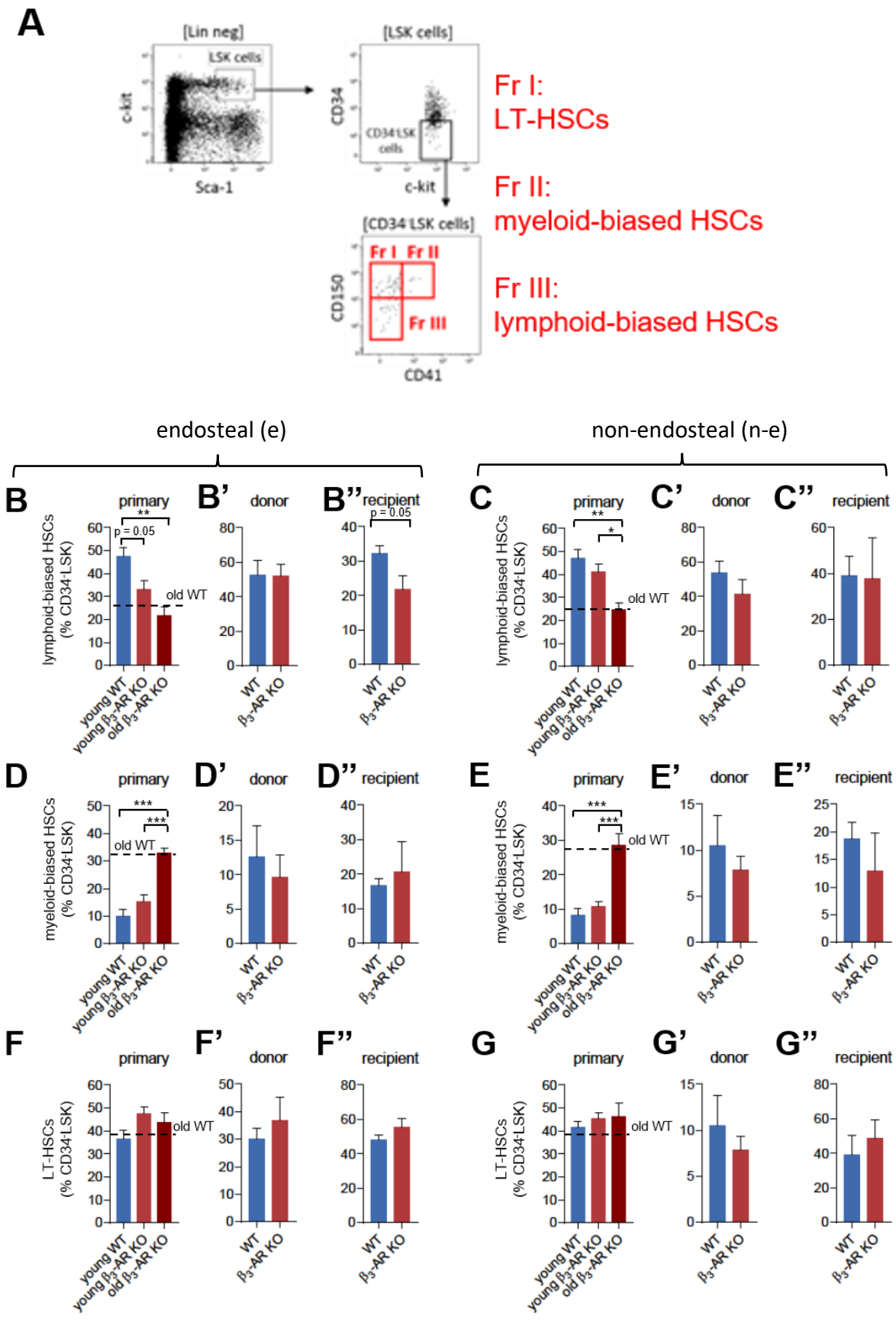
A
[Lin neg]
LSK cells
c-kit
Sca-1
[LSK cells]
CD34
CD34-LSK cells
c-kit
[CD34-LSK cells]
Fr I
Fr II
Fr III
CD150
CD41
Fr I:
LT-HSCs
Fr II:
myeloid-biased HSCs
Fr III:
lymphoid-biased HSCs
endosteal (e)
non-endosteal (n-e)
B
primary
B'
donor
B''
recipient
C
primary
C'
donor
C''
recipient
lymphoid-biased HSCs (% CD34-LSK)
p = 0.05
**
*
old WT
young WT
young β3-AR KO
old β3-AR KO
WT
β3-AR KO
D
primary
D'
donor
D''
recipient
E
primary
E'
donor
E''
recipient
myeloid-biased HSCs (% CD34-LSK)
***
old WT
F
primary
F'
donor
F''
recipient
G
primary
G'
donor
G''
recipient
LT-HSCs (% CD34-LSK)

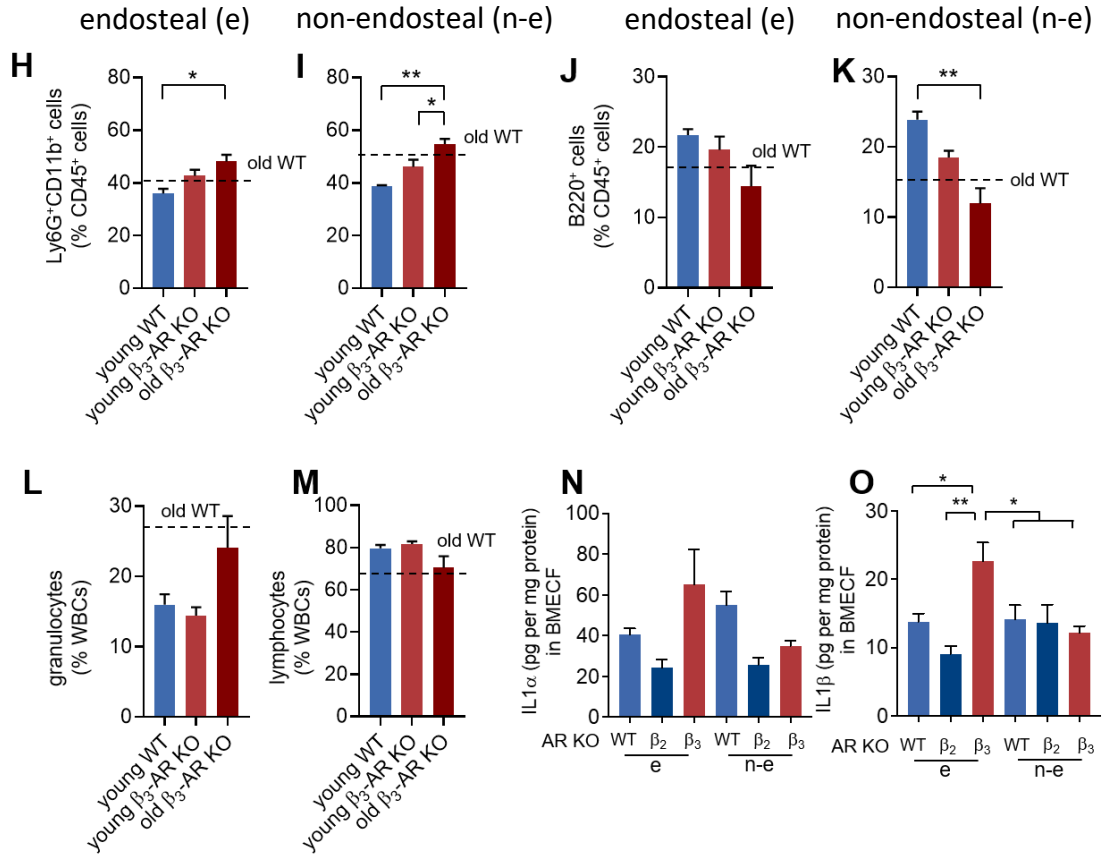

Figure 23. Lack of β3-AR in endosteal BM impairs lymphoid-biased HSCs. (A) Representative flow cytometry diagram of HSC populations based on CD41 and CD150 expression. (B-G'') Frequency of (B-C'') $CD150^{lo/-}CD41^{-}$ lymphoid-biased HSCs, (D-E'') $CD150^{+}CD41^{+}$ myeloid-biased HSCs or (F-G) $CD150^{+}CD41^{-}$ LT-HSCs in (B, D, F) endosteal or (C, E, G) non-endosteal BM $CD34^{-}$LSK cells from the following mice: (B, C, D, E, F, G) young WT (n = 7), young *Adrb3*$^{-/-}$ (n = 7) or old *Adrb3*$^{-/-}$ (n = 5) mice; (B', C', D', E', F',G') lethally-irradiated WT recipients of WT (n = 5) or *Adrb3*$^{-/-}$ (n = 5) BM cells; (B'', C'', D'', E'', F'', G'') lethally-irradiated WT (n = 4) or *Adrb3*$^{-/-}$ (n = 3) recipients of WT BM cells. (H-K) Frequency of (H, I) $Ly6G^{+}CD11b^{+}$ granulocytes or (J, K) $B220^{+}$ lymphocytes in (H, J) endosteal or (I, K) non-endosteal BM $CD45^{+}$ cells from young WT (n = 3), young *Adrb3*$^{-/-}$ (n = 4) or old *Adrb3*$^{-/-}$ (n = 5) mic. (L-M) Frequency of (L) granulocytes and (M) lymphocytes in white blood cells (WBCs) in young WT (n = 10), young *Adrb3*$^{-/-}$ (n = 4) or old *Adrb3*$^{-/-}$ (n = 6) mice. Data are means ± SEM. (N-O) Concentration of (N) IL-1α and (O) IL-1β in endosteal (e) or nonendosteal (n-e) BM extracellular fluid (BMECF) from adult WT mice (n = 6), *Adrb2*$^{-/-}$ mice (n = 4), or *Adrb3*$^{-/-}$ mice (n = 7). (B', C', D', E', F', G', B'', C'', D'', E'', F'', G'') Unpaired two-tailed t test. (B, C, D, E, F, G, H-O) One-way ANOVA and Bonferroni pairwise comparisons.

4.7 β3-AR signalling regulates lymphoid-biased HSCs partially through Nos1-dependent pathway

The precise mechanisms by which β3-AR balances myeloid/lymphoid output have yet to be elucidated. Whereas all β-ARs transduce signals through activating G-proteins, it has been reported that NO is a second messenger restricted to β3-AR activation (Gauthier et al., 1998). A recent publication indicates that NO synthesis pathways bridge ageing of the microenvironment and HSCs (Hennrich et al., 2018). Dr. Monika Wittner and Dr. Fawzia Louache (collaborators of the lab) discovered that NO synthase 1 (Nos1) deficient mice exhibit increased platelet/granulocytes but decreased B lymphocytes in the circulation (Ho et al., 2019). Supporting the observation on peripheral myeloid-skewing differentiation, immunofluorescence staining of CD41 and c-kit demonstrates that adult Nos1 deficient mice expand myeloid/megakaryocytic progenitors ($CD41^+ckit^+$ cells), specifically near endosteal BM (Fig. 24A, C and D). Consistently, adult β3-AR deficient mice exhibit increased BM myeloid/megakaryocytic progenitors near endosteum (Figure 24A, B and D), despite terminal differentiated cells being unchanged in the circulation (Fig. 23L). These lines of evidence suggest that β3-AR in endosteal niches might regulate lymphoid-biased HSCs through Nos1-dependent NO generation, leading to an expansion of myeloid progenitors in the BM. In WT mice, NO concentration is remarkably higher in endosteal BM compared to non-endosteal BM (Fig. 24H). This can be explained by twice the difference of Nos1 (but not Nos2 or Nos3) mRNA transcripts in the two niches (Fig. 24E). Interestingly, NO concentration and Nos1 mRNA are significantly reduced in endosteal BM of β3-AR deficient mice (Fig. 24E-H). To study the functional role of Nos1 in β3-AR-dependent haematopoiesis, the aforementioned primary culture system was performed. In this regard, BM cells were obtained from Vwf-eGFP mice, which allows to stringently distinguish platelet/myeloid-

biased HSCs from lymphoid-biased HSCs by eGFP (Fig. 24I). Selective β3-AR agonist and/or Nos1 inhibitor were added to the culture during TPO induction. Pharmacological activation of β3-AR expands the number of Vwf-eGFP$^-$ (lymphoid-biased) HSCs, while Vwf-eGFP$^+$ (platelet/myeloid-biased) HSCs are unaffected. Nos1 inhibition abrogates the enhancing effect of β3-AR agonist on lymphoid-biased HSCs (Fig. 24J and K), confirming that β3-AR regulates lymphoid-biased HSCs through Nos1-dependent pathway.

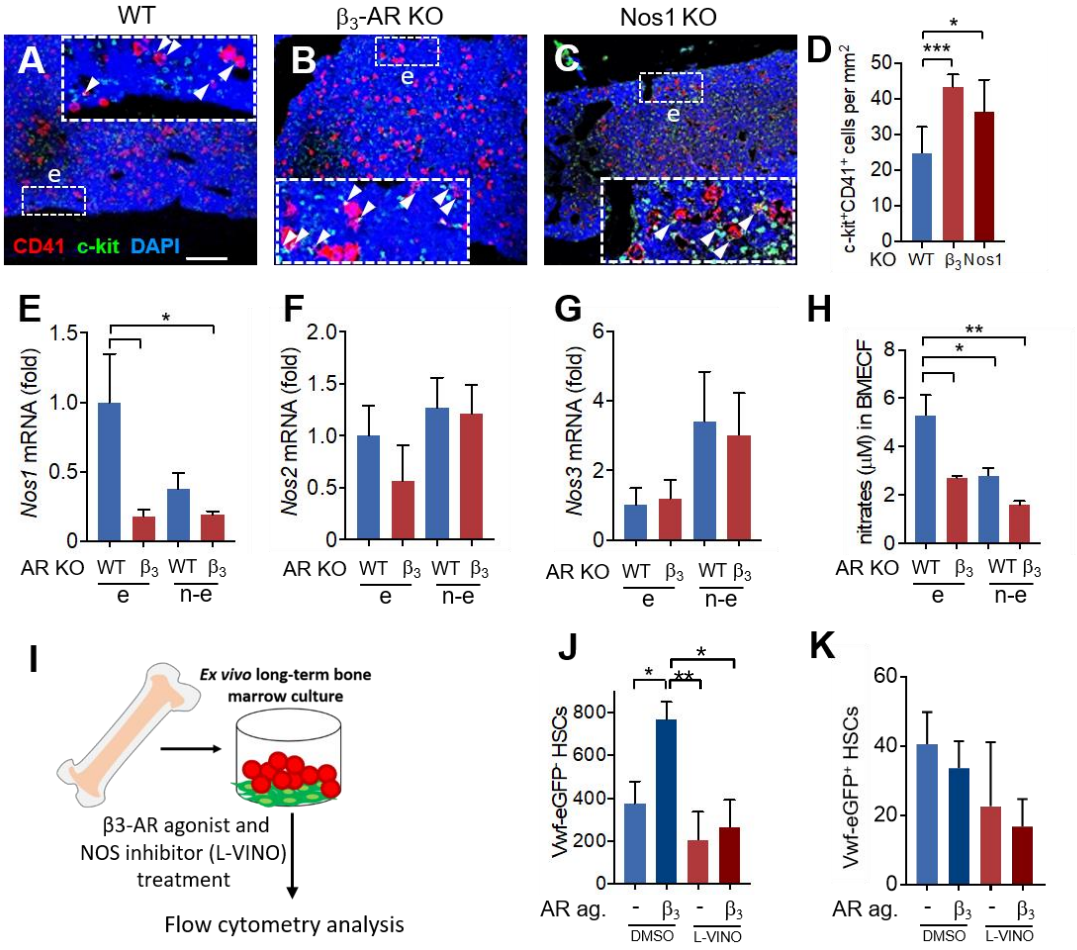

Figure 24. β3-AR regulates lymphoid-biased HSCs through Nos-1-dependent pathway.

(A–D) Representative immunofluorescence (A–C) and quantification (D) of c-kit+ (green) CD41+ (red) myeloid or megakaryocyte progenitors (arrowheads) in endosteal BM of WT (n = 10), *Adrb3*$^{-/-}$ (n = 8), or *Nos1*$^{-/-}$ (n = 4) mice. Endosteal BM is considered as regions within one-fifth marrow width from the bone surface. Scale bar, 300 mm. (E-G) mRNA levels (fold) of (E) Nos1 (F) Nos2 and (G) Nos3 in the endosteal (e) or non-endosteal (n-e) BM of adult WT mice (n = 6) and β3-AR KO mice (n = 7). (H) Nitrate concentration in BM extracellular fluid (BMECF) of young WT (n = 6) or *Adrb3*$^{-/-}$ (n = 7) mice. (I) Scheme of long-term BM culture from Vwf-eGFP mice. (J-K) Number of (J) lin^{-}sca-1^{+}c-kit^{+}CD34^{-} CD48^{-}CD150^{+}Vwf-eGFP^{-} lymphoid-biased HSCs or (K) lin^{-}sca-1^{+}c-kit^{+}CD34^{-} CD48^{-}CD150^{+}Vwf-eGFP^{+} platelet/myeloid-biased HSCs in primary BM culture from Vwf-eGFP mice treated with β3-AR agonist (BRL37344, 10 mM), Nos1 inhibitor (L-VINO, 100 mM), or vehicle for 4 days (n = 8). Data are means ± SEM. *p < 0.05; **p < 0.01; ***p < 0.001. One-way ANOVA and Bonferroni pairwise comparisons. AR: adrenergic receptor.

4.8 Lack of β3-AR-Nos1 signalling accelerates haematopoietic ageing by remodelling HSC-supporting niches

The previous results suggest that impaired β3-AR-Nos1 signalling accelerates ageing of the haematopoietic system (mainly expansion of myeloid/megakaryocytic progenitors) by promoting lymphoid deficiency at the level of HSCs. Given the regulation is not HSC cell-autonomous, whether adult β3-AR and Nos1 deficient mice display age-related BM niche remodelling was further tested. It has been reported that the overall BM vessel density is increased in aged mice. However, endosteal vascular niches contract while non-endosteal vascular niches expand (Ho et al., 2019). Whole-mount confocal imaging of thick femur sections was performed in order to study endothelial architecture at a 3D-resolution level. Immunofluorescence staining of CD31 and EMCN reveals that TZVs, specialized endosteal vessels that connect arterioles and sinusoids, are decreased in β3-AR and Nos1 deficient mice (Fig. 25E-H). In contrast, small capillaries are expanded in central marrow (Fig. 25I). Mks tightly control HSC quiescence and proliferation under homeostasis. A drastic remodelling of Mk niches is found in aged mice, characterised by Mk increasing PPF, being closer to sinusoids but distant from HSCs (Maryanovich et al., 2019). To examine Mks and their interaction with sinusoids, immunofluorescence staining of CD41 and EMCN was performed. Adult β3-AR and Nos1 deficient mice show higher frequency of Mks ($CD41^+$ cells) adjacent with sinusoids ($EMCN^+$ cells) compared to age-matched WT controls (Fig. 25A-D). Immunofluorescence staining of BM $CD150^+lin^-CD48^-$ HSCs and $CD42^+$ Mks uncovers that HSCs redistribute away from Mks in β3-AR deficient BM, to a similar extent as normally aged BM (Fig. 25J-M). These results together suggest that lack of β3-

AR-Nos1 signalling alters Mk and vascular niches, which correlates with HSCs apposition to Mks.

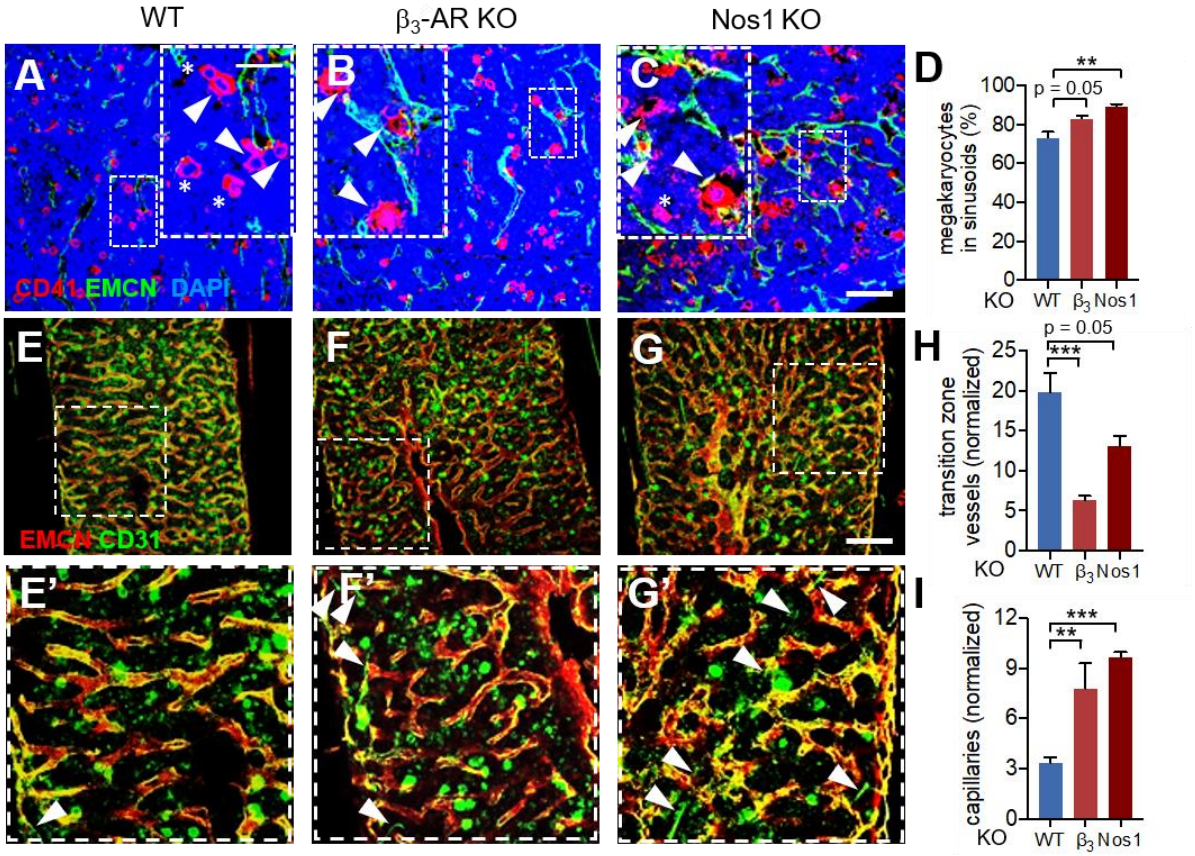
WT
β3-AR KO
Nos1 KO
A
B
C
CD41 EMCN DAPI
D
megakaryocytes in sinusoids (%)
p = 0.05
**
KO WT β3 Nos1
E
F
G
EMCN CD31
H
transition zone vessels (normalized)
p = 0.05
***
KO WT β3 Nos1
E'
F'
G'
I
capillaries (normalized)
***
**
KO WT β3 Nos1

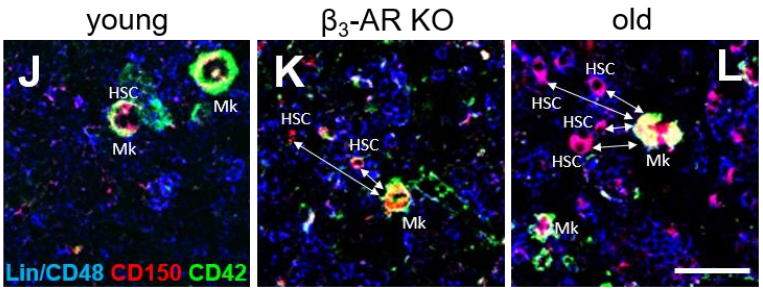
young
β3-AR KO
old
J
HSC
Mk
Mk
Lin/CD48 CD150 CD42
K
HSC
HSC
Mk
L
HSC
HSC
HSC
HSC
Mk
Mk

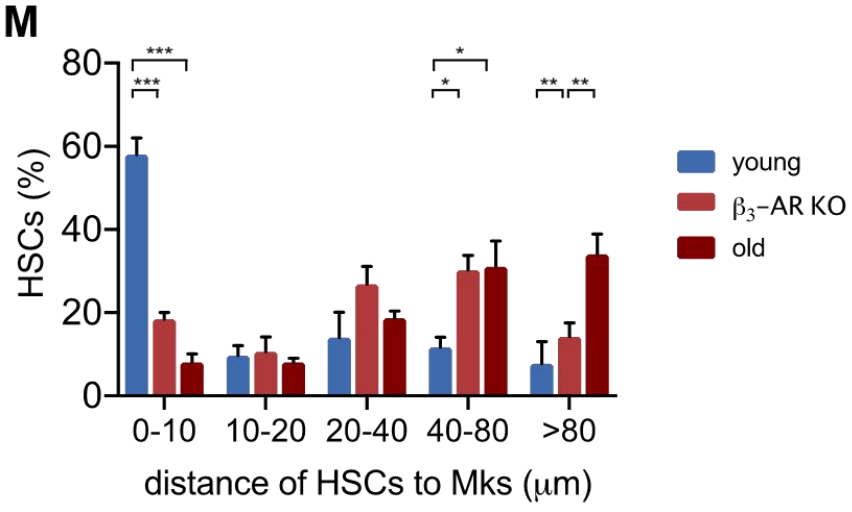
M
HSCs (%)
***
***
*
*
**
**
young
β3−AR KO
old
0-10
10-20
20-40
40-80
>80
distance of HSCs to Mks (μm)

Figure 25. Deficient β3-AR accelerates BM niche ageing.
(A–D) Representative immunofluorescence (A-C) and quantification (D) of CD41+ (red) megakaryocytes adjacent (arrowheads) or nonadjacent (asterisks) to EMCN+ (green) BM vasculature of WT (n = 9), *Adrb3*$^{-/-}$ (n = 6), or *Nos1*$^{-/-}$ (n = 4) mice. Scale bar, 250 mm. (E–G) Representative whole-mount immunofluorescence of CD31 (green) and EMCN (red) in WT (n = 7), Adrb3$^{-/-}$ (n = 5), or *Nos1*$^{-/-}$ (n = 4) BM. Arrowheads in insets (E'), (F'), and (G') depict CD31^{hi}EMCN^{-} capillaries. (H, I) Quantification of (H) CD31^{hi}EMCN^{hi} transition zone vessels and (I) CD31^{hi}EMCN^{-} capillaries with <6 mm diameter. Scale bar, 250 mm. (J-M) Representative immunofluorescence (J-L) and distribution (M) of BM CD150^{+} (red) HSCs (negative for mature haematopoietic lineage markers, blue) adjacent (asterisks) or nonadjacent (arrows) to CD42^{+} (green) megakaryocytes in femoral BM sections of young WT mice (n = 3), adult *Adrb3*$^{-/-}$ mice (n = 5) and old WT mice (n = 3). Scale bar, 50 μm. Data are means ± SEM. * $p < 0.05$; ** $p < 0.01$; *** $p < 0.001$. (D, H, I) One-way ANOVA and Bonferroni pairwise comparisons. (M) Two-way ANOVA and Bonferroni pairwise comparisons.

4.9 BM niche remodelling in *Lmna*$^{G609G/G609G}$ progeria mouse model

It has been reported that HGPS recapitulates certain hallmarks of haematopoietic ageing. Using the *Lmna*$^{G609G/G609G}$ mouse model of HGPS, increased platelet counts and myeloid-biased differentiation in circulation were observed (Ho et al., 2019). Importantly, these features appeared to be driven by the microenvironment, since chimera mice with *Lmna*$^{G609G/G609G}$ donor BM cells did not reproduce the phenotype. Analysis of BM histology of progeroid mice reveals that Th^+ nerve fibres are not expanded. Vessel dilation is present in progeroid BM, while reduced TZVs and increased small capillaries (vascular remodelling in normal ageing) are not observed. However, progeroid mice suffer the same Mk niche remodelling found in normal ageing: Mk being closer to sinusoids (Fig. 26A-C) with increasing PPF (Fig. 26D-F). Moreover, age-related pro-inflammatory cytokines are augmented in progeroid BM (Fig. 26G-K). These results highlight the differences (vasculature and nerve fibres) between normal and pathological conditions, but also suggest that similar microenvironmental alterations (Mk niche remodelling and increased inflammatory cytokines) contribute to premature ageing in HGPS.

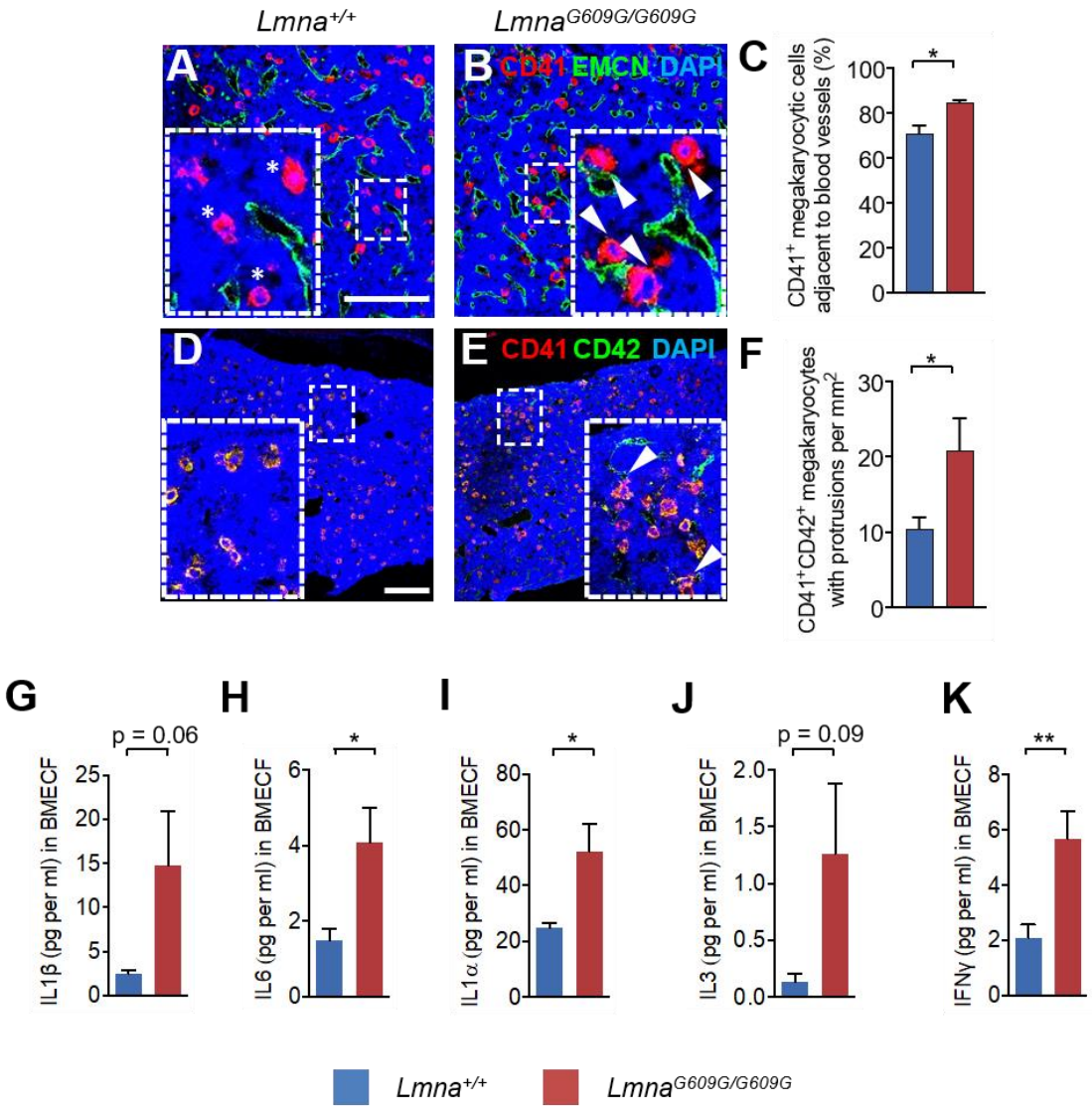

Figure 26. Premature haematopoietic ageing in HGPS concurs with BM Mk niche remodelling and inflammation.

(A, B) Representative immunofluorescence staining for CD41 (red) and EMCN (green) in femoral BM sections of adult WT (*Lmna*$^{+/+}$; n = 3) and *Lmna*$^{G609G/G609G}$ (n = 4) mice. White stars, CD41^{+} cells nonadjacent to EMCN^{+} vasculature; White arrows, CD41^{+} cells adjacent to EMCN^{+} vasculature. Scale bar, 100 μm. (C) Frequency of CD41+ cells in contact with EMCN^{+} vasculature. (D, E) Representative immunofluorescence staining for CD41 (red) and CD42 (green) in femoral BM sections of adult WT (*Lmna*$^{+/+}$; n = 3) and *Lmna*$^{G609G/G609G}$ (n = 4) mice. Scale bar, 250 μm. (F) CD41^{+}CD42^{+} megakaryocytes with protrusions (clear cell body extensions, depicted by white arrows in E) per BM area. (G–K) Concentration of (G) IL-1β, (H) IL-6, (I) IL-1α, (J) IL-3, and (K) IFNγ in the BM extracellular fluid (BMECF) of adult WT (*Lmna*$^{+/+}$; n = 9) and *Lmna*$^{G609G/G609G}$ (n = 9) male mice. Data are means ± SEM. *p < 0.05; **p < 0.01 (unpaired two-tailed t test).

4.10 Chronic β3-AR agonist treatment partially rejuvenates haematopoietic ageing in HGPS

Previous results suggest that β3-AR deficient mice and progeroid mice exhibit similar microenvironmental alterations found in normal ageing. Additionally, a recent publication reported that chronic treatment of β3-AR agonist can rejuvenate old HSCs (Maryanovich et al., 2019). Therefore, whether pharmacological targeting β3-AR can also improve pathological haematopoietic ageing in HGPS was tested. *Lmna*$^{G609G/G609G}$ mice were daily injected with the selective β3-AR agonist for over 2 months (experiment carried out by our collaborator Cristina Gonzalez). Mice were sacrificed at the end of the treatment for histology and flow cytometry analysis. Circulating granulocytes are decreased, while lymphocytes are increased in response to chronic β3-AR activation (Fig. 27A and B). Consistently, expansion of BM granulocytes and B-lymphoid deficiency are rescued (Figure 27C and D). The normalisation of myeloid-biased differentiation correlates with altered HSC composition, in that high frequency of LT-HSCs are reduced while impaired lymphoid-biased HSCs are restored (Fig. 27E-H). Given that progeroid mice appear to follow the same Mk remodelling signature, it is hypothesized that rejuvenation of progeroid HSCs under β3-AR activation is mainly due to restored HSC-Mk interaction. To test the hypothesis, immunofluorescence staining of HSCs ($CD150^+lin^-CD48^-$ cells), haematopoietic progenitors (c-kit^+ cells) and Mks ($CD42^+$ cells or $CD41^+$ cells) was performed. Similar to β3-AR deficient mice and normally aged mice, HSCs locate more distantly from Mks in HGPS. However, this alienation is partially restored by β3-AR agonist treatment (Fig. 27L-N and P). Likewise, lower frequency of progeroid Mks ($CD41^+$ cells) are found adjacent with haematopoietic progenitors (c-kit^+ cells), but this association is normalised in response to chronic β3-AR activation

(Fig. 27I-K and O). These results suggest that activating β3-AR can improve certain haematopoietic and niche ageing features in HGPS.

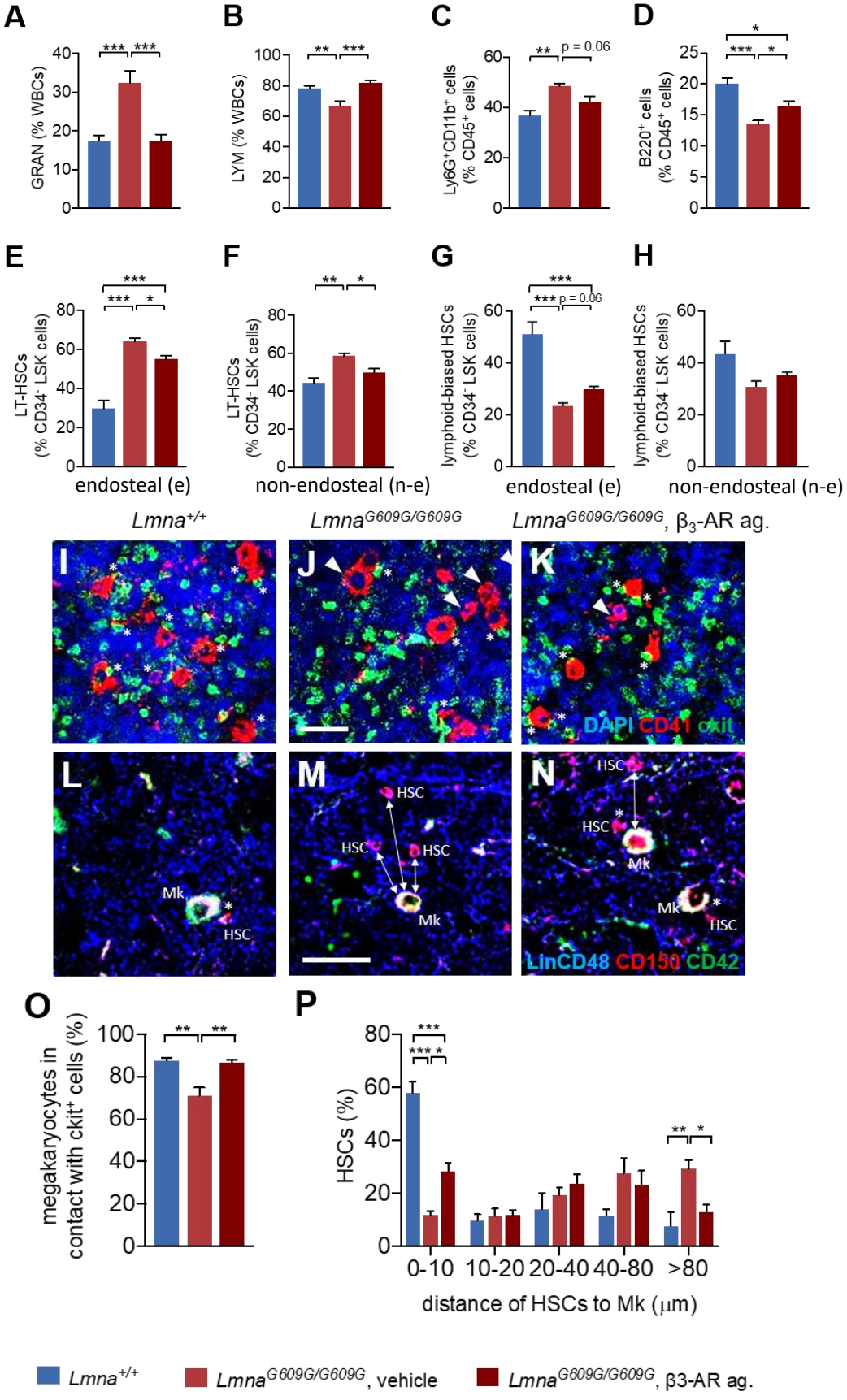
A
B
C
D
GRAN (% WBCs)
LYM (% WBCs)
Ly6G+CD11b+ cells (% CD45+ cells)
B220+ cells (% CD45+ cells)
p = 0.06
E
F
G
H
LT-HSCs (% CD34- LSK cells)
lymphoid-biased HSCs (% CD34- LSK cells)
p = 0.06
endosteal (e)
non-endosteal (n-e)
Lmna+/+
LmnaG609G/G609G
LmnaG609G/G609G, β3-AR ag.
I
J
K
DAPI CD41 ckit
L
M
N
HSC
Mk
LinCD48 CD150 CD42
O
megakaryocytes in contact with ckit+ cells (%)
P
HSCs (%)
0-10
10-20
20-40
40-80
>80
distance of HSCs to Mk (μm)
Lmna+/+
LmnaG609G/G609G, vehicle
LmnaG609G/G609G, β3-AR ag.

Figure 27. β3-AR agonist improves HSC number, lineage skewing and localization near Mks in HGPS.
(A and B) Frequency of (A) granulocytes and (B) lymphocytes in white blood cells (WBCs) of WT mice (n = 8) or *Lmna*$^{G609G/G609G}$ mice (n = 6) treated with β3-AR agonist (BRL37344, 2 mg/kg/day, intraperitoneally [i.p.]) or vehicle for 8 weeks. (C, D) Frequency of BM (C) Ly6G+CD11b+ neutrophils or (D) B220+ B cells in these mice. (E-H) Frequency of (E, F) LT-HSCs and (G, H) lymphoid-biased HSCs in CD34^{-}LSK cells in (E, G) endosteal or (F, H) non-endosteal BM of these mice (n = 6). (I–K, O) Representative immunofluorescence (I–K) and quantification (O) of CD41^{+} megakaryocytes adjacent (asterisks) or nonadjacent (arrowheads) to c-kit^{+} (green) HSPCs in BM of WT mice (n = 3) and *Lmna*$^{G609G/G609G}$ mice (n = 5) treated with β3-AR agonist or vehicle. Scale bar, 50 mm. (L–N, P) Representative immunofluorescence (L–N) and distribution (P) of BM CD150^{+} (red) HSCs (negative for mature haematopoietic lineage markers, blue) adjacent (asterisks), or nonadjacent (arrows) to CD42^{+} (green) megakaryocytes. Scale bar, 50 mm. Data are means ± SEM. *p < 0.05; **p < 0.01; ***p < 0.001. (A–H, O) One-way ANOVA and Bonferroni pairwise comparisons. (P) Two-way ANOVA and Bonferroni pairwise comparisons.

4.11 Chronic β3-AR agonist treatment improves exacerbated megakaryopoiesis in MPNs

Since modulating sympathetic signalling was able to reverse myeloid-skewing in premature ageing, whether it can also be applied to the treatment of age-related blood disorders was tested. MPNs share several haematopoietic features with normal ageing, such as BM inflammation, increased HSC proliferation and myeloid-biased differentiation toward platelet production. A previous study by our group reported that the development of MPNs is accelerated in β3-AR deficient microenvironment. Chronic treatment of β3-AR agonist or neuroprotective agents mitigates disease progression by lowering peripheral platelet/neutrophil counts and improving myelofibrosis (Arranz et al., 2014). BM histology from the same cohort of experiments (MPN mice treated with β3-AR agonist and β3-AR deficient mice carrying MPN BM cells) was analysed in order to get insight into the biology of Mks. H&E staining shows a significant reduction of Mk numbers in β3-AR agonist-treated MPN mice (Fig. 28A and B). Atypical Mk clusters and aberrant Mk distribution, a hallmark of myelofibrosis, are also normalised (Fig. 28A-C). Immunofluorescence staining of CD41 and CD42 cells was performed, confirming that both Mk precursors (small $CD41^{+}CD42^{+}$ cells) and mature Mks (large $CD41^{+}CD42^{+}$ cells) are decreased (Fig. 28H-K). In contrast, higher number of megakaryocytic cells was observed in β3-AR deficient mice with MPN, as compared to WT recipients (Fig. 28D-G). BM trephines of MPN patients from a follow-up clinical study led by Dr. Drexler et al. were subjected to histology analysis. Immunohistochemistry staining of CD34 (which labels HSPCs and vessels) reveals that Mk (identified by cell size)-vessel contact is decreased after β3-AR agonist treatment (Fig. 28L-N), despite thrombocytosis reportedly being unimproved (Drexler et al., 2019). Taking into consideration the relatively low dose and duration of treatment in the human study, these results

suggest that chronic β3-AR agonist treatment could potentially improve exacerbated megakaryopoiesis in MPNs.

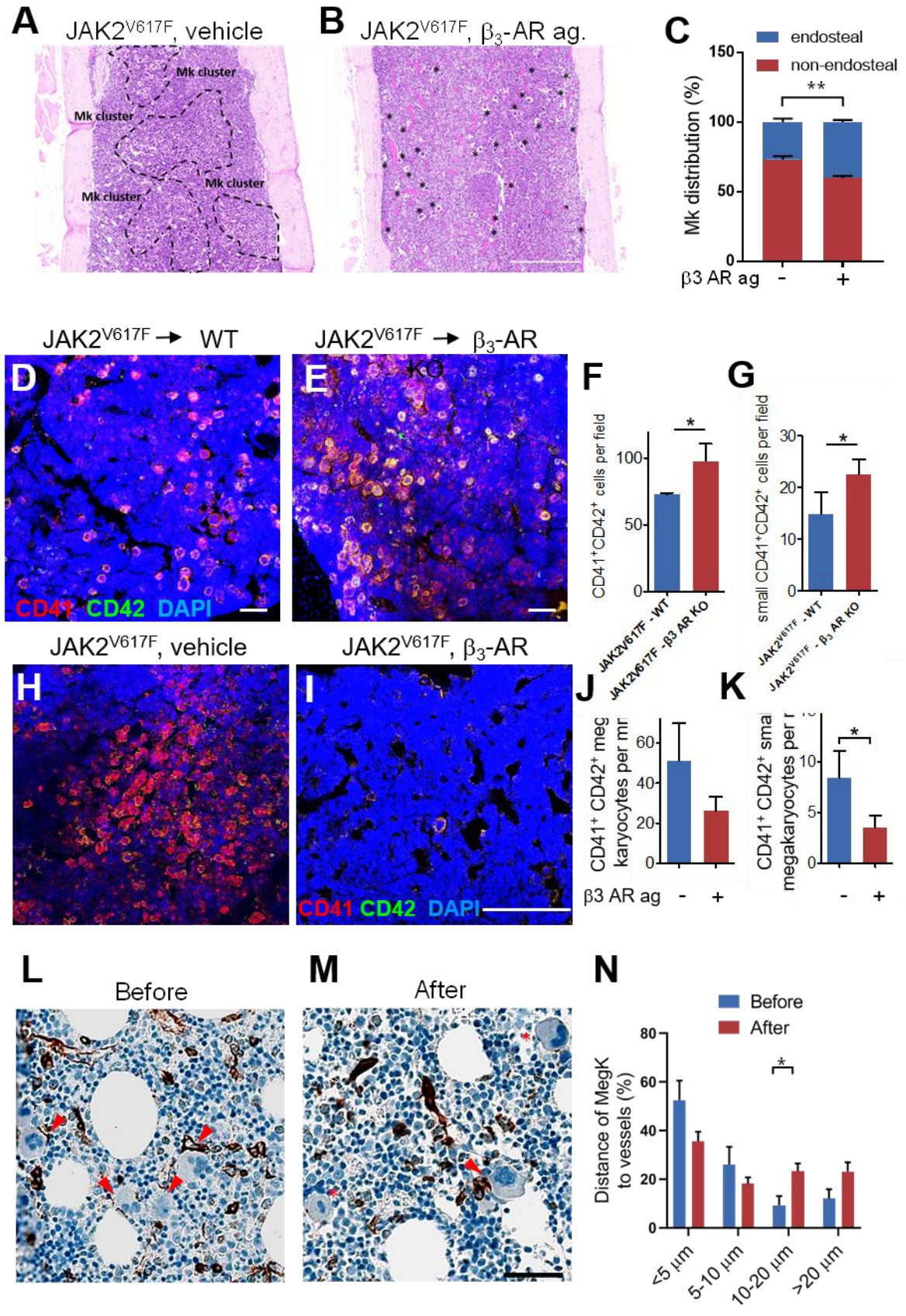
A
JAK2V617F, vehicle
Mk cluster
Mk cluster
Mk cluster
Mk cluster
B
JAK2V617F, β3-AR ag.
C
endosteal
non-endosteal
**
Mk distribution (%)
150
100
50
0
β3 AR ag - +
JAK2V617F → WT
JAK2V617F → β3-AR KO
D
E
CD41 CD42 DAPI
F
G
CD41+CD42+ cells per field
small CD41+CD42+ cells per field
*
JAK2V617F - WT
JAK2V617F - β3 AR KO
H
JAK2V617F, vehicle
I
JAK2V617F, β3-AR
CD41 CD42 DAPI
J
K
CD41+ CD42+ megakaryocytes per mm
β3 AR ag - +
L
Before
M
After
N
Before
After
Distance of MegK to vessels (%)
<5 μm
5-10 μm
10-20 μm
>20 μm

Figure 28. β3-AR agonist improves exacerbated megakaryopoiesis in MPNs. (A, B) Representative H&E staining in femoral BM sections of MPN mice (Mx1-cre;JAK2(V617F)) treated with (A) vehicle (n = 3) or (B) β3-AR agonist (n = 4). Scale bar, 250 μm. Megakaryocyte clusters are shown in vehicle treated group. Single megakaryocyte (labelled with star) was shown in β3-AR agonist treated group. (C) Quantification of megakaryocyte distribution. Endosteal region was defined as the area within 1/5 of the BM width from the bone surface. Quantification was done by averaging the results from at least 3 random fields (10X magnification) per mouse. (D-E) Representative immunofluorescence staining for CD41 (red) and CD42 (green) in femoral BM sections of (D) WT mouse and (E) β3-AR KO mouse transplanted with Mx1-cre;JAK2(V617F) mouse BM cells. Scale bar, 75 μm. (F) $CD41^+CD42^+$ cells per BM field (n = 3). (G) Small (< 300 μm^2) $CD41^+CD42^+$ cells (n = 3). (H, I) Representative immunofluorescence staining for CD41 (red) and CD42 (green) in femoral BM sections of mice treated with (Q) vehicle or (R) β3-AR agonist (BRL37344, 2 mg kg^{-1}) for 12 weeks. Scale bar, 75 μm. (J) $CD41^+CD42^+$ megakaryocytes per BM field (n = 3). (K) Small (< 300 μm^2) $CD41^+CD42^+$ megakaryocytes (n = 3) per BM field. Average of ≥6 random fields. (L-M) Representative immunohistochemistry staining for CD34 (brown) in BM trephines from MPN patients treated with β3-AR agonist (mirabegron) for 24 weeks. Vessels are identified as $CD34^+$ tubular structure while megakaryocytes are identified by morphology. Arrowheads depict megakaryocytes adjacent with vessels. Asterisks depict megakaryocytes nonadjacent with vessels. Scale bar, 50 μm. (N) Quantification of the distance of megakaryocytes to $CD34^+$ vessels. Data are means ± SEM * $p < 0.05$; ** $p < 0.01$. (C, F, G, J, K) Unpaired two-tailed t test. (N) Two-way ANOVA and Bonferroni pairwise comparisons.

5. Conclusions and Discussions

HSC ageing was initially considered to be driven mostly by cell-autonomous mechanisms. However, it is important to note that not only HSCs, but all the other cell types, suffer biological changes with age. The close relationship between BM HSCs and their neighbouring cells suggests that upon ageing, alterations in both compartments (HSC and the microenvironment) might have influences on each other. Given that most HSCs are maintained in perivascular regions, vessels and vessel-adjacent niche populations in response to ageing have been reported by many groups. Common findings are that cells near endosteum (transition zone vessels, or TZVs, arterioles and their associated MSCs) contract while cells away from bone surfaces (Mks, sinusoids, small capillaries and their associated MSCs) expand or remain unchanged. However, studies regarding age-related changes in the size of BM sympathetic neurons are controversial, and the mechanisms by which sympathetic signalling regulates haematopoietic ageing are largely unexplored. Based on the observation that Th^+ nerve fibres are augmented in aged mice, the current study expands this observation to further dissecting neuronal regulation of HSC ageing through the microenvironment, centred on myeloid/megakaryocytic-biased differentiation of HSCs.

5.1 Key findings of the study

The current study demonstrates that increased sympathetic activity causes increased myelopoiesis during ageing, majorly through activating β2-AR, since high peripheral platelets and BM megakaryocytic cells are present in old WT mice but absent in old *Adrb2*$^{-/-}$ mice (or *Adrb2*$^{-/-}$*Adrb3*$^{-/-}$ mice), but not in old *Adrb3*$^{-/-}$ mice (Fig. 19 and Fig. 21). The effect appears to be dominant in the endosteal BM, where the alteration of Mk lineage cells is more prominent,

compared to non-endosteal compartments (Fig. 19R and S, and Fig. 21H-K). The chimera mouse studies further indicate that the regulation of Mk differentiation by β2-AR in endosteal niches is dependent on the microenvironment (Fig. 21H-K). Supported by *in vitro* coculture experiments, β2-AR agonist promotes Mk differentiation only when stromal cells are present (Fig. 20). TPO is indispensable for driving Mk differentiation, while cytokines upregulated in ageing, such as IL-1, IL-3 and IL-6, have been reported to promote the process. The study confirms that IL-6 concentration is higher in old mice, but is reduced in adult β2-AR deficient mice and specifically in the endosteal BM (Fig. 22B). MS-5 stromal cells increase IL-6 mRNA transcripts under β2-AR activation (Fig. 22C), revealing MSC-like cell as one possible source of IL-6 in the endosteal niches. Moreover, β2-AR agonist treatment fails to enhance Mk differentiation when IL-6 is depleted from the microenvironment (Fig. 22I). These results strongly suggest that β2-AR in endosteal niches contributes to Mk differentiation during ageing, which relies on stromal cell-derived IL-6. However, certain haematopoietic cell-autonomous effects on MkPs in non-endosteal niches are also observed (Fig. 21I and K), despite the results neither showing significant difference nor supported by the coculture experiment. β2-AR is reportedly expressed by a wide range of cell types, including both haematopoietic and non-haematopoietic cells. Therefore, a direct activation of β2-AR on haematopoietic progenitors contributing to megakaryopoiesis during ageing in non-endosteal niches cannot be excluded. Dr. Chen et al. have reported that α-AR directly regulates Mk migration, adhesion and proplatelet formation under stress (Chen et al., 2016). Given compensatory mechanisms of α-ARs and β-ARs being reported, it is also likely that deficient β2-AR upregulates α-AR to promote Mk maturation. Future studies on the coordinating roles of α-ARs and β-ARs in regulating HSC ageing are expected and will certainly provide additional value to the field.

Interestingly, β3-AR exhibits opposing effects on myelopoiesis compared to β2-AR. Coculture experiments (HPC-7 cells and MS-5 cells) show that β3-AR agonist treatment inhibits Mk differentiation in the presence of stromal cells (Fig. 20D). The effect seems to be explained by differentiation blockade at the HSC level, since terminally differentiated population ($CD41^{hi}$ cells) declines whereas the most primitive, uncommitted population ($CD41^{lo}c\text{-}kit^{hi}$ cells) expands. Supporting this concept, in the long-term BM primary culture system, the number of HSCs, or more specifically the *Vwf*-$eGFP^{-}$ lymphoid-biased HSCs, is significantly increased under β3-AR activation (Fig. 24J). These results suggest that β3-AR might suppress myelopoiesis/megakaryopoiesis by preferentially activating the lymphoid-primed HSC compartment. Indeed, adult β3-AR deficient mice exhibit lower frequency of lymphoid-biased HSCs in endosteal BM (Fig. 23B and C), and a tendency toward increased granulocytes at the expense of B-cells (Fig. 23H-K). The chimera experiments confirm β3-AR signalling acts through the microenvironment (Fig. 23B and C), in line with the fact that HSCs do not express β3-AR. The endosteal-specific loss of lymphoid-biased HSCs correlates with higher concentration of IL-1, which have been reported to promote myeloid/megakaryocytic expansion (Beaulieu et al., 2014; Nishimura et al., 2015) (Pietras et al., 2016) or inhibit lymphopoiesis (Kennedy and Knight, 2015). Mechanistically, Nos-1-dependent NO production is a likely downstream pathway. β3-AR deficient mice have lower levels of Nos-1 transcripts and NO content in endosteal BM (Fig. 24E-H), and pharmacological inhibition of Nos-1 abrogates the effect of β3-AR agonist on lymphoid-biased HSCs (Fig. 24J). Strikingly, adult Nos-1 deficient mice and β3-AR deficient mice both display premature ageing of the BM architecture: diminished TZVs, increased numbers of small capillaries, and Mks apposition to sinusoids (Fig. 25A-I). Contraction of endosteal vessels possibly causes lymphoid deficiency in β3-AR deficient mice, since the majority of lymphoid-primed HSPCs is

reportedly present near endosteum. Moreover, LT-HSCs are found redistributing away from their putative Mk niches in β3-AR deficient mice (Fig. 25J-M). Altogether, these results suggest that lack of β3-AR remodels HSC-supporting niches into an ageing-permissive microenvironment, which accelerates lymphoid deficiency partially through Nos-1-NO dependent pathway.

These findings are consistent with a recent publication by Dr. Maryanovich et al. in that certain degree of premature ageing happens in β3-AR deficient mice. However, some differences also exist. In their study, imbalanced myeloid-lymphoid output is evident in BM HSPC compartments and the mature progenies in circulation, whereas in the present study only BM HSPCs (but not circulating blood cells) display myeloid skewing. In addition, Maryanovich et al claim that administration of a β3-AR agonist in old mice rejuvenates overall aged haematopoiesis. The present study demonstrates that the same β3-AR agonist can restore myeloid/megakaryocytic expansion in a mouse model of MPNs (Arranz et al., 2014) (Fig. 28) and progeria syndrome (Fig. 27). However, haematopoietic rejuvenation is not observed (evidenced by unchanged peripheral platelet counts) in WT mice treated with β3-AR agonist over 40 weeks (data not shown). Likewise, old MPN patients treated with β3-AR agonist render normal HSC-Mk distribution in the BM (Fig. 28L-N), but do not show rejuvenation in the peripheral blood system (Drexler et al., 2019). Furthermore, Dr. Maryanovich et al. propose that Th^+ fibres are reduced in ageing, aggravating HSC functions in a β3-AR-dependent manner. In contrast, investigators from our lab have observed increased Th^+ fibres in old mice (Ho et al., 2019), consistent with the well-known increase in sympathetic activity in the elderly. The present study further reveals that sympathetic activation of β2-AR is indispensable for myeloid-bias toward platelet production during ageing. These discrepancies suggest that neuronal regulation of HSC ageing cannot be attributed to β3-AR signalling alone. Of note,

changes of Th^+ fibres shown in BM sections does not equal to the levels of innervation. Myeloid and lymphoid cells are sources of neurotransmitters (Cosentino et al., 2015), meaning that BM neuronal activities incompletely depend on the area covered by nerve fibres. Sympathetic regulation of HSC myeloid-skewing is more likely explained by the activation or inactivation of different adrenergic receptors. A functional switch of neurotransmission (β2-AR overriding β3-AR) with age, rather than a general decline of innervation might initiate BM niche remodelling and subsequently promote HSC myeloid-skewing toward platelet production (Fig. 29).

In contrast to normal physiological ageing, the pathological ageing models show opposite phenotype in BM Th^+ fibres: either unchanged in progeria (HGPS) (Ho et al., 2019) or decreased in age-related myeloid disorders (MPNs) (Arranz et al., 2014). However, similar BM microenvironment alterations, such as inflammation (compare Fig. 18 and Fig. 26G-K) and Mk niche remodelling (compare Fig. 19A-H an Fig. 26A-F), are shared among normal ageing, pathological ageing, and β3-AR deficient mice. These results suggest that instead of overstimulating β2-AR, inactive β3-AR might play a dominant role in the development of pathological ageing. Therefore, this study has tested whether activating β3-AR can rejuvenate certain ageing features in progeria and myeloproliferative disorders. In progeroid mice, chronic β3-AR agonist treatment normalises imbalanced myeloid/lymphoid output (Fig. 27A-D), reduces the frequency of LT-HSCs (Fig. 27E-H) and restores the proximal association of HSCs to Mks (Fig. 27I-P). In MPNs mice, chronic β3-AR agonist treatment improves exacerbated megakaryopoiesis by normalising Mk clusters (Fig. 28D-K) and atypical Mk distribution (Fig. 28A-C). Of note, despite MPN patients also showing improvement in Mk distribution after treatment (Fig. 28L-N), JAK2(V617F) allele burden and high platelet/myeloid blood counts are reportedly not decreased (Drexler et al., 2019). These

differences might be drug-dependent (different drugs were used for humans and mice), explained by different dose, stage and duration of treatment, and/or reveal differences in BM microenvironment between murine and humans. They also suggest that targeting single neuronal pathway might not be sufficient to rejuvenate overall haematopoiesis. Combining selective β3-AR agonist and β2-AR antagonist could be a better therapeutic approach that could be tested in the future.

Finally, the present study provides insights into the typical ‘’chicken or egg’’ question in ageing: microenvironmental alterations initiate HSC ageing or old HSCs trigger niche remodelling? Haematopoietic ageing features seem to emerge at distinct ages. In murine ageing, defective lymphopoiesis starts early at the age of 8 months old (Young et al., 2016), while increased platelet counts doesn’t seem to be pronounced until 18 months (Ho et al., 2019). BM Th^+ sympathetic nerve fibres appear to be decreased in 12-month-olds mice (Maryanovich et al., 2018), but they are expanded in old (20 months-old) mice (Ho et al., 2019). Deficient β3-AR accelerates the loss of endosteal lymphoid-biased HSCs in 4-month-olds mice, but it does not exacerbate myeloid-skewing in the periphery of old mice (Fig. 23). In contrast, deficient β2-AR impairs megakaryopoiesis in both young and old mice, and double knockout of β2-AR and β3-AR recapitulates the haematopoietic phenotype of single β2-AR deficient mice. An adrenergic remodelling model contributing to imbalanced lymphoid/myeloid output through the microenvironment is proposed (Fig. 30): lack of β3-AR activity near endosteum initiates the contraction of endosteal niches, which attenuates lymphopoiesis, favours myeloid-bias and pushes HSCs away from the endosteum. Adrenergic switch from β3-AR to β2-AR promotes megakaryopoiesis, and possibly feedbacks to worsen the reduction of endosteal niches, since activation of β2-AR in osteoblasts is known to restrain bone formation (Kajimura et al.,

2011). Deficient β3-AR also alters Mk niches by promoting Mk apposition to sinusoids, which might facilitate the proliferation of neighbouring HSCs. As a secondary outcome, HSCs might exit from quiescence and become more susceptible to acquire somatic mutations and initiate myeloid malignancies. Future studies are warranted to determine whether the aged niche can facilitate the expansion of myeloid clones carrying clonal-haematopoiesis-related somatic mutations. These clones become dominant during ageing and are candidate prerequisites for the development of many myeloid malignancies and cardiovascular diseases (Busque et al., 2012; Fuster et al., 2017; Genovese et al., 2014; Jaiswal et al., 2014; Jaiswal et al., 2017; McKerrell et al., 2015; Xie et al., 2014; Zink et al., 2017). Therefore, strategies targeting the microenvironmental regulation of myelopoiesis might be able to affect clonal size or dominance.

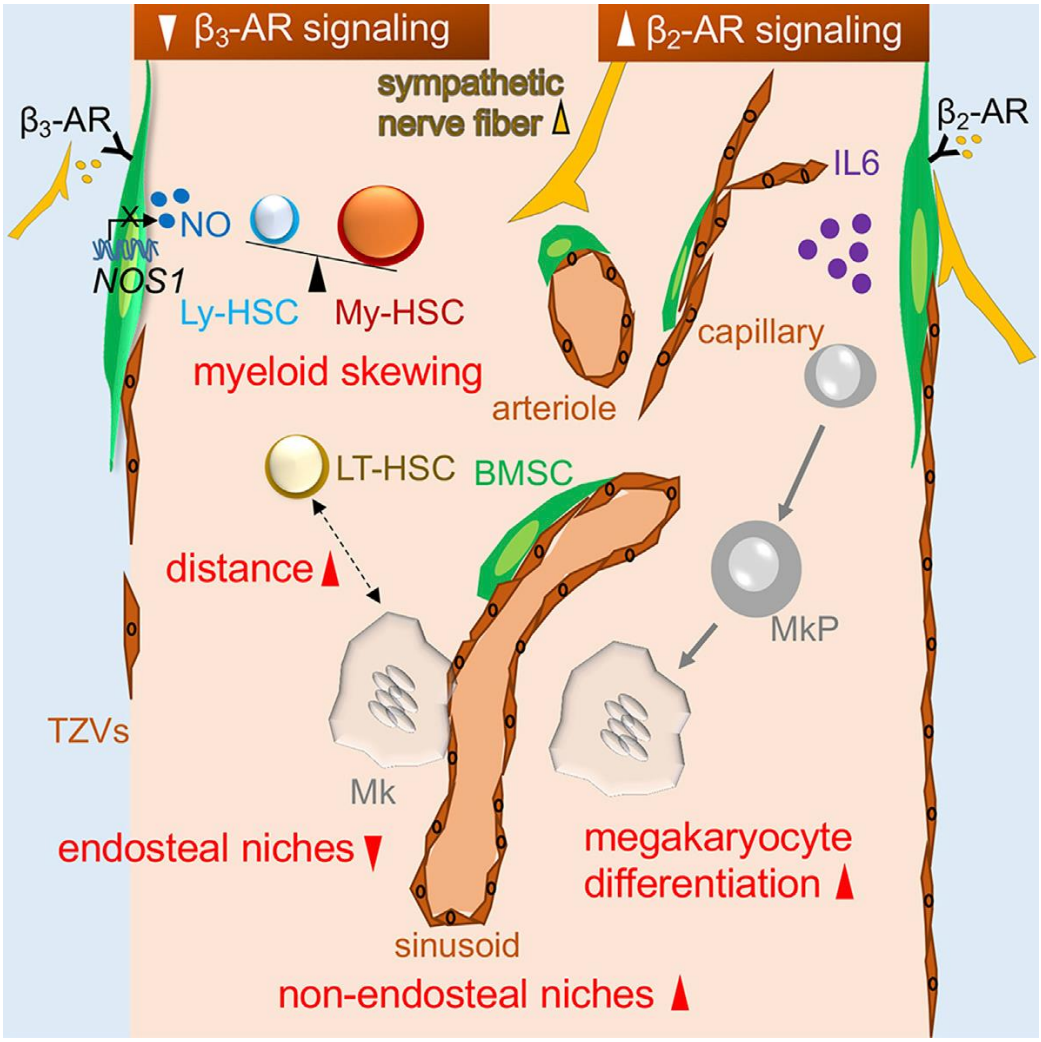

Figure 29. Working model of adrenergic remodelling contributing to HSC ageing.

Loss of β3-AR activity contracts endosteal niches by inhibiting NO production from the microenvironment (endothelial cells and/or stromal cells), which pushes HSCs away from the endosteum and favours myeloid-bias at the expense of lymphopoiesis. Adrenergic switch from β3-AR to β2-AR promotes Mk differentiation toward platelet production by increasing stromal cell-derived IL6. Accumulation of aged HSCs remodels the microenvironment by reinforcing β2-AR activity overriding β3-AR activity, expanding non-endosteal niches and altering the proximal association of HSCs to Mks. LT-HSC: long-term haematopoietic stem cell. My-HSC: myeloid-biased haematopoietic stem cell. Ly-HSC: lymphoid-biased haematopoietic stem cell. TZVs: transitional zone vessels. MkP: megakaryocyte progenitor. Mk: megakaryocyte. NO: nitric oxide. NOS1: nitric oxide synthase 1. BMSC: bone marrow stromal cells. IL6: interleukin 6

5.2 Potential implications of the study

Ageing is the major risk factor for haematological malignancies, such as MPNs, myelodysplastic syndrome (MDS), and acute myelogenous leukaemia (AML). The progression of myeloid neoplasms has been explained by clonal haematopoiesis: HSC clones acquiring leukaemia-associated somatic mutations are selected with age, take over normal HSCs and ultimately predispose haematological malignancies. HSC-autonomous dysregulations in ageing (Dykstra et al., 2011), such as epigenetic deregulation (Chambers et al., 2007), replication stress (Flach et al., 2014), deficient DNA repair (Rossi et al., 2007), and transition from canonical to non-canonical Wnt signalling (Florian et al., 2013), are potential drivers for disease development. Old HSCs also suffer metabolic changes (Chandel et al., 2016; Ito and Suda, 2014), impaired autophagy (Ho et al., 2017) and altered protein homeostasis (Vilchez et al., 2014), which contribute to the decline of their regenerative potential. However, the selection pressure is not dependent on these intrinsic mechanisms alone. Microenvironment challenges also govern the expansion of HSC clones with specific functional properties. Recent studies suggest that HSCs are heterogenous, and HSC subpopulations might occupy different niches. For instance, lymphoid-biased HSCs lodge near endosteum, whereas platelet/myeloid-biased HSCs are found adjacent with Mks in sinusoids. As a result, changes of endosteal and non-endosteal niche size in ageing might favour the selection of platelet/myeloid-biased HSCs over lymphoid-biased HSCs, leading to declined immunity and myeloid-skewing as an overall net outcome. The specific effect of β3-AR on lymphoid-biased HSCs supports the concept that clonal shift can result from relative loss of certain HSC clones rather than promoting the others. BM inflammation is another selection force. Traditional views believe that myeloid cells are a major source of inflammation, yet current studies argue that haematopoietic cells do not inflame the aged BM alone. Senescence of MSCs,

accumulation of adipocytes (Mancuso and Bouchard, 2019), decreased NO production and increased sympathetic innervation all contribute to abnormal inflammation, which promotes myeloid expansion by indirectly facilitating niche remodelling, and positively selecting mutant and/or myeloid-biased HSC clones. Of note, leukaemia stem cells can also hijack normal HSC niches to reinforce the selection (Behrmann et al., 2018), suggesting an important interplay between HSCs and HSC-supporting niches. This study connects ageing and age-related cancers from the microenvironmental aspects, focuses on impaired neuronal regulation as one key example, and sheds lights on the possible implications on inhibiting myeloid clone expansion by targeting aberrant niche functions.

Cardiovascular diseases are more frequent in the elderly. Blood cells overproduced in ageing, such as platelets and neutrophils, are essential players in cardiovascular diseases, suggesting a close relationship between cardiovascular dysfunctions and the haematopoietic systems. In atherosclerosis, for example, cardiovascular risk factors are known to promote myelopoiesis and megakaryopoiesis by providing external cues from the liver (Nagareddy et al., 2018). Obesity indirectly causes myelopoiesis through liver macrophage-derived IL-1β (Nagareddy et al., 2014). Hyperglycaemia induces S100A8/A9 expression by neutrophils, which stimulates IL-6 and subsequent production of TPO from the liver to drive BM megakaryopoiesis (Lee and Bergmeier, 2017). Clinically, β-blockers (mainly targeting β1-AR and β2-AR) are widely used in cardiovascular medicine. The effect is reported to be mediated mainly through reducing platelet aggregation and/or hypertension (Bonten et al., 2014). However, the specific role of β2-AR found in the present study raises the possibility that β-blockers might also affect BM Mk differentiation, which helps explain why some β-blockers are more effective than the others.

Over the last decade, efforts have been made to optimize platelet production *in vitro* in transfusion medicine. Challenges include inefficient Mk differentiation, poor production of end-stage mature cells and expensive cytokine cocktails. The present study applies an MSC-coculture system, in which minimum amounts of haematopoietic cytokines (only TPO and IL-1β) are required, successfully doubling the numbers of megakaryocytic cells from human cord blood-derived HSPCs under β2-AR agonist treatment. One future direction will be to test whether platelet production is also significantly enhanced followed by increased megakaryopoiesis. If yes, translating the setting into manufacturing processes will be a promising approach to treat thrombocytopenia.

5.3 Conclusion remarks and the future scope

In conclusion, this study demonstrates for the first time that different β adrenergic signals have microenvironment-dependent, but opposite effects on HSC lineage commitment during ageing. β2-AR promotes Mk differentiation through stromal cell-derived IL-6, whereas β3-AR regulates BM niche remodelling, balancing myeloid/lymphoid-biased HSCs partially through Nos1-NO-dependent manner. Premature ageing and myeloid disorders can be improved by targeting the microenvironment using β3-AR agonist. Herein, several interesting questions arise, and could potentially develop into follow-up projects in the future. Firstly, what are the cell types involved in aged haematopoiesis under β2-AR and/or β3-AR regulation? Secondly, how does the proposed adrenergic switch from β3-AR to β2-AR happen during ageing? A possible answer to the questions is that cells highly expressing β2-AR replace those with high expression of β3-AR over time. Another possibility is that BM niche cells ubiquitously increase β2-AR while

decrease β3-AR upon ageing. These hypotheses require to be validated since the experiments were performed using global knockouts. Tissue-specific deletion of β2-AR/β3-AR in endothelial or mesenchymal lineages will be an ideal approach. Last but not the least, what is the role of β2-AR in MPNs? Generating β2-AR deficient mice with chimeric JAK2(V617F) BM cells, or treating MPNs mice with selective β2-AR antagonist will certainly add to the field.

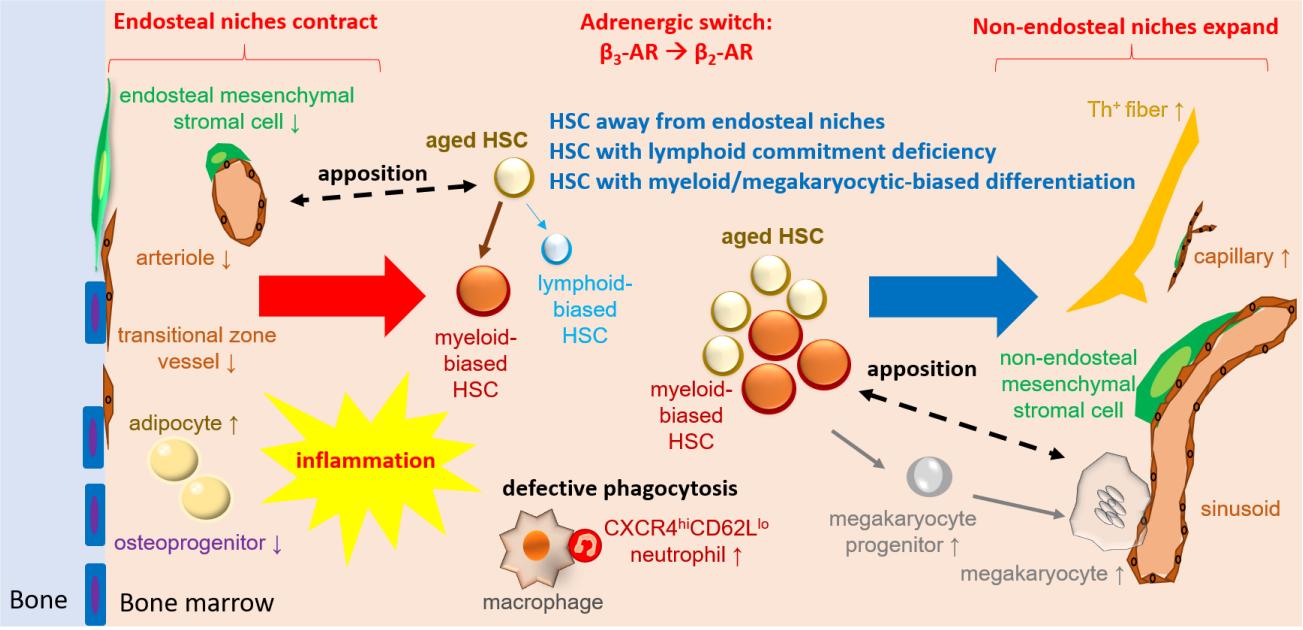

Figure 30. Schematic representation of the interplay between HSCs and the microenvironment during ageing.

Loss of β3-AR activity contracts endosteal niches by decreasing endosteal vessels and the associated BMSCs, which disadvantage lymphoid-biased HSCs. As a secondary outcome, HSCs are pushed away from the endosteum to central marrow, favoring myeloid bias at the expense of lymphopoiesis. Accumulation of aged HSCs remodels the microenvironment by reinforcing adrenergic activity through β2-AR, expanding non-endosteal niches and promotes megakaryocyte differentiation toward platelet production. The damaged endosteal niches, increased sympathetic innervation on myeloid cells, and defective phagocytosis of senescent neutrophils by macrophages promote BM inflammation. An inflammatory cytokine storm positively selects myeloid-biased HSCs clones over lymphoid/non-biased HSCs and predispose myeloid malignancies.

Players	Size	Functions/Mechanisms
Mesenchymal lineages	■ Decreased endosteal Nestin-GFP⁺ cells ■ Increased non-endosteal Nestin-GFP⁺ cells ■ Decreased αSMA⁺ cells, NG2⁺ cells, PDGFβ⁺ cells	➢ Increased adipogenesis ➢ Decreased osteogenic differentiation ➢ Cellular senescence ➢ Altered nitric oxide (NO), urea cycle pathways ➢ Reduced secretion of niche factors ➢ HSC closer to non-endosteal niches, away from endosteal niches
Endothelial cells	■ Increased overall vascular density ■ Decreased arterioles; shortened arteriole segments ■ Unchanged/preserved sinusoids ■ Decreased transitional zone vessels ■ Increased small capillaries	➢ Increased vascular leakiness ➢ Vasodilation ➢ Decreased angiogenic potential ➢ Decreased Notch activity ➢ HSC away from arterioles ➢ HSC preserved in sinusoids ➢ DLL4 regulating HSC myeloid-skewing ➢ Sinusoidal Jag2 regulating HSC proliferation
Inflammatory cytokines	■ Increased IL-1, IL-3, IL-6, TNFα, INFγ, TGFβ	➢ IL-1β regulating HSC myeloid-skewing ➢ IL-6 regulating megakaryocyte differentiation ➢ TNFα protecting HSC from necroptosis ➢ TGF-β regulating megakaryopoiesis ➢ IFN regulating megakaryocytic-bias
Sympathetic nervous system	■ Increased Th⁺ nerve fibers	➢ β2-AR activation regulating HSC myeloid-skewing toward platelet production ➢ β3-AR inactivation regulating niche remodeling, HSC lymphoid deficiency ➢ Functional switch of β adrenergic signaling (β_2-AR overriding β_3-AR)
Others	■ Increased megakaryocytes ■ Accumulation of CXCR4^{high}CD62L^{low} senescent neutrophils	➢ Megakaryocytes closer to sinusoids ➢ HSC away from megakaryocytes ➢ Macrophages with impaired phagocytosis

Table 6. Summary of BM microenvironmental alterations during ageing.

6. References

Adams, G.B., Chabner, K.T., Alley, I.R., Olson, D.P., Szczepiorkowski, Z.M., Poznansky, M.C., Kos, C.H., Pollak, M.R., Brown, E.M., and Scadden, D.T. (2006). Stem cell engraftment at the endosteal niche is specified by the calcium-sensing receptor. Nature *439*, 599-603.

Agarwal, A., Morrone, K., Bartenstein, M., Zhao, Z.J., Verma, A., and Goel, S. (2016). Bone marrow fibrosis in primary myelofibrosis: pathogenic mechanisms and the role of TGF-beta. Stem Cell Investig *3*, 5.

Ambrosi, T.H., Scialdone, A., Graja, A., Gohlke, S., Jank, A.M., Bocian, C., Woelk, L., Fan, H., Logan, D.W., Schurmann, A.*, et al.* (2017). Adipocyte Accumulation in the Bone Marrow during Obesity and Aging Impairs Stem Cell-Based Hematopoietic and Bone Regeneration. Cell stem cell *20*, 771-784 e776.

Arai, F., Hirao, A., Ohmura, M., Sato, H., Matsuoka, S., Takubo, K., Ito, K., Koh, G.Y., and Suda, T. (2004). Tie2/angiopoietin-1 signaling regulates hematopoietic stem cell quiescence in the bone marrow niche. Cell *118*, 149-161.

Arranz, L., Sanchez-Aguilera, A., Martin-Perez, D., Isern, J., Langa, X., Tzankov, A., Lundberg, P., Muntion, S., Tzeng, Y.S., Lai, D.M.*, et al.* (2014). Neuropathy of haematopoietic stem cell niche is essential for myeloproliferative neoplasms. Nature *512*, 78-81.

Bain, B.J. (2010). Megakaryocyte dysplasia in primary myelofibrosis. Am J Hematol *85*, 886.

Balzano, M., De Grandis, M., Vu Manh, T.P., Chasson, L., Bardin, F., Farina, A., Serge, A., Bidaut, G., Charbord, P., Herault, L.*, et al.* (2019). Nidogen-1 Contributes to the Interaction Network Involved in Pro-B Cell Retention in the Peri-sinusoidal Hematopoietic Stem Cell Niche. Cell Rep *26*, 3257-3271 e3258.

Beaulieu, L.M., Lin, E., Mick, E., Koupenova, M., Weinberg, E.O., Kramer, C.D., Genco, C.A., Tanriverdi, K., Larson, M.G., Benjamin, E.J.*, et al.* (2014). Interleukin 1 receptor 1 and interleukin 1beta regulate megakaryocyte maturation,

platelet activation, and transcript profile during inflammation in mice and humans. Arterioscler Thromb Vasc Biol *34*, 552-564.

Beerman, I., Bhattacharya, D., Zandi, S., Sigvardsson, M., Weissman, I.L., Bryder, D., and Rossi, D.J. (2010). Functionally distinct hematopoietic stem cells modulate hematopoietic lineage potential during aging by a mechanism of clonal expansion. Proc Natl Acad Sci U S A *107*, 5465-5470.

Behrmann, L., Wellbrock, J., and Fiedler, W. (2018). Acute Myeloid Leukemia and the Bone Marrow Niche-Take a Closer Look. Front Oncol *8*, 444.

Bonten, T.N., Plaizier, C.E., Snoep, J.J., Stijnen, T., Dekkers, O.M., and van der Bom, J.G. (2014). Effect of beta-blockers on platelet aggregation: a systematic review and meta-analysis. British journal of clinical pharmacology *78*, 940-949.

Boulais, P.E., and Frenette, P.S. (2015). Making sense of hematopoietic stem cell niches. Blood *125*, 2621-2629.

Boyd, A.L., Reid, J.C., Salci, K.R., Aslostovar, L., Benoit, Y.D., Shapovalova, Z., Nakanishi, M., Porras, D.P., Almakadi, M., Campbell, C.J.V.*, et al.* (2017). Acute myeloid leukaemia disrupts endogenous myelo-erythropoiesis by compromising the adipocyte bone marrow niche. Nat Cell Biol *19*, 1336-1347.

Bruns, I., Lucas, D., Pinho, S., Ahmed, J., Lambert, M.P., Kunisaki, Y., Scheiermann, C., Schiff, L., Poncz, M., Bergman, A.*, et al.* (2014). Megakaryocytes regulate hematopoietic stem cell quiescence through CXCL4 secretion. Nat Med *20*, 1315-1320.

Busque, L., Patel, J.P., Figueroa, M.E., Vasanthakumar, A., Provost, S., Hamilou, Z., Mollica, L., Li, J., Viale, A., Heguy, A.*, et al.* (2012). Recurrent somatic TET2 mutations in normal elderly individuals with clonal hematopoiesis. Nat Genet *44*, 1179-1181.

Calvi, L.M., Adams, G.B., Weibrecht, K.W., Weber, J.M., Olson, D.P., Knight, M.C., Martin, R.P., Schipani, E., Divieti, P., Bringhurst, F.R.*, et al.* (2003). Osteoblastic cells regulate the haematopoietic stem cell niche. Nature *425*, 841-

846.

Casanova-Acebes, M., Pitaval, C., Weiss, L.A., Nombela-Arrieta, C., Chevre, R., N, A.G., Kunisaki, Y., Zhang, D., van Rooijen, N., Silberstein, L.E., *et al.* (2013). Rhythmic modulation of the hematopoietic niche through neutrophil clearance. Cell *153*, 1025-1035.

Chambers, S.M., Shaw, C.A., Gatza, C., Fisk, C.J., Donehower, L.A., and Goodell, M.A. (2007). Aging hematopoietic stem cells decline in function and exhibit epigenetic dysregulation. PLoS Biol *5*, e201.

Chandel, N.S., Jasper, H., Ho, T.T., and Passegue, E. (2016). Metabolic regulation of stem cell function in tissue homeostasis and organismal ageing. Nat Cell Biol *18*, 823-832.

Chen, S., Du, C., Shen, M., Zhao, G., Xu, Y., Yang, K., Wang, X., Li, F., Zeng, D., Chen, F., *et al.* (2016). Sympathetic stimulation facilitates thrombopoiesis by promoting megakaryocyte adhesion, migration, and proplatelet formation. Blood *127*, 1024-1035.

Choi, E.S., Hokom, M.M., Chen, J.L., Skrine, J., Faust, J., Nichol, J., and Hunt, P. (1996). The role of megakaryocyte growth and development factor in terminal stages of thrombopoiesis. Br J Haematol *95*, 227-233.

Cordeiro Gomes, A., Hara, T., Lim, V.Y., Herndler-Brandstetter, D., Nevius, E., Sugiyama, T., Tani-Ichi, S., Schlenner, S., Richie, E., Rodewald, H.R., *et al.* (2016). Hematopoietic Stem Cell Niches Produce Lineage-Instructive Signals to Control Multipotent Progenitor Differentiation. Immunity *45*, 1219-1231.

Cosentino, M., Marino, F., and Maestroni, G.J. (2015). Sympathoadrenergic modulation of hematopoiesis: a review of available evidence and of therapeutic perspectives. Front Cell Neurosci *9*, 302.

de Haan, G., and Lazare, S.S. (2018). Aging of hematopoietic stem cells. Blood *131*, 479-487.

De Sandre-Giovannoli, A., Bernard, R., Cau, P., Navarro, C., Amiel, J., Boccaccio,

I., Lyonnet, S., Stewart, C.L., Munnich, A., Le Merrer, M., *et al.* (2003). Lamin a truncation in Hutchinson-Gilford progeria. Science *300*, 2055.

del Toro, R., and Méndez-Ferrer, S. (2013). Autonomic regulation of hematopoiesis and cancer. Haematologica *98*, 1663-1666.

Ding, L., and Morrison, S.J. (2013). Haematopoietic stem cells and early lymphoid progenitors occupy distinct bone marrow niches. Nature *495*, 231-235.

Drexler, B., Passweg, J.R., Tzankov, A., Bigler, M., Theocharides, A.P., Cantoni, N., Keller, P., Stussi, G., Ruefer, A., Benz, R., *et al.* (2019). The sympathomimetic agonist mirabegron did not lower JAK2-V617F allele burden, but restored nestin-positive cells and reduced reticulin fibrosis in patients with myeloproliferative neoplasms: results of phase II study SAKK 33/14. Haematologica *104*, 710-716.

Dykstra, B., Olthof, S., Schreuder, J., Ritsema, M., and de Haan, G. (2011). Clonal analysis reveals multiple functional defects of aged murine hematopoietic stem cells. J Exp Med *208*, 2691-2703.

Ema, H., Morita, Y., and Suda, T. (2014). Heterogeneity and hierarchy of hematopoietic stem cells. Exp Hematol *42*, 74-82 e72.

Ergen, A.V., Boles, N.C., and Goodell, M.A. (2012). Rantes/Ccl5 influences hematopoietic stem cell subtypes and causes myeloid skewing. Blood *119*, 2500-2509.

Eriksson, M., Brown, W.T., Gordon, L.B., Glynn, M.W., Singer, J., Scott, L., Erdos, M.R., Robbins, C.M., Moses, T.Y., Berglund, P., *et al.* (2003). Recurrent de novo point mutations in lamin A cause Hutchinson-Gilford progeria syndrome. Nature *423*, 293-298.

Eto, K., and Kunishima, S. (2016). Linkage between the mechanisms of thrombocytopenia and thrombopoiesis. Blood *127*, 1234-1241.

Fazeli, P.K., Horowitz, M.C., MacDougald, O.A., Scheller, E.L., Rodeheffer, M.S., Rosen, C.J., and Klibanski, A. (2013). Marrow fat and bone--new perspectives. The Journal of clinical endocrinology and metabolism *98*, 935-945.

Feldberg, W.S. (1952). The physiology of the autonomic nervous system. Lect Sci Basis Med *2*, 343-374.

Flach, J., Bakker, S.T., Mohrin, M., Conroy, P.C., Pietras, E.M., Reynaud, D., Alvarez, S., Diolaiti, M.E., Ugarte, F., Forsberg, E.C.*, et al.* (2014). Replication stress is a potent driver of functional decline in ageing haematopoietic stem cells. Nature *512*, 198-202.

Florian, M.C., Dorr, K., Niebel, A., Daria, D., Schrezenmeier, H., Rojewski, M., Filippi, M.D., Hasenberg, A., Gunzer, M., Scharffetter-Kochanek, K.*, et al.* (2012). Cdc42 activity regulates hematopoietic stem cell aging and rejuvenation. Cell Stem Cell *10*, 520-530.

Florian, M.C., Nattamai, K.J., Dorr, K., Marka, G., Uberle, B., Vas, V., Eckl, C., Andra, I., Schiemann, M., Oostendorp, R.A.*, et al.* (2013). A canonical to non-canonical Wnt signalling switch in haematopoietic stem-cell ageing. Nature *503*, 392-396.

Frisch, B.J., Hoffman, C.M., Latchney, S.E., LaMere, M.W., Myers, J., Ashton, J., Li, A.J., Saunders, J., 2nd, Palis, J., Perkins, A.S.*, et al.* (2019). Aged marrow macrophages expand platelet-biased hematopoietic stem cells via Interleukin1B. JCI Insight *5*.

Fuster, J.J., Maclauchlan, S., Zuriaga, M.A., Polackal, M.N., and Walsh, K. (2017). Clonal Hematopoiesis Associated with Tet2 Deficiency Accelerates Atherosclerosis in Hyperlipidemic Mice. Atherosclerosis *263*, E14-E14.

Garcia-Garcia, A., Korn, C., Garcia-Fernandez, M., Domingues, O., Villadiego, J., Martin-Perez, D., Isern, J., Bejarano-Garcia, J.A., Zimmer, J., Perez-Simon, J.A.*, et al.* (2018). Dual cholinergic signals regulate daily migration of hematopoietic stem cells and leukocytes. Blood.

Garcia-Prat, L., Sousa-Victor, P., and Munoz-Canoves, P. (2013). Functional dysregulation of stem cells during aging: a focus on skeletal muscle stem cells. The FEBS journal *280*, 4051-4062.

Gauthier, C., Leblais, V., Kobzik, L., Trochu, J.N., Khandoudi, N., Bril, A., Balligand, J.L., and Le Marec, H. (1998). The negative inotropic effect of beta3-adrenoceptor stimulation is mediated by activation of a nitric oxide synthase pathway in human ventricle. J Clin Invest *102*, 1377-1384.

Genovese, G., Kahler, A.K., Handsaker, R.E., Lindberg, J., Rose, S.A., Bakhoum, S.F., Chambert, K., Mick, E., Neale, B.M., Fromer, M.*, et al.* (2014). Clonal hematopoiesis and blood-cancer risk inferred from blood DNA sequence. N Engl J Med *371*, 2477-2487.

Greenbaum, A.M., Revollo, L.D., Woloszynek, J.R., Civitelli, R., and Link, D.C. (2012). N-cadherin in osteolineage cells is not required for maintenance of hematopoietic stem cells. Blood *120*, 295-302.

Grigoryan, A., Guidi, N., Senger, K., Liehr, T., Soller, K., Marka, G., Vollmer, A., Markaki, Y., Leonhardt, H., Buske, C.*, et al.* (2018). LaminA/C regulates epigenetic and chromatin architecture changes upon aging of hematopoietic stem cells. Genome biology *19*, 189.

Grover, A., Sanjuan-Pla, A., Thongjuea, S., Carrelha, J., Giustacchini, A., Gambardella, A., Macaulay, I., Mancini, E., Luis, T.C., Mead, A.*, et al.* (2016). Single-cell RNA sequencing reveals molecular and functional platelet bias of aged haematopoietic stem cells. Nat Commun *7*, 11075.

Guidi, N., Sacma, M., Standker, L., Soller, K., Marka, G., Eiwen, K., Weiss, J.M., Kirchhoff, F., Weil, T., Cancelas, J.A.*, et al.* (2017). Osteopontin attenuates aging-associated phenotypes of hematopoietic stem cells. EMBO J *36*, 840-853.

Haas, S., Hansson, J., Klimmeck, D., Loeffler, D., Velten, L., Uckelmann, H., Wurzer, S., Prendergast, A.M., Schnell, A., Hexel, K.*, et al.* (2015). Inflammation-Induced Emergency Megakaryopoiesis Driven by Hematopoietic Stem Cell-like Megakaryocyte Progenitors. Cell stem cell *17*, 422-434.

Hamczyk, M.R., Villa-Bellosta, R., Gonzalo, P., Andres-Manzano, M.J., Nogales, P., Bentzon, J.F., Lopez-Otin, C., and Andres, V. (2018). Vascular Smooth

Muscle-Specific Progerin Expression Accelerates Atherosclerosis and Death in a Mouse Model of Hutchinson-Gilford Progeria Syndrome. Circulation *138*, 266-282.

Hart, E.C., and Charkoudian, N. (2014). Sympathetic neural regulation of blood pressure: influences of sex and aging. Physiology (Bethesda) *29*, 8-15.

Haylock, D.N., and Nilsson, S.K. (2006). Osteopontin: a bridge between bone and blood. Br J Haematol *134*, 467-474.

Hennrich, M.L., Romanov, N., Horn, P., Jaeger, S., Eckstein, V., Steeples, V., Ye, F., Ding, X., Poisa-Beiro, L., Lai, M.C.*, et al.* (2018). Cell-specific proteome analyses of human bone marrow reveal molecular features of age-dependent functional decline. Nature communications *9*, 4004.

Heo, H.R., Chen, L., An, B., Kim, K.S., Ji, J., and Hong, S.H. (2015). Hormonal regulation of hematopoietic stem cells and their niche: a focus on estrogen. Int J Stem Cells *8*, 18-23.

Ho, T.T., Warr, M.R., Adelman, E.R., Lansinger, O.M., Flach, J., Verovskaya, E.V., Figueroa, M.E., and Passegue, E. (2017). Autophagy maintains the metabolism and function of young and old stem cells. Nature *543*, 205-210.

Ho, Y.H., Del Toro, R., Rivera-Torres, J., Rak, J., Korn, C., Garcia-Garcia, A., Macias, D., Gonzalez-Gomez, C., Del Monte, A., Wittner, M.*, et al.* (2019). Remodeling of Bone Marrow Hematopoietic Stem Cell Niches Promotes Myeloid Cell Expansion during Premature or Physiological Aging. Cell stem cell.

Huang, H., and Cantor, A.B. (2009). Common features of megakaryocytes and hematopoietic stem cells: what's the connection? J Cell Biochem *107*, 857-864.

Ito, K., and Suda, T. (2014). Metabolic requirements for the maintenance of self-renewing stem cells. Nat Rev Mol Cell Biol *15*, 243-256.

Jackson, C.W. (1990). Megakaryocyte endomitosis: a review. Int J Cell Cloning *8*, 224-226.

Jaiswal, S., Fontanillas, P., Flannick, J., Manning, A., Grauman, P.V., Mar, B.G.,

Lindsley, R.C., Mermel, C.H., Burtt, N., Chavez, A., *et al.* (2014). Age-related clonal hematopoiesis associated with adverse outcomes. N Engl J Med *371*, 2488-2498.

Jaiswal, S., Natarajan, P., Silver, A.J., Gibson, C.J., Bick, A.G., Shvartz, E., McConkey, M., Gupta, N., Gabriel, S., Ardissino, D., *et al.* (2017). Clonal Hematopoiesis and Risk of Atherosclerotic Cardiovascular Disease. N Engl J Med *377*, 111-121.

Ju, Z., Jiang, H., Jaworski, M., Rathinam, C., Gompf, A., Klein, C., Trumpp, A., and Rudolph, K.L. (2007). Telomere dysfunction induces environmental alterations limiting hematopoietic stem cell function and engraftment. Nat Med *13*, 742-747.

Kajimura, D., Hinoi, E., Ferron, M., Kode, A., Riley, K.J., Zhou, B., Guo, X.E., and Karsenty, G. (2011). Genetic determination of the cellular basis of the sympathetic regulation of bone mass accrual. J Exp Med *208*, 841-851.

Kaser, A., Brandacher, G., Steurer, W., Kaser, S., Offner, F.A., Zoller, H., Theurl, I., Widder, W., Molnar, C., Ludwiczek, O., *et al.* (2001). Interleukin-6 stimulates thrombopoiesis through thrombopoietin: role in inflammatory thrombocytosis. Blood *98*, 2720-2725.

Katayama, Y., Battista, M., Kao, W.M., Hidalgo, A., Peired, A.J., Thomas, S.A., and Frenette, P.S. (2006). Signals from the sympathetic nervous system regulate hematopoietic stem cell egress from bone marrow. Cell *124*, 407-421.

Kawano, Y., Fukui, C., Shinohara, M., Wakahashi, K., Ishii, S., Suzuki, T., Sato, M., Asada, N., Kawano, H., Minagawa, K., *et al.* (2017). G-CSF-induced sympathetic tone provokes fever and primes antimobilizing functions of neutrophils via PGE2. Blood *129*, 587-597.

Kennedy, D.E., and Knight, K.L. (2015). Inhibition of B Lymphopoiesis by Adipocytes and IL-1-Producing Myeloid-Derived Suppressor Cells. J Immunol *195*, 2666-2674.

Kim, M., Kim, C., Choi, Y.S., Kim, M., Park, C., and Suh, Y. (2012). Age-related alterations in mesenchymal stem cells related to shift in differentiation from osteogenic to adipogenic potential: implication to age-associated bone diseases and defects. Mech Ageing Dev *133*, 215-225.

Kim, S.Y., Im, K., Park, S.N., Kwon, J., Kim, J.A., and Lee, D.S. (2015). CALR, JAK2, and MPL mutation profiles in patients with four different subtypes of myeloproliferative neoplasms: primary myelofibrosis, essential thrombocythemia, polycythemia vera, and myeloproliferative neoplasm, unclassifiable. Am J Clin Pathol *143*, 635-644.

Kinashi, T., and Springer, T.A. (1994). Adhesion molecules in hematopoietic cells. Blood cells *20*, 25-44.

Korn, C., and Mendez-Ferrer, S. (2017). Myeloid malignancies and the microenvironment. Blood *129*, 811-822.

Kornicka, K., Marycz, K., Tomaszewski, K.A., Maredziak, M., and Smieszek, A. (2015). The Effect of Age on Osteogenic and Adipogenic Differentiation Potential of Human Adipose Derived Stromal Stem Cells (hASCs) and the Impact of Stress Factors in the Course of the Differentiation Process. Oxid Med Cell Longev *2015*, 309169.

Kovtonyuk, L.V., Fritsch, K., Feng, X., Manz, M.G., and Takizawa, H. (2016). Inflamm-Aging of Hematopoiesis, Hematopoietic Stem Cells, and the Bone Marrow Microenvironment. Frontiers in immunology *7*, 502.

Kunisaki, Y., Bruns, I., Scheiermann, C., Ahmed, J., Pinho, S., Zhang, D., Mizoguchi, T., Wei, Q., Lucas, D., Ito, K.*, et al.* (2013). Arteriolar niches maintain haematopoietic stem cell quiescence. Nature *502*, 637-643.

Kusumbe, A.P., Ramasamy, S.K., and Adams, R.H. (2014). Coupling of angiogenesis and osteogenesis by a specific vessel subtype in bone. Nature *507*, 323-328.

Kusumbe, A.P., Ramasamy, S.K., Itkin, T., Mae, M.A., Langen, U.H., Betsholtz,

C., Lapidot, T., and Adams, R.H. (2016). Age-dependent modulation of vascular niches for haematopoietic stem cells. Nature *532*, 380-384.

Lee, J., Yoon, S.R., Choi, I., and Jung, H. (2019). Causes and Mechanisms of Hematopoietic Stem Cell Aging. Int J Mol Sci *20*.

Lee, R.H., and Bergmeier, W. (2017). Sugar makes neutrophils RAGE: linking diabetes-associated hyperglycemia to thrombocytosis and platelet reactivity. J Clin Invest *127*, 2040-2043.

Liang, Y., Van Zant, G., and Szilvassy, S.J. (2005). Effects of aging on the homing and engraftment of murine hematopoietic stem and progenitor cells. Blood *106*, 1479-1487.

Majka, M., Janowska-Wieczorek, A., Ratajczak, J., Kowalska, M.A., Vilaire, G., Pan, Z.K., Honczarenko, M., Marquez, L.A., Poncz, M., and Ratajczak, M.Z. (2000). Stromal-derived factor 1 and thrombopoietin regulate distinct aspects of human megakaryopoiesis. Blood *96*, 4142-4151.

Malara, A., Abbonante, V., Di Buduo, C.A., Tozzi, L., Currao, M., and Balduini, A. (2015). The secret life of a megakaryocyte: emerging roles in bone marrow homeostasis control. Cell Mol Life Sci *72*, 1517-1536.

Malherbe, J.A., Fuller, K.A., Mirzai, B., Kavanagh, S., So, C.C., Ip, H.W., Guo, B.B., Forsyth, C., Howman, R., and Erber, W.N. (2016). Dysregulation of the intrinsic apoptotic pathway mediates megakaryocytic hyperplasia in myeloproliferative neoplasms. J Clin Pathol.

Mancuso, P., and Bouchard, B. (2019). The Impact of Aging on Adipose Function and Adipokine Synthesis. Front Endocrinol (Lausanne) *10*, 137.

Mann, M., Mehta, A., de Boer, C.G., Kowalczyk, M.S., Lee, K., Haldeman, P., Rogel, N., Knecht, A.R., Farouq, D., Regev, A.*, et al.* (2018). Heterogeneous Responses of Hematopoietic Stem Cells to Inflammatory Stimuli Are Altered with Age. Cell Rep *25*, 2992-3005 e2995.

Maryanovich, M., Zahalka, A.H., Pierce, H., Pinho, S., Nakahara, F., Asada, N.,

Wei, Q., Wang, X., Ciero, P., Xu, J., *et al.* (2018). Adrenergic nerve degeneration in bone marrow drives aging of the hematopoietic stem cell niche. Nat Med.

Maryanovich, M., Zahalka, A.H., Pierce, H., Pinho, S., Nakahara, F., Asada, N., Wei, Q., Wang, X., Ciero, P., Xu, J., *et al.* (2019). Author Correction: Adrenergic nerve degeneration in bone marrow drives aging of the hematopoietic stem cell niche. Nat Med *25*, 701.

McCranor, B.J., Langdon, J.M., Prince, O.D., Femnou, L.K., Berger, A.E., Cheadle, C., Civin, C.I., Kim, A., Rivera, S., Ganz, T., *et al.* (2013). Investigation of the role of interleukin-6 and hepcidin antimicrobial peptide in the development of anemia with age. Haematologica *98*, 1633-1640.

McKerrell, T., Park, N., Moreno, T., Grove, C.S., Ponstingl, H., Stephens, J., Understanding Society Scientific, G., Crawley, C., Craig, J., Scott, M.A., *et al.* (2015). Leukemia-associated somatic mutations drive distinct patterns of age-related clonal hemopoiesis. Cell Rep *10*, 1239-1245.

Mendez-Ferrer, S., Battista, M., and Frenette, P.S. (2010). Cooperation of beta(2)- and beta(3)-adrenergic receptors in hematopoietic progenitor cell mobilization. Ann N Y Acad Sci *1192*, 139-144.

Merideth, M.A., Gordon, L.B., Clauss, S., Sachdev, V., Smith, A.C., Perry, M.B., Brewer, C.C., Zalewski, C., Kim, H.J., Solomon, B., *et al.* (2008). Phenotype and course of Hutchinson-Gilford progeria syndrome. N Engl J Med *358*, 592-604.

Mohrin, M., Shin, J., Liu, Y., Brown, K., Luo, H., Xi, Y., Haynes, C.M., and Chen, D. (2015). Stem cell aging. A mitochondrial UPR-mediated metabolic checkpoint regulates hematopoietic stem cell aging. Science *347*, 1374-1377.

Montecino-Rodriguez, E., Kong, Y., Casero, D., Rouault, A., Dorshkind, K., and Pioli, P.D. (2019). Lymphoid-Biased Hematopoietic Stem Cells Are Maintained with Age and Efficiently Generate Lymphoid Progeny. Stem cell reports *12*, 584-596.

Nagareddy, P.R., Kraakman, M., Masters, S.L., Stirzaker, R.A., Gorman, D.J.,

Grant, R.W., Dragoljevic, D., Hong, E.S., Abdel-Latif, A., Smyth, S.S., *et al.* (2014). Adipose tissue macrophages promote myelopoiesis and monocytosis in obesity. Cell Metab *19*, 821-835.

Nagareddy, P.R., Noothi, S.K., Flynn, M.C., and Murphy, A.J. (2018). It's reticulated: the liver at the heart of atherosclerosis. J Endocrinol *238*, R1-R11.

Nakahara, F., Borger, D.K., Wei, Q., Pinho, S., Maryanovich, M., Zahalka, A.H., Suzuki, M., Cruz, C.D., Wang, Z., Xu, C., *et al.* (2019). Engineering a haematopoietic stem cell niche by revitalizing mesenchymal stromal cells. Nat Cell Biol *21*, 560-567.

Nakamura-Ishizu, A., Takubo, K., Fujioka, M., and Suda, T. (2014). Megakaryocytes are essential for HSC quiescence through the production of thrombopoietin. Biochem Biophys Res Commun *454*, 353-357.

Nakamura-Ishizu, A., Takubo, K., Kobayashi, H., Suzuki-Inoue, K., and Suda, T. (2015). CLEC-2 in megakaryocytes is critical for maintenance of hematopoietic stem cells in the bone marrow. J Exp Med *212*, 2133-2146.

Nangalia, J., Grinfeld, J., and Green, A.R. (2016). Pathogenesis of Myeloproliferative Disorders. Annu Rev Pathol *11*, 101-126.

Naveiras, O., Nardi, V., Wenzel, P.L., Hauschka, P.V., Fahey, F., and Daley, G.Q. (2009). Bone-marrow adipocytes as negative regulators of the haematopoietic microenvironment. Nature *460*, 259-263.

Ng, A.V., Callister, R., Johnson, D.G., and Seals, D.R. (1993). Age and gender influence muscle sympathetic nerve activity at rest in healthy humans. Hypertension *21*, 498-503.

Nilsson, S.K., Johnston, H.M., Whitty, G.A., Williams, B., Webb, R.J., Denhardt, D.T., Bertoncello, I., Bendall, L.J., Simmons, P.J., and Haylock, D.N. (2005). Osteopontin, a key component of the hematopoietic stem cell niche and regulator of primitive hematopoietic progenitor cells. Blood *106*, 1232-1239.

Nishikii, H., Kurita, N., and Chiba, S. (2017). The Road Map for

Megakaryopoietic Lineage from Hematopoietic Stem/Progenitor Cells. Stem Cells Transl Med *6*, 1661-1665.

Nishimura, S., Nagasaki, M., Kunishima, S., Sawaguchi, A., Sakata, A., Sakaguchi, H., Ohmori, T., Manabe, I., Italiano, J.E., Jr., Ryu, T.*, et al.* (2015). IL-1alpha induces thrombopoiesis through megakaryocyte rupture in response to acute platelet needs. J Cell Biol *209*, 453-466.

Osorio, F.G., Navarro, C.L., Cadinanos, J., Lopez-Mejia, I.C., Quiros, P.M., Bartoli, C., Rivera, J., Tazi, J., Guzman, G., Varela, I.*, et al.* (2011). Splicing-directed therapy in a new mouse model of human accelerated aging. Science translational medicine *3*, 106ra107.

Patel, S.R., Hartwig, J.H., and Italiano, J.E., Jr. (2005). The biogenesis of platelets from megakaryocyte proplatelets. J Clin Invest *115*, 3348-3354.

Pietras, E.M. (2017). Inflammation: a key regulator of hematopoietic stem cell fate in health and disease. Blood *130*, 1693-1698.

Pietras, E.M., Mirantes-Barbeito, C., Fong, S., Loeffler, D., Kovtonyuk, L.V., Zhang, S., Lakshminarasimhan, R., Chin, C.P., Techner, J.M., Will, B.*, et al.* (2016). Chronic interleukin-1 exposure drives haematopoietic stem cells towards precocious myeloid differentiation at the expense of self-renewal. Nat Cell Biol *18*, 607-618.

Pimkin, M., Kossenkov, A.V., Mishra, T., Morrissey, C.S., Wu, W., Keller, C.A., Blobel, G.A., Lee, D., Beer, M.A., Hardison, R.C.*, et al.* (2014). Divergent functions of hematopoietic transcription factors in lineage priming and differentiation during erythro-megakaryopoiesis. Genome Res *24*, 1932-1944.

Pinho, S., Marchand, T., Yang, E., Wei, Q., Nerlov, C., and Frenette, P.S. (2018). Lineage-Biased Hematopoietic Stem Cells Are Regulated by Distinct Niches. Dev Cell *44*, 634-641 e634.

Pongratz, G., and Straub, R.H. (2014). The sympathetic nervous response in inflammation. Arthritis Res Ther *16*, 504.

Poulos, M.G., Ramalingam, P., Gutkin, M.C., Llanos, P., Gilleran, K., Rabbany, S.Y., and Butler, J.M. (2017). Endothelial transplantation rejuvenates aged hematopoietic stem cell function. J Clin Invest *127*, 4163-4178.

Reynaud, D., Pietras, E., Barry-Holson, K., Mir, A., Binnewies, M., Jeanne, M., Sala-Torra, O., Radich, J.P., and Passegue, E. (2011). IL-6 controls leukemic multipotent progenitor cell fate and contributes to chronic myelogenous leukemia development. Cancer Cell *20*, 661-673.

Rossi, D.J., Bryder, D., Seita, J., Nussenzweig, A., Hoeijmakers, J., and Weissman, I.L. (2007). Deficiencies in DNA damage repair limit the function of haematopoietic stem cells with age. Nature *447*, 725-729.

Rossi, D.J., Bryder, D., Zahn, J.M., Ahlenius, H., Sonu, R., Wagers, A.J., and Weissman, I.L. (2005). Cell intrinsic alterations underlie hematopoietic stem cell aging. Proc Natl Acad Sci U S A *102*, 9194-9199.

Sacma, M., Pospiech, J., Bogeska, R., de Back, W., Mallm, J.-P., Sakk, V., Soller, K., Marka, G., Vollmer, A., Karns, R.*, et al.* (2019). Haematopoietic stem cells in perisinusoidal niches are protected from ageing. Nature Cell Biology *(submitted)*.

Sakamaki, S., Hirayama, Y., Matsunaga, T., Kuroda, H., Kusakabe, T., Akiyama, T., Konuma, Y., Sasaki, K., Tsuji, N., Okamoto, T.*, et al.* (1999). Transforming growth factor-beta1 (TGF-beta1) induces thrombopoietin from bone marrow stromal cells, which stimulates the expression of TGF-beta receptor on megakaryocytes and, in turn, renders them susceptible to suppression by TGF-beta itself with high specificity. Blood *94*, 1961-1970.

Sanchez-Aguilera, A., and Mendez-Ferrer, S. (2017). The hematopoietic stem-cell niche in health and leukemia. Cell Mol Life Sci *74*, 579-590.

Scaffidi, P., and Misteli, T. (2006). Lamin A-dependent nuclear defects in human aging. Science *312*, 1059-1063.

Schulze, H., Korpal, M., Hurov, J., Kim, S.W., Zhang, J., Cantley, L.C., Graf, T., and Shivdasani, R.A. (2006). Characterization of the megakaryocyte demarcation

membrane system and its role in thrombopoiesis. Blood *107*, 3868-3875.

Schwartz, A.V. (2015). Marrow fat and bone: review of clinical findings. Front Endocrinol (Lausanne) *6*, 40.

Siegel, G., Kluba, T., Hermanutz-Klein, U., Bieback, K., Northoff, H., and Schafer, R. (2013). Phenotype, donor age and gender affect function of human bone marrow-derived mesenchymal stromal cells. BMC Med *11*, 146.

Spiegel, A., Shivtiel, S., Kalinkovich, A., Ludin, A., Netzer, N., Goichberg, P., Azaria, Y., Resnick, I., Hardan, I., Ben-Hur, H.*, et al.* (2007). Catecholaminergic neurotransmitters regulate migration and repopulation of immature human CD34+ cells through Wnt signaling. Nat Immunol *8*, 1123-1131.

Stegner, D., vanEeuwijk, J.M.M., Angay, O., Gorelashvili, M.G., Semeniak, D., Pinnecker, J., Schmithausen, P., Meyer, I., Friedrich, M., Dutting, S.*, et al.* (2017). Thrombopoiesis is spatially regulated by the bone marrow vasculature. Nature communications *8*, 127.

Stewart, M.H., Gutierrez-Martinez, P., Beerman, I., Garrison, B., Gallagher, E.J., LeRoith, D., and Rossi, D.J. (2014). Growth hormone receptor signaling is dispensable for HSC function and aging. Blood *124*, 3076-3080.

Stier, S., Ko, Y., Forkert, R., Lutz, C., Neuhaus, T., Grunewald, E., Cheng, T., Dombkowski, D., Calvi, L.M., Rittling, S.R.*, et al.* (2005). Osteopontin is a hematopoietic stem cell niche component that negatively regulates stem cell pool size. J Exp Med *201*, 1781-1791.

Stolzing, A., Jones, E., McGonagle, D., and Scutt, A. (2008). Age-related changes in human bone marrow-derived mesenchymal stem cells: consequences for cell therapies. Mech Ageing Dev *129*, 163-173.

Sudo, K., Ema, H., Morita, Y., and Nakauchi, H. (2000). Age-associated characteristics of murine hematopoietic stem cells. J Exp Med *192*, 1273-1280.

Sugiyama, T., Kohara, H., Noda, M., and Nagasawa, T. (2006). Maintenance of the hematopoietic stem cell pool by CXCL12-CXCR4 chemokine signaling in

bone marrow stromal cell niches. Immunity *25*, 977-988.

Taichman, R.S., and Emerson, S.G. (1994). Human osteoblasts support hematopoiesis through the production of granulocyte colony-stimulating factor. J Exp Med *179*, 1677-1682.

Thiele, J., Kvasnicka, H.M., Mullauer, L., Buxhofer-Ausch, V., Gisslinger, B., and Gisslinger, H. (2011). Essential thrombocythemia versus early primary myelofibrosis: a multicenter study to validate the WHO classification. Blood *117*, 5710-5718.

Tijssen, M.R., and Ghevaert, C. (2013). Transcription factors in late megakaryopoiesis and related platelet disorders. J Thromb Haemost *11*, 593-604.

Tikhonova, A.N., Dolgalev, I., Hu, H., Sivaraj, K.K., Hoxha, E., Cuesta-Dominguez, A., Pinho, S., Akhmetzyanova, I., Gao, J., Witkowski, M.*, et al.* (2019). The bone marrow microenvironment at single-cell resolution. Nature *569*, 222-228.

Tripathi, P., Tripathi, P., Kashyap, L., and Singh, V. (2007). The role of nitric oxide in inflammatory reactions. FEMS Immunol Med Microbiol *51*, 443-452.

Vainchenker, W., Besancenot, R., and Favale, F. (2013). [Megakaryopoiesis: regulation of platelet production by thrombopoietin]. Bull Acad Natl Med *197*, 395-406.

Veith, R.C., Featherstone, J.A., Linares, O.A., and Halter, J.B. (1986). Age differences in plasma norepinephrine kinetics in humans. Journal of gerontology *41*, 319-324.

Vilchez, D., Simic, M.S., and Dillin, A. (2014). Proteostasis and aging of stem cells. Trends Cell Biol *24*, 161-170.

Villa-Bellosta, R., Rivera-Torres, J., Osorio, F.G., Acin-Perez, R., Enriquez, J.A., Lopez-Otin, C., and Andres, V. (2013). Defective extracellular pyrophosphate metabolism promotes vascular calcification in a mouse model of Hutchinson-Gilford progeria syndrome that is ameliorated on pyrophosphate treatment.

Circulation *127*, 2442-2451.

Vytrva, N., Stacher, E., Regitnig, P., Zinke-Cerwenka, W., Hojas, S., Hubmann, E., Porwit, A., Bjorkholm, M., Hoefler, G., and Beham-Schmid, C. (2014). Megakaryocytic morphology and clinical parameters in essential thrombocythemia, polycythemia vera, and primary myelofibrosis with and without JAK2 V617F. Arch Pathol Lab Med *138*, 1203-1209.

Wagner, W., Bork, S., Horn, P., Krunic, D., Walenda, T., Diehlmann, A., Benes, V., Blake, J., Huber, F.X., Eckstein, V.*, et al.* (2009). Aging and replicative senescence have related effects on human stem and progenitor cells. PloS one *4*, e5846.

Wintges, K., Beil, F.T., Albers, J., Jeschke, A., Schweizer, M., Claass, B., Tiegs, G., Amling, M., and Schinke, T. (2013). Impaired bone formation and increased osteoclastogenesis in mice lacking chemokine (C-C motif) ligand 5 (Ccl5). Journal of bone and mineral research : the official journal of the American Society for Bone and Mineral Research *28*, 2070-2080.

Woolthuis, C.M., and Park, C.Y. (2016). Hematopoietic stem/progenitor cell commitment to the megakaryocyte lineage. Blood *127*, 1242-1248.

Xie, M., Lu, C., Wang, J., McLellan, M.D., Johnson, K.J., Wendl, M.C., McMichael, J.F., Schmidt, H.K., Yellapantula, V., Miller, C.A.*, et al.* (2014). Age-related mutations associated with clonal hematopoietic expansion and malignancies. Nat Med *20*, 1472-1478.

Xing, Z., Ryan, M.A., Daria, D., Nattamai, K.J., Van Zant, G., Wang, L., Zheng, Y., and Geiger, H. (2006). Increased hematopoietic stem cell mobilization in aged mice. Blood *108*, 2190-2197.

Yamashita, M., and Passegue, E. (2019). TNF-alpha Coordinates Hematopoietic Stem Cell Survival and Myeloid Regeneration. Cell Stem Cell.

Yoshihara, H., Arai, F., Hosokawa, K., Hagiwara, T., Takubo, K., Nakamura, Y., Gomei, Y., Iwasaki, H., Matsuoka, S., Miyamoto, K.*, et al.* (2007).

Thrombopoietin/MPL signaling regulates hematopoietic stem cell quiescence and interaction with the osteoblastic niche. Cell stem cell *1*, 685-697.

Young, K., Borikar, S., Bell, R., Kuffler, L., Philip, V., and Trowbridge, J.J. (2016). Progressive alterations in multipotent hematopoietic progenitors underlie lymphoid cell loss in aging. J Exp Med *213*, 2259-2267.

Zhang, D.Y., Wang, H.J., and Tan, Y.Z. (2011). Wnt/beta-catenin signaling induces the aging of mesenchymal stem cells through the DNA damage response and the p53/p21 pathway. PloS one *6*, e21397.

Zhang, J., Niu, C., Ye, L., Huang, H., He, X., Tong, W.G., Ross, J., Haug, J., Johnson, T., Feng, J.Q.*, et al.* (2003). Identification of the haematopoietic stem cell niche and control of the niche size. Nature *425*, 836-841.

Zhao, M., Perry, J.M., Marshall, H., Venkatraman, A., Qian, P., He, X.C., Ahamed, J., and Li, L. (2014). Megakaryocytes maintain homeostatic quiescence and promote post-injury regeneration of hematopoietic stem cells. Nat Med *20*, 1321-1326.

Zheng, Y., He, L., Wan, Y., and Song, J. (2013). H3K9me-enhanced DNA hypermethylation of the p16INK4a gene: an epigenetic signature for spontaneous transformation of rat mesenchymal stem cells. Stem Cells Dev *22*, 256-267.

Zhou, B.O., Yu, H., Yue, R., Zhao, Z., Rios, J.J., Naveiras, O., and Morrison, S.J. (2017). Bone marrow adipocytes promote the regeneration of stem cells and haematopoiesis by secreting SCF. Nat Cell Biol *19*, 891-903.

Ziegler, M.G., Lake, C.R., and Kopin, I.J. (1976). Plasma noradrenaline increases with age. Nature *261*, 333-335.

Zink, F., Stacey, S.N., Norddahl, G.L., Frigge, M.L., Magnusson, O.T., Jonsdottir, I., Thorgeirsson, T.E., Sigurdsson, A., Gudjonsson, S.A., Gudmundsson, J.*, et al.* (2017). Clonal hematopoiesis, with and without candidate driver mutations, is common in the elderly. Blood *130*, 742-752.